UNIVERSITÉ DU QUÉBEC

LE RÔLE DU ZOOPLANCTON DANS LE CYCLE DU MERCURE DANS LES LACS BORÉAUX : COUPLAGE D'APPROCHES COMPARATIVES ET EXPÉRIMENTALES

THÈSE PRÉSENTÉE
COMME EXIGENCE PARTIELLE DU
DOCTORAT EN SCIENCES DE L'ENVIRONNEMENT

OFFERT PAR L'UNIVERSITÉ DU QUÉBEC À MONTRÉAL
EN ASSOCIATION AVEC
L'UNIVERSITÉ DU QUÉBEC À TROIS-RIVIÈRES

PAR
FAN QIN

DÉCEMBRE 2022

UNIVERSITÉ DU QUÉBEC

DOCTORAT EN SCIENCES DE L'ENVIRONNEMENT (PH. D.)

Programme offert par l'Université du Québec à Montréal (UQAM)

en association avec

l'Université du Québec à Chicoutimi (UQAC)

l'Université du Québec à Rimouski (UQAR)

l'Université du Québec en Abitibi-Témiscamingue (UQAT)

et l'Université du Québec à Trois-Rivières (UQTR)

Direction de recherche :

Andrea Bertolo	Directeur de recherche
Marc Amyot	Codirecteur de recherche

Jury d'évaluation :

Andrea Bertolo	Directeur de recherche
Marc Amyot	Codirecteur de recherche
Vincent Fugère	Président de jury
Michael Twiss	Évaluateur externe
Zofia Taranu	Évaluatrice externe

Thèse soutenue le 24 août 2022

In loving memory of

my beloved grandmother

吴英秀 (1935-2019)

and my dearest uncle

樊京川 (1968-2018)

"These are the people who first spoke out against the reckless and irresponsible poisoning of the world that man shares with all other creatures, and who are even now fighting the thousands of small battles that in the end will bring victory for sanity and common sense in our accommodation to the world that surrounds us."

"The 'control of nature' is a phrase conceived in arrogance, born of the Neanderthal age of biology and philosophy, when it was supposed that nature exists for the convenience of man. The concepts and practices of applied entomology for the most part date from that Stone Age of science. It is our alarming misfortune that so primitive a science has armed itself with the most modern and terrible weapons, and that in turning them against the insects it has also turned them against the earth."

<< Silent Spring>> Rachel Carson 1962

ACKNOWLEDGMENTS

The darkest years in my life were the first two years in Canada, nine years ago, when I just arrived in Canada with hopes and dreams to work in the fishery research area with my enthusiasm. Lucky, I got help. I would like to thank firstly Liza Poirier, my psychologist, who helped me to get out of the depression, and Mme Boyz, the lawyer who helped me to confront the bullying and for the immigration papers, so I can continue chase my dream in Canada. I would like also to thank my dear friends, Sylvain Lebargy, Dorrie Campbell and Marc Leblanc. Thank you for being with me through the difficult time of my life.

I would like to express my gratitude to my supervisors, Andrea Bertolo and Marc Amyot, for offering me the opportunity to work on this research project. Thank you for your patient guidance, encouragement, and advice in my research. Especially for Andrea, after seeing my PTSD symptom during the period of my experiments, you were supportive and always listening. The moment I got the email from Marc, asking for my school transcript after I quit my last job, I felt like I was reborn again. Thank you for finding me, always being available, and providing prompt answers to my questions.

I thank the members of the jury, Vincent Fugère, Michael Twiss, and Zofia Taranu, for agreeing to evaluate my dissertation. I am very grateful to them for the time they have dedicated to reading and commenting on my work.

I appreciate the help from Pre Isabel Desgagné-Penix, Pre Helene Glémet, and Pr Simon Barnabé, and Pr Raphaël Proulx for their generosity of free algae source, the working space and lab equipements to accomplish my experiments. I would also like to thank Valérie Godbout, Joanie Guay, and Elois Veilleux from CEAEQ for their generous help with the free source of *D. magna*.

Thanks to all who had the courage to accompany me during the field and laboratory experiments. I know it was hard, especially the 24 h rotating of sampling. Thank you, Caroline Macarez and Catherine Dunn, for your supportive effort and encouragement during the difficult time of work. I would also like to acknowledge other colleagues, who gave a hand during the work, namely Maxime Clermont, Joëlle Guitard, Francis Sévigny, Stéphanie L'Italien Simard, Laurie Fortin, Alexis Baribeau Rondeau, Sabrina Gignac Brassard and Judith Pichon. Thanks to Antoine Filion and Matteo Giacomazzo, for the help when I needed to return to the field for missing data.

To my team in Montréal, I would like to thank Maxime Leclerc and Dominic Ponton for the supportive help and enlightening discussion on my project. Special thanks to Gwyneth MacMillan for talking me through when I wanted to quit the project because of the depression at the biological station of UdeM in 2016. It was a rainy day, beside the Lake Geai. I appreciate greatly the help from the technique team, namely Dominic Bélanger, Maria Chrifi Alaoui, and Kathy St-Fort for sample analysis during the lockdown in 2020 and 2021. Special thanks to Dominic Bélanger, you are not just a teacher, but also a friend. Thank you for the hosting, the teaching, and the comforting words during my stay in the lab.

I appreciate the help from the administration at the UQTR and UQAM. Namely Catarina Leote Franco Pio, Christine Guillerm, and Chantal Fournier, for their technical support and their outstanding communication and problem-solving skills that helped me through many arduous times. Mme Marie-Claude Brulé at the international student service at the UQTR, thank you for your support and help and those papers of immigration during my time in school. Geneviève Bureau, Natalie Bourdeau, Marguerite Cinq-Mars for the collaboration during my experiment. And last the security team at the UQTR, especially M. Guylain Pronovost for checking me and keeping me alive, during my 24 h experiments besides the human anatomy lab.

Thanks to my friend Arthur de Grandpré and Corentin Flinois, for the help on the French version of part of my thesis. Roxanne Giguère-Tremblay, Marc Pepino and

Vincent Marie for the fun time of preparating the numerilab and the statistic workshop for the ECOTOQ conference. And many other friends I have met and gave me a hand during a certain moment of my life.

I'm indebted to my parents for their support during different periods of my life, their open teaching philosophy has made me an open-minded person who is willing to take on any future challenges.

Finally, I want to thank my mentors Pr Jean-Paul Robin and Pre Katrine Costil from the University of Caen Basse-Normandy, my dear friend Dr. Michaël Gras from the European Commission, and the supervisor of my internship at the University of Lorraine Pre Marielle Thomas. Thank you for your faith in me and were willing to redo the recommendation letter for me for this job. Words cannot describe my gratitude. Thank you for helping me to correct my life trajectory back to my beloved ecotoxicology.

This doctoral project was supported by grants from the Research Centre for Watershed – Aquatic Ecosystem Interactions, University of Québec at Trois-Rivières, the Fonds Québécois de la recherche sur la nature et les technologies (FQRNT) (Grant No. 2016-PR-189982), and the Groupe de Recherche Interuniversitaire en Limnologie (a FQRNT Strategic Network) to Andrea Bertolo and Marc Amyot, and the Canadian Foundation for Innovation and the Canada Research Chair Program to Marc Amyot.

I dedicated this thesis to my persistence and my beloved research work
on ecotoxicology, and to my family, friends, and coworkers
who have faith in me for the realization of this work:
my deepest gratitude for your support and encouragement.

RÉSUMÉ

Le mercure (Hg) est un des polluants le plus étudiés dans les écosystèmes aquatiques, principalement en raison de sa forte toxicité sous forme organique (monométhylmercure, MeHg) et de sa capacité à être bio-accumulé et bio-amplifié dans les réseaux trophiques à des niveaux très préoccupants pour la santé de l'homme. L'étude du cycle du Hg dans les systèmes lacustres d'eau douce est importante non seulement parce qu'elle aide à comprendre les mécanismes de production de MeHg et de son transfert dans les réseaux trophiques, mais fournit également des informations utiles pour les futurs projets de restauration des écosystèmes aquatiques contaminés. Bien que le zooplancton soit considéré comme une composante importante dans le transfert trophique du Hg dans les écosystèmes aquatiques, son comportement, tel que le broutage et la migration à courte échelle, n'a pas suffisamment attiré l'attention sur l'image du cycle du Hg dans les écosystèmes aquatiques. Dans ce projet de doctorat, nous avons étudié les effets du broutage du zooplancton ainsi que les fluctuations de température liées à la migration à courte échelle et l'abondance dans la colonne d'eau afin de mieux comprendre le rôle du zooplancton dans le cycle du Hg dans les lacs boréaux.

Dans le 1^{e} chapitre, nous avons questionné l'efficacité du transfert trophique des polluants métalliques traces dans les réseaux trophiques en réalisant des expériences en laboratoire pour étudier l'effet du broutage du zooplancton sur la régénération des métaux traces en eau douce. Nous avons utilisé des algues vertes (*Chlorella* sp.) marquées par des isotopes du Hg (^{200}Hg inorganique, Me^{198}Hg) comme source de nourriture. Pour mettre en évidence le rôle du comportement de broutage, nous avons comparé un grand filtreur (*Daphni magna*) et un consommateur sélectif (copépodes calanoïdes), en faisant l'hypothèse que ce dernier provoquerait plus d'effets de type *sloppy feeding* (comportement d'alimentation inefficace) que le premier. Nos résultats ont montré que les activités du zooplancton libéraient jusqu'à 11 % du Hg qui avait été inoculé dans les algues après 30 minutes. Cependant, cette efficacité de libération dépendait à la fois de la taxonomie du zooplancton et de la spéciation du Hg dans l'eau. *D. magna* a fortement affecté la libération des éléments dissous, tandis que les copépodes calanoïdes ont fortement affecté la libération des éléments dans la phase particulaire. Nous avons également trouvé d'autres métaux traces, y compris des éléments de terres rares, qui sont également libérés à partir des algues par le broutage du zooplancton après 30 minutes d'incubation. Ces résultats mettent en évidence une voie négligée de recyclage de Hg inorganique (IHg) et du MeHg dans la colonne d'eau des écosystèmes d'eau douce avec des conséquences potentiellement importantes pour le transfert trophique.

Dans le 2^{e} chapitre, nous avons étudié les effets des variations de la température sur l'accumulation de métaux traces chez le zooplancton (*D. magna*) dans des conditions simulant les cycles journaliers de température pouvant être rencontrés dans les milieux naturels. Plus précisément, nous avons étudié l'impact des oscillations de température (7/23 ^{o}C, 24 h/cycle) sur l'accumulation d'IHg et de MeHg chez *D. magna*, en le comparant à un traitement avec une température constante ayant la même température

moyenne (15 ºC). Les effets de la température moyenne ont été testés en comparant cette dernière à un traitement similaire avec une température constante plus élevée (23 ºC). Nous avons aussi comparé l'importance relative des voies trophique et aqueuse en comparant l'accumulation des différentes formes de Hg par des daphnies nourris avec des *Chlorella* marquées avec des isotopes stables de Hg à d'autres qui étaient incubées dans milieux enrichis en isotopes de Hg, mais nourrirez avec des *Chlorella* non marquées. Les résultats de cette étude ont montré que les concentrations d'IHg chez *D. magna* exposées à des conditions de température oscillante étaient inférieures à celles mesurées dans des conditions de température constante, aussi bien par la voie trophique (diminution de 42 %) que par la voie aqueuse (diminution de 25 %). En revanche, l'accumulation de MeHg a été réduite dans la voie trophique mais a été augmentée par la voie aqueuse. Cette étude jette un nouvel éclairage sur l'accumulation de métaux traces dans des conditions de température proches des conditions naturelles.

Dans le 3^{e} chapitre, nous avons étudié le rôle de l'hétérogénéité dans colonne d'eau sur le cycle du Hg, en particulier concernant le rôle du zooplancton, en échantillonnant quatre lacs boréaux avec des caractéristiques contrastées (transparence et présence/absence de poissons) dans le Parc National de la Mauricie au Canada. Les caractéristiques contrastées sélectionnées des lacs visaient à maximiser l'hétérogénéité de l'abondance du zooplancton à la fois entre les lacs et au niveau des profils verticaux dans la colonne d'eau de chacun des lacs ainsi qu'à analyser leurs liens potentiels avec l'hétérogénéité verticale du Hg. Les résultats ont montré que la présence de grands copépodes et de cladocères de taille moyenne diminuait significativement la concentration de Hg dissous dans l'eau à une profondeur donnée, alors que la présence de copépodes de taille moyenne diminuait significativement la concentration de Hg total. La présence de cladocères a significativement affecté le ratio entre les formes dissoutes de MeHg et de Hg. Des variations quotidiennes ont également été observées dans les concentrations de Hg dissous et total, les échantillons de nuit étant significativement plus élevés que les échantillons de jour. Ces résultats ont mis en évidence le rôle clé de l'hétérogénéité de la colonne d'eau, en particulier la présence de zooplancton, sur le cycle du Hg dans l'eau dans les lacs boréaux.

Mots-clés : Polluants métalliques à l'état de trace, mercure, monométhylmercure, régénération des métaux, *Daphnia magna*, calanoïdes, broutage du zooplancton, sloppy feeding, transferts trophiques, bioconcentration, température oscillante, migration verticale journalière, prédation des poissons, prédateurs d'invertébrés, lacs d'eau douce

ABSTRACT

Mercury (Hg) is one of the most studied trace metal pollutants in aquatic ecosystems, mainly due to its high toxicity as a neurotoxin in the organic form (monomethylmercury, MeHg), and its ability to be bioaccumulated and bioamplified in food webs to levels of great concern for human health. Studying the cycling of Hg in freshwater lake systems is important not only because it helps to understand the mechanisms of MeHg production and its transfer in the food webs, but also provides useful information for future projects on the restoration of the contaminated aquatic ecosystems. Although zooplankton is considered an important component in the trophic transfer of Hg in the food webs, its behavior, such as grazing and short scale migration (both temporal and spatial), has not drawn enough attention to the paradigm of Hg cycling in aquatic ecosystems. In this doctoral project, we studied the effects of zooplankton grazing on Hg remineralization, together with the short-term effects of temperature fluctuations on bioaccumulation by zooplankton, and the relationship between zooplankton abundance in the water column and the concentration of different Hg species to better understand the role of zooplankton in the cycling of Hg in boreal lakes.

In the 1st chapter, we analyzed the trophic transfer efficiency of trace metal pollutants in the food webs by performing laboratory experiments to study the effect of zooplankton grazing on trace metal regeneration in freshwater. We used isotopic labeled *Chlorella* (inorganic ^{200}Hg, $Me^{198}Hg$) as food sources. To highlight the role of feeding behavior, we compared a large filter-feeder (*Daphnia magna*) and a smaller selective feeder (calanoid copepods), with the latter being expected to cause more sloppy feeding than the former. Our results showed that zooplankton activities released up to 11% of spiked Hg from algae within 30 min. However, this release efficiency was species-specific, depending on both the taxonomy of zooplankton and the speciation of Hg in water. *D. magna* strongly affected the release of dissolved elements, whereas calanoid copepods strongly affected the release of elements into the particulate phase. We found also the release of other trace metals, including rare earth elements, from algae by zooplankton grazing within 30 min of incubation. These results highlight a neglected pathway of inorganic Hg (IHg) and MeHg recycling in the water column in freshwater ecosystems with potentially important consequences for trophic transfer.

In the 2nd chapter, we studied the thermal effects on trace metal accumulation in zooplankton (*D. magna*) under a near realistic condition with temperature fluctuation within a short time cycle (24 h). The impact of oscillating temperature (7/23 ºC, 24h/cycle) on the accumulation of IHg and MeHg in *Daphnia* was investigated, by comparing it to a constant temperature treatment with the same average temperature (15 ºC). The effects of mean temperature were tested by comparing this latter to a similar treatment with a higher temperature (23 ºC). Both trophic and water pathways were estimated by using *Chlorella* labeled with stable Hg isotopes and by directly spiking Hg isotope solutions into the microcosm, respectively. The results of this study showed that the concentrations of IHg were decreased in *Daphnia* under oscillating temperature for both food and water

pathways by at least 42% and 25%, respectively, compared to the treatment with the temperature maintained constantly at 15 ^{o}C. In contrast, the accumulation of MeHg was reduced in the trophic pathway but was enhanced in the water pathway. This study sheds new light on trace metal accumulation in a near realistic temperature condition.

In the 3rd chapter, we studied the role of water column heterogeneity on Hg cycling, especially concerning the role of zooplankton, by sampling four boreal lakes with contrasting characteristics (transparency and the presence/absence of fish) in La mauricie National Park of Canada. The selected characteristics of lakes aimed to maximize the heterogeneity in zooplankton abundance both among and within lakes and analyze their potential links with Hg vertical heterogeneity. The results showed that the presence of large copepods and medium cladocera significantly decreased the concentration of dissolved Hg in the water at a given depth, whereas the presence of medium copepods significantly decrease the concentration of total Hg. The presence of cladocera significantly affected the ratio between dissolved forms of MeHg and Hg. Diel variations have also been observed in the concentrations of both dissolved and total Hg, with night samples significantly higher than day samples. These results highlighted the key role of water column heterogeneity, especially the presence of zooplankton, on the cycling of Hg in boreal lakes.

Keywords: trace metal pollutants, mercury, monomethylmercury, metal regeneration, *Daphnia magna*, calanoids, zooplankton grazing, sloppy feeding, trophic transfers, bioconcentration, oscillating temperature, diel vertical migration, fish predation, invertebrate predators, freshwater lakes

TABLE DES MATIÈRES

LISTE DES FIGURES

INTRODUCTION GÉNÉRALE

Contexte général

Dû à l'augmentation de la population mondiale, l'urbanisation rapide, l'évolution des régimes alimentaires et la croissance économique, les écosystèmes aquatiques attirent de plus en plus d'attention de la part de l'homme. Ces écosystèmes sont particulièrement importants pour les sociétés humaines, non seulement en raison de leur vaste superficie, mais aussi de leur rôle important pour la production alimentaire mondiale (Dalin et Outhwaite, 2019; Golden et al., 2021). Par exemple, la production halieutique mondiale a atteint un nouveau record en 2018 avec 180 millions de tonnes de produits alimentaires (FAO, 2020). Au sein de cette production, la pêche en eau douce a pris une place importante avec une croissance plus rapide par rapport aux autres secteurs d'activités (Figure 1), notamment dans le secteur de l'aquaculture en eaux continentales, où la production a presque triplé en 20 ans (19 millions de tonnes en 2000, 51 millions de tonnes en 2018) (FAO, 2020). De plus, les écosystèmes d'eau douce jouent un rôle fondamental dans le soutien de l'environnement et de la société. Par exemple, ils fournissent des services tels que l'eau potable, la production d'énergie, des habitats pour la vie aquatique, des solutions naturelles pour la purification de l'eau et la protection contre les inondations, et bien d'autres encore.

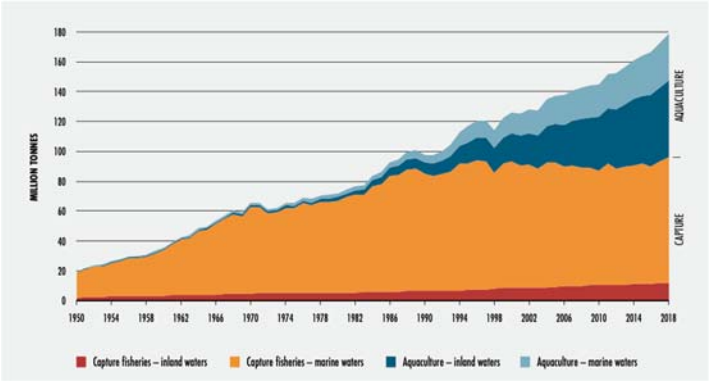

Figure 1. Production mondiale des pêcheries et de l'aquaculture (à l'exclusion des mammifères aquatiques, crocodiles, alligators, caïmans, algues et autres plantes aquatiques). (Source : FAO 2020)

Les écosystèmes d'eau douce sont considérés parmi les premiers et les plus grands compartiments environnementaux à recevoir une grande variété de contaminants chimiques provenant de la nature et des activités anthropiques, tels que les polluants organiques persistants (p. ex., PCBs, HAP, pesticide, etc.) et inorganiques (p. ex., métaux lourds). Parmi ceux-ci, le mercure (Hg) est le polluant métallique le plus étudié dans les écosystèmes d'eau douce, principalement en raison de sa haute toxicité sous forme organique (monomethylmercure, MeHg), et sa capacité d'être bio-accumulé et bio-amplifié dans la chaîne trophique à des niveaux très préoccupants pour la santé humaine (Ullrich et al., 2001; Lehnherr, 2014). En Amérique du Nord, le Hg se situe au cœur de la législation sur la consommation des produits de la pêche en eau douce. Au Canada, par exemple, les guides de consommation des poissons d'eau douce sont établis par la présence de mercure dans les tissus, car il s'agit du seul contaminant dépassant fréquemment la directive ministérielle (pour le mercure, limite de 0.5 mg/kg dans la chair du poisson) pour plusieurs espèces de poissons (Ministre du Développement durable, de l'Environnement et de la Lutte contre les changements climatiques, Québec). Il devient alors important de comprendre les facteurs qui déterminent la disponibilité du Hg en milieu aquatique.

Cycle du Hg dans les systèmes d'eau douce

Le cycle biogéochimique du Hg dans les écosystèmes aquatiques est complexe. Dans le paradigme couramment accepté au sein de la littérature (Figure 2) (Hudson et al., 1994), la source principale de Hg pour les systèmes lacustres dans des territoires non anthropisés provient de l'atmosphère, soit par la déposition sèche ou humide, en raison de sa capacité à parcourir de longues distances depuis sa source d'émission (Jitaru et Adams, 2004 ; Mason et al., 2012). Dans les lacs, le Hg inorganique, principalement sous forme divalente (Hg^{II}), peut être méthylé par des micro-organismes méthylateurs lorsqu'il se trouve en condition anoxiques. Le MeHg produit peut ensuite être absorbé à la base des réseaux trophiques et être transféré et bio-amplifié vers les niveaux trophiques supérieurs (Figure 2). Certains auteurs incluent également la production de Hg gazeuse dissous (angl. : *dissolved gaseous mercury*, DGM) parmi les mécanismes favorisants une

diminution de la charge de Hg dans les écosystèmes aquatiques, ce qui permet un certain contrôle des quantités de Hg accumulé dans les réseaux trophiques (Jitaru et Adams, 2004; Poulain et al., 2004). Les sédiments sont généralement considérés comme un lieu important pour la production de MeHg, principalement en raison de leurs conditions anoxiques qui favorisent les activités des bactéries méthylatrices, telles que les bactéries sulfato-réductrices (SRB), les bactéries réductrices de fer (IRB), et dans une moindre mesure, les archées méthanogènes (Compeau et al., 1985 ; Lovley et al., 1987; Fleming et al., 2006 ; Kerin et al., 2006; Hamelin et al., 2011). Cependant, de plus en plus d'indices montrent que le MeHg produit dans les sédiments n'est peut-être pas significativement important dans le transfert trophique des écosystèmes d'eau douce, à cause de la barrière entre les sédiments et la couche d'eau couverte (Steffan et al., 1988).

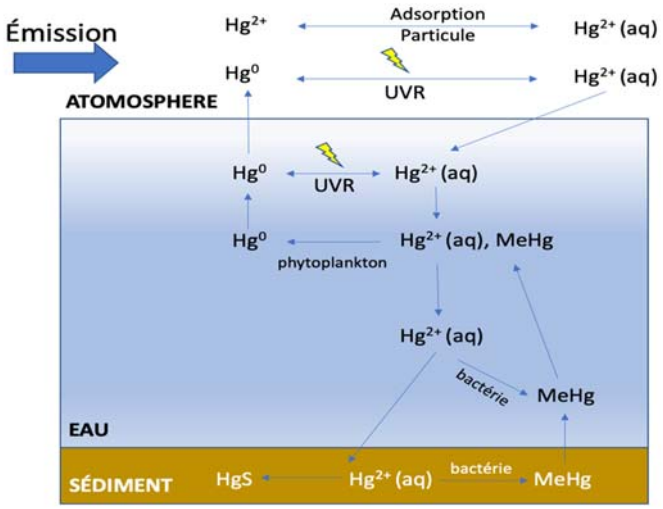

Figure 2. Cycle biogéochimique simplifié du Hg dans l'air, l'eau et le sédiment.

Des études récentes ont démontré que la colonne d'eau pourrait être un lieu important pour la production de MeHg, qui à son tour peut avoir un impact significatif sur l'accumulation de Hg dans les réseaux trophiques aquatiques. Ces études ont montré que la couche d'eau anoxique étendue en surface des sédiments, combinée avec le pic de biomasse du phytoplancton dans la colonne d'eau (angl : *deep chlorophyll maximum;* DCM) avait une corrélation positive avec la concentration de MeHg dans l'eau (Watras et al., 1994; Eckley et Hintelmann, 2006). Il a été suggéré que, dans des conditions

anoxiques, le phytoplancton pourrait servir à la fois de substrat pour la croissance des bactéries méthylatrices et de source d'énergie provenant d'exsudation pour favoriser la production de MeHg (Huguet et al., 2010; Grégoire et Poulain, 2018). La découverte du rôle du périphyton dans la production de MeHg a renforcé l'hypothèse que dans certains lacs, la contribution majeure de MeHg dans les réseaux trophiques ne provient peut-être pas des sédiments, mais de la colonne d'eau où la végétation submergée peut agit comme un support pour le développement du périphyton (Cleckner et al., 1999; Guimarães et al., 2006; Achá et al., 2011; Bouchet et al., 2018). En outre, similairement au phénomène dit de « neige marine » observé dans l'océan, la « neige de lac » peut également fournir un micro-environnement optimal pour la production de MeHg dans lequel la dégradation de matière organique au sein des noyaux d'agrégation favoriserait l'anoxie (Grossart et Simon, 1993; Ortiz et al., 2015). De plus, bien que le rôle du broutage de zooplancton dans cycle de carbone dans la colonne d'eau des océans est bien documenté (Ducklow et al., 2001), les rôles potentiels de ce comportement sur le cycle du Hg dans la colonne d'eau sont encore mal connus. Plus précisément, ses effets potentiels sur le recyclage du Hg via son broutage sur le phytoplancton, tels que démontrés en conditions expérimentales (Qin et al., 2022), n'ont pas été pris en compte explicitement dans le paradigme actuel décrivant ces cycles.

Migration verticale journalière du zooplancton

Selon un paradigme couramment accepté, le zooplancton s'alimente majoritairement par le broutage nocturne du phytoplancton durant la DVM dans la colonne d'eau, un des phénomènes migratoires les plus importants sur la planète. En général, la DVM est représentée par une ascension du zooplancton vers les couches superficielles au coucher du soleil et une redescente vers les couches profondes à l'aube du soleil dans les lacs et les océans (Ringelberg, 2009). La prédation visuelle par les poissons est considérée comme un des déterminants clé de ce phénomène (Ringelberg, 2009; Bollens et al., 2011). Pendant la nuit, les organismes composant le zooplancton, notamment ceux de grande taille, plus susceptibles aux prédateurs, remontent à la surface de l'eau, en profitant de la source de nourriture et en augmentant ainsi leur valeur sélective

(Winder et al., 2004; Ringelberg, 2009). Ce comportement constitue une stratégie adaptative pour le zooplancton et peut avoir des conséquences majeures sur la biogéochimie dans les écosystèmes de l'eau douce (Le Jeune et al., 2012 ; Li et al., 2014).

Lors du broutage, le zooplancton a le potentiel d'affecter le cycle du Hg dans les écosystèmes de l'eau douce ainsi que son accumulation chez les organismes. Comme il a été montré dans une étude préliminaire concernant le lac Bédard (situé dans la forêt Montmorency, 80 km au nord de la ville de Québec), une différence dans les profils de la concentration de mercure total a été observée entre le jour et la nuit dans l'épilimnion (Figure 3; M. Amyot, Université de Montréal; communication personnelle). Cette différence a été interprétée comme étant due au comportement du broutage du zooplancton, car la variation dans les profils de mercure total a été détectée au moment approximatif de la remontée nocturne du zooplancton dans l'épilimnion. Les composés du mercure, situés dans le cytoplasme des algues ou fixés sur leur paroi par leurs exsudats (Mason et al., 1996; Leclerc et al., 2015), seraient ainsi libérés de façon directe par ce comportement. De plus, la libération de carbone organique dissous (COD) par le broutement de type 'sloppy feeding' (comportement alimentaire inefficace) et l'excrétion, a le potentiel d'affecter la spéciation des composés du Hg dans l'eau. Malheureusement, les analyses effectuées aux Lac Bédard n'avaient pas inclus la distribution verticale du zooplancton et ne permettent donc pas de tester cette hypothèse.

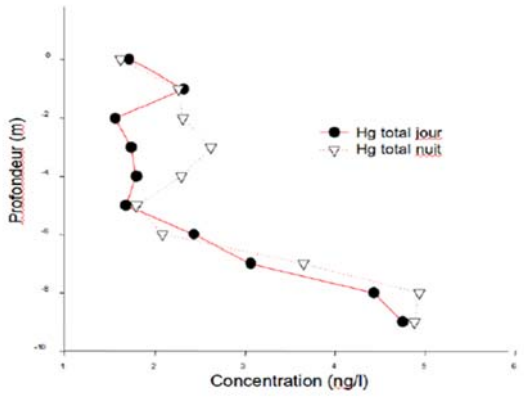

Figure 3. Observation de la différence de [Hg total] entre le jour et la nuit, Lac Bédard, 2002 (M. Amyot, Université de Montréal, données non publiées utilisées avec permission).

En considérant la stratification thermique dans la colonne d'eau, il existe des contraintes physiologiques et comportementales associées avec la capacité de la bioaccumulation de contaminants chez les individus (Tsui et Wang, 2004). Le Jeune et al. (2012), par exemple, ont montré que la capacité de bioaccumulation de MeHg dans les lacs boréaux varie en fonction du mode de vie chez des espèces de *Chaoborus*, avec des concentrations moindres de MeHg retrouvées chez les espèces migratrices, qui subissent une grande variation de température durant la DVM, comparé avec les espèces sédentaires, qui restent constamment à la surface d'eau durant l'été (Figure 4). Cependant, les études réalisées par Watkins et Simkiss (1988a, b) en laboratoire dans des conditions contrôlées, ont montré une accumulation plus élevée d'éléments traces métalliques essentiels, tels que le zinc (Zn), chez *Mytilus edulis* exposés à une température oscillante par rapport à des traitements à température constante (Figure 5). En plus de ces informations rares et contradictoires, il n'est pas clair si l'oscillation des températures pourrait affecter différemment l'accumulation des polluants inorganiques par rapport aux polluants organométalliques (p. ex., Hg inorganique et MeHg). En outre, il n'est pas certain que des conditions de température oscillante auraient des effets similaires sur les différentes voies d'absorption des contaminants métalliques, telles que les voies trophiques et aqueuses (Kainz et Fisk., 2009).

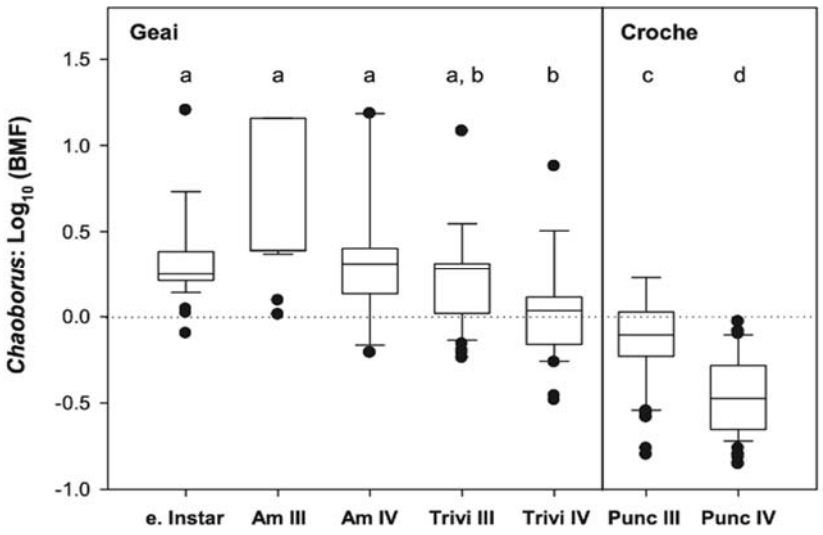

Figure 4. Facteur de biomagnification (angl. : *biomagnification factors*, BMFs; en $\log_{10}$) des larves de *Chaoborus* dans le lacs Geai et Croche à trois dates d'échantillonnage. Légende : e. Instar : premiers stades larvaires; III : stade III; IV : stade IV; Am : C. amer-canus (espèce

sédentaire, qui reste constamment à la surface à des températures relativement élevées); Trivi : C. trivittatus; Punc : C. punctipennis (ces deux dernières espèces subissent des fluctuations de température durant la migration verticale). (Tirée de Le Jeune et al., 2012.)

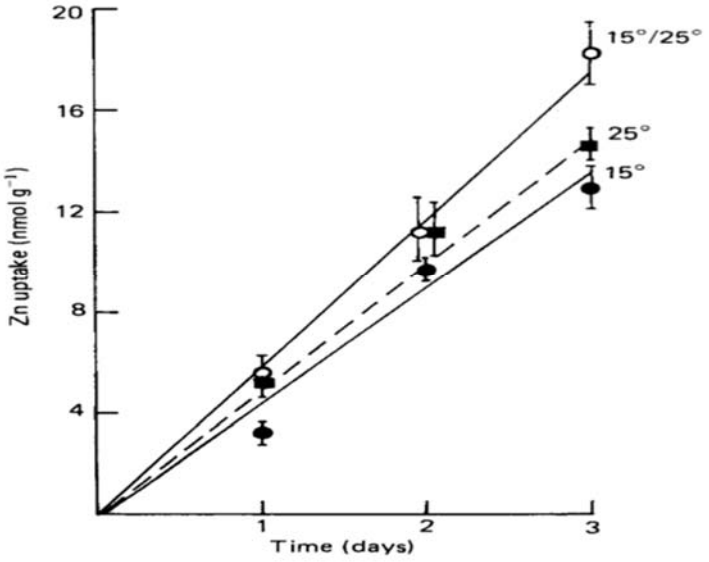

Figure 5. Effets de variations de température sur l'absorption de ^{65}Zn chez *Mytilus edulis*. (Tirée de Watkins et Simkiss, 1988b.)

Objectifs de recherche

Il existe encore des aspects méconnus du cycle du Hg dans les écosystèmes d'eau douce, en particulier concernant le rôle des consommateurs primaires et sa relation avec les producteurs primaires dans le transfert trophique de ces polluants remarquables. Le comportement du zooplancton n'a pas été pris en compte dans le paradigme du cycle de Hg dans les écosystèmes aquatiques, et son rôle pourrait être sous-estimé concernant le cycle biogéochimique de ces polluants dans les lacs.

Dans le **premier chapitre**, nous avons testé expérimentalement l'impact de l'efficacité de broutage du zooplancton ainsi que des processus d'excrétion/égestion sur les concentrations de métaux dans l'eau douce. Nous avons utilisé des algues enrichies avec des isotopes du Hg ($^{200}HgCl_2$, $Me^{198}HgCl$) comme source de nourriture et suivi le transfert de ces isotopes vers le milieu de culture durant le broutage. En parallèle, nous avons également exploré les effets potentiels sur le recyclage des principaux ions et

métaux, y compris certains métaux essentiels et non essentiels qui pourraient aider à suivre les effets du *sloppy feeding*. Pour mettre en évidence le rôle du comportement alimentaire, nous avons comparé un filtreur non sélectif (*Daphnia*) à un taxon de zooplancton sélectif (copépodes calanoïdes), ce dernier étant censé provoquer un effet *sloppy feeding* plus important par rapport au premier.

L'oscillation de la température est un autre élément qui n'a pas été pris en compte dans le paradigme actuel du cycle du Hg dans les écosystèmes aquatiques. Ce manque de connaissances peut biaiser les modèles présents sur le transfert trophique de ces polluants dans les lacs, et plusieurs chercheurs ont déjà souligné que les observations faites dans des conditions de température constante ne peuvent pas être appliquées pour prédire les effets en conditions naturelles (Hagstrum et Hagstrum 1970; Niehaus et al., 2011). Ainsi, dans le **deuxième chapitre**, nous avons réalisé des expériences en laboratoire pour étudier l'impact d'une température oscillante (7/23 ºC, 24 h/cycle) sur l'accumulation de Hg inorganique (IHg) et de monométhylmercure (MeHg) chez *Daphnia magna*, en la comparant à un traitement à une température constante ayant la même température moyenne (15 ºC). Les effets de la température moyenne ont été testés en comparant cette dernière à un traitement avec une température constante plus élevée (23 ºC). Les voies trophique et aqueuse ont été estimées en utilisant dans le premier car des *Chlorella* préalablement marquées avec des isotopes stables de Hg et en ajoutant directement des solutions d'isotopes de Hg dans les microcosmes dans le deuxième.

Enfin, dans le **troisième chapitre** nous avons réalisé une étude comparative afin d'établir un lien direct entre l'hétérogénéité des facteurs abiotiques (p. ex., température et pH) et biotiques (p. ex., phytoplancton et zooplancton) dans la colonne d'eau et les variations journalières des profils de Hg dans les lacs boréaux oligotrophes. Nous avons échantillonné quatre lacs boréaux (Table 1, Chapitre III) dans le Parc national de la Mauricie (Shawinigan, Québec), en tenant compte des caractéristiques contrastées, telles que la présence versus l'absence de poissons et la clarté de l'eau, qui pourraient avoir des effets importants sur l'hétérogénéité de la distribution du zooplancton dans la colonne d'eau (Ringelberg. 2009), augmentant ainsi la gamme d'hétérogénéité verticale au sein et entre les lacs d'étude.

CHAPITRE I

GRAZER-MEDIATED REGENERATION OF METHYLMERCURY, INORGANIC MERCURY, AND OTHER METALS IN FRESHWATER

Cet article a été publié dans le périodique *Science of the Total Environment*.
https://doi.org/10.1016/j.scitotenv.2022.154553

Fan Qin[1,2], Marc Amyot[2,3], Andrea Bertolo[1,2*]

[1] Centre de recherche sur les interactions bassins versants – écosystèmes aquatiques (RIVE) and Département des sciences de l'environnement, Université du Québec à Trois-Rivières, 3351 Boul. des Forges, C.P. 500, Trois-Rivières, QC G8Z 4M3, Canada

[2] Groupe de Recherche Interuniversitaire en Limnologie (GRIL), Université de Montréal, Campus MIL, C.P. 6128, Succ. Centre-ville, Montréal, QC H3C 3J7, Canada

[3] Département de sciences biologiques, Université de Montréal, Campus MIL, C.P. 6128, Succ. Centre-ville, Montréal, QC H3C 3J7, Canada

Abstract

Whereas it is well established that zooplankton can transfer various pollutants such as mercury (Hg) from primary producers to higher trophic levels, less is known on the effects of their activities on the recycling of Hg in aquatic ecosystems. This study tested experimentally the impact of zooplankton grazing efficiency and excretion/egestion processes on metal concentrations in freshwater. Isotopically labeled algae ($^{200}HgCl_2$, $Me^{198}HgCl$) were used as a food source and the transfer of the selected isotopes to the culture medium was followed during grazing. In parallel, this study also explored the recycling of major ions and metals, including selected essential and non-essential metals that could help to track the effects of sloppy feeding. To highlight the role of feeding behavior, this study compared a large filter-feeder (*Daphnia magna*) to a smaller selective feeder zooplankton taxon (calanoid copepods), with the latter being expected to cause more sloppy feeding than the former. The results of the experiments demonstrated that zooplankton grazing of both taxa significantly influenced the concentrations of the particulate portion of both inorganic Hg (IHg) and monomethylmercury (MeHg) in water. In contrast, only *Daphnia* significantly increased the concentration of dissolved IHg, whereas the concentration of dissolved MeHg was not affected by either grazer. The results also suggested that both taxa affected the concentrations of dissolved Fe, Zn, SO_4^{2-} and rare earth elements via sloppy feeding, whereas only *Daphnia* significantly increased the concentration of dissolved Cu via this mechanism. The effects of excretion/egestion were negligible except for dissolved IHg and Cu in *Daphnia* treatment. These results highlight a neglected pathway of IHg and MeHg recycling in the water column in freshwater ecosystems with potentially important consequences for trophic transfer.

Keywords: trace metal pollutants, metal regeneration, sloppy feeding, zooplankton grazing, *Daphnia*, calanoids

Introduction

Grazer-mediated elemental regeneration plays a crucial role in metal recycling and could have a significant impact on the functioning of aquatic ecosystems (Smetacek et al., 2004). For example, it has been shown that zooplankton grazing can have a substantial influence on iron (Fe) recycling in the ocean and contribute to the early spring phytoplankton bloom in Fe-deficient areas (Hutchins et al., 1993). A similar phenomenon has also been found in a large freshwater lake (Lake Erie), where it has been shown that zooplankton grazing on phytoplankton is responsible for the regeneration of trace metals such as cadmium (Cd) and zinc (Zn) (Twiss et al., 1996). Several laboratory studies have confirmed that zooplankton grazing activity is responsible for the release of almost all life-essential trace metals including Fe, Zn, copper (Cu), cobalt (Co), manganese (Mn), as well as some non-essential metals like lead (Pb) and silver (Ag) (Hutchins et al., 1994; 1995; Wang and Fisher, 1998; Xu and Wang, 2003). However, there is a lack of understanding of the exact mechanism by which zooplankton feeding behavior (e.g., sloppy feeding vs. excretion/egestion) affects these elements in small freshwater ecosystems. More notably, the effects of zooplankton grazing on trace metal pollutants are still poorly known, especially concerning inorganic mercury (IHg) and methylmercury (MeHg).

As a ubiquitous trace element, Hg can be found in all environmental compartments due to its volatility at room temperature and mobility in both water and the atmosphere. This element is of major concern at a global scale because of its massive release due to anthropogenic activities and its eventual deposition into aquatic ecosystems with potential consequences for human health (Stein et al., 1996; Ullrich et al., 2001; Jitaru et al., 2004). Generally, some freshwater lakes are considered as hotspots for the production of the highly toxic pollutant MeHg due to the activity of bacteria and archaea, such as sulfate-reducing bacteria (SRB), iron-reducing bacteria (IRB), and methanogens (Oremland et al., 1991; Choi et al., 1994; Ekstrom et al., 2003; Fleming et al., 2006). The produced MeHg, as well as IHg, can both be assimilated by phytoplankton from the surrounding water at the base of the aquatic food webs, and then transferred towards higher trophic levels (Morel et al., 1998). However, according to some studies, only a small fraction of

absorbed IHg (about 10% of total mass) is concentrated in the cytoplasm of phytoplankton relatively to the cell wall, whereas about 60% of absorbed MeHg is found in the cytoplasm (Mason et al., 1996, Wu and Wang, 2011). This distribution pattern of IHg and MeHg in primary producers may lead to a more efficient trophic transfer of MeHg to consumers, which is considered particularly toxic and a threat to human health, in addition to displaying high bioaccumulation and bioamplification potential in the food webs (Reinfelder and Fisher, 1991; Wang and Fisher, 1996). Although it is widely assumed that zooplankton plays a central role in the transfer of IHg and MeHg from primary producers to higher trophic levels, their feeding behavior on the recycling of Hg species in freshwater has been poorly studied (Le Faucheur et al., 2014; Branfireun et al., 2020).

The general perception of trophic transfer of Hg in the aquatic ecosystems is usually seen as being conservative, meaning that the standing stock of Hg (MeHg in particular) in the primary producers is fully exploited and bioaccumulated by consumers (Watras and Bloom, 1992; Westcott and Kalff, 1996; Al-Majed and Preston, 2000; Pickhardt et al., 2005). However, zooplankton feeding behavior may have the potential to decrease the trophic transfer efficiency of Hg species as shown for other trace elements in the aquatic ecosystems, for instance sloppy feeding, which is a process of importance in freshwater as in marine ecosystems (Williamson et al., 2007; Tang et al., 2010; Perhar et al., 2013; Bess et al., 2021). As a result, zooplankton grazing may change the daily dynamic of Hg concentration in the water column and modify certain parameters in the modeling of Hg recycling in freshwater ecosystems. This study addressed this issue here by comparing the relative roles of sloppy feeding and excretion/egestion of zooplankton. Moreover, this study tested if two zooplankton taxa can have different effects on Hg recycling when exposed to the same contaminated algae (5–10 µm *Chlorella vulgaris*) depending on their feeding mode. Thus, this study compared here relatively small-bodies calanoid copepods, which are known to be selective feeders able to handle and eventually grind particles (Schnack, 1989), to large-bodied *Daphnia,* which is expected to swallow *Chlorella* of this size without breaking the cells, with the former being expected to release more Hg by sloppy feeding than the latter (Sommer et al., 2001; Møller, 2005; Thorp and Covich, 2009).

In addition to Hg, which is at the core, this study expanded the approach by analyzing other potential tracers of sloppy feeding such as some selected essential (e.g., Fe, Zn, Cu) and non-essential metals (rare earth elements, REE) that could help to document the effects of zooplankton feeding behavior. Dissolved organic carbon (DOC) was also measured as another proxy of sloppy feeding, since phytoplankton cell lysis due to zooplankton grazing is expected to increase its concentration in the water (Hygum et al., 1997; Kamjunke and Zehrer, 1999; He and Wang, 2006). Similarly, trace elements such as essential and non-essential metals might follow the same fate as DOC. Furthermore, it is known that these trace metals play an important role in Hg recycling in aquatic ecosystems (Hodson, 1988; Deb and Fukushima, 1999; Mountouris et al., 2002; Ajitha et al., 2021). Thus, this study took the advantage of the work to compare the response of zooplankton grazing on Hg to that of other essential trace metals. REE were also included in the study in order to fill a gap of knowledge about their potential recycling in aquatic ecosystems and their behaviour in trophic networks. It only has limited knowledge about the ecological effects of these metals, which are increasingly used in many areas (e.g., agriculture, medicine, digital technologies, etc.) and are considered as emerging pollutants in aquatic ecosystems. Whereas most REE have similar chemical behaviors in aquatic systems (Gladilovich et al., 1988; Liu et al., 2018), cerium (Ce) has a distinctive redox chemistry; hence, the results are presented by separating Ce from the sum of all the other rare earth elements (hereafter ΣREE).

Based on these premises, a few hypotheses have been established for this study: i) zooplankton grazing releases IHg, MeHg, DOC, and other elements including various ions from freshwater phytoplankton, because of sloppy feeding. Regardless of the extra/intra cellular partitioning of IHg and MeHg in algae, it was expected that ii) more MeHg than IHg would be released during the experiment since it is anticipated that more MeHg than IHg is accumulated in the cytoplasm of phytoplankton relatively to the cell wall. Moreover, this study hypothesized that iii) the efficiency of elemental release (including IHg and MeHg) depends on zooplankton taxa because of their different feeding modes. More precisely, it was expected that calanoids would cause more release of

elements than *Daphnia* due to a higher sloppy feeding effect due to their smaller size and feeding behaviour.

Material and methods

Study design summary

A laboratory experiment was conducted under controlled conditions to study the effects of zooplankton grazing activity on the release of both inorganic (Hg^{2+}) and organic (MeHg) mercury in water by using freshwater phytoplankton (*Chlorella vulgaris*) cultivated in a medium enriched with Hg stable isotopes ($^{200}HgCl_2$, $Me^{198}HgCl$). This method allowed distinguishing spiked Hg sources from natural ones and to better track the dynamic of Hg during zooplankton grazing. Two crustacean taxa (calanoid copepods and *Daphnia magna*) with different size and feeding behaviors have been tested, with medium-sized calanoids (0.79 ± 0.05 mm) expected to have stronger sloppy feeding effects than large *Daphnia* (2.42 ± 0.55 mm). The aim of this study was twofold: first, to single out the effects of zooplankton grazing on Hg recycling due to "sloppy feeding" (i.e., the lysis of algal cells during the feeding process) (Lampert, 1978; Darchambeau et al., 2005), and second, to assess the combined effect of grazing and excretion/egestion on Hg recycling by taking the advantage of using traceable Hg forms (i.e., stable isotopes not found in measurable concentrations in the medium nor the zooplankton used here). Therefore, samples were taken both before (30 min) and after (1 to 3 h) the excretion/egestion processes fully took place. This allowed isolating the short-term effects of sloppy feeding before they sum up to that of the other processes potentially influencing the Hg concentration in the water.

Sampling and Hg stock solutions preparation

Glassware (beakers used as microcosms and mercury sampling bottles) was washed with a strong acid solution (50% HNO_3, 5%HCl, 45% ultrapure water) before the experiments. High-density polyethylene (HDPE) bottles for anion sampling and other

plastic instruments, including the filter holder (Thermo Scientific™ Nalgene™ reusable filter units) used for filtered water sampling, were first washed with 10% HCl solution overnight to remove trace elements, and then rinsed with ultrapure water before being dried under a laminar flow cabinet. Glass sampling bottles for dissolved organic carbon analysis and glass fiber filters for algae collection (1 µm, Cytiva Whatman™ binder-free glass microfiber filters, grade GF/B) were heated to 550 ºC in an oven for 3 hours before being used for experiments. Non-powdered latex gloves were worn all the time during experiments or manipulation with mercury spiked solutions.

Enriched inorganic ^{200}Hg and $Me^{198}Hg$ solutions ($^{200}HgCl_2$, $Me^{198}HgCl$, respectively) were purchased from Trace Sciences International Corp. Canada (#18b, 98.29%) and the National Research Council of Canada's (NRC) Metrology Research Centre (EMMS-1, 96.45%), respectively. Stock solutions were prepared with ultrapure water in the Chemical Laboratory of GRIL at the University of Montreal, with the final concentrations of 400 ng mL^{-1} for ^{200}Hg, and 107.5 ng mL^{-1} for $Me^{198}Hg$. Stock solutions were kept at 4 ºC before being used.

Algae culture and mercury spiking

A non-axenic strain of a green unicellular algae (CPCC 90 *Chlorella vulgaris*) bought from Canadian Phycological Culture Centre (CPCC); Toronto was used as food source for zooplankton. The initial inoculum was collected from a seed culture at the stationary phase with a density of 5 x 10^7 cells mL^{-1}. Cultures were grown in a 1 L glass bottle with 500 mL Bold Basal nutrient Medium (BBM) (Bischoff and Bold, 1963) made with demineralized water. They were agitated by using a magnetic stirrer to prevent the sedimentation of algae cells, under cool white lighting with a 12 h per day photoperiod and an intensity of 20 µmol photons m^{-2} sec^{-1} (Bourdeau, 2016). An aluminum cover with a downward beak opening was placed on top of the glass bottle to prevent airborne contamination (e.g., bacteria/protozoa) and to allow the air flux for the growth of algae. The temperature was maintained at 21 ºC, and the pH was measured on a weekly basis to

ensure the maintenance of *Chlorella* culture (BioBasic^{TM} pH/mV/^{o}C meters, accumet^{TM} AB15, Fisherbrand^{TM}).

Hg-contaminated algae were prepared one week before the experiments. An initial culture of 1 L with a density of 2.8 x 10^6 cells mL^{-1} was made with a modified BBM medium in which Cu, Zn and EDTA were not included. The lack of EDTA aims to minimize the chelation effects and maximize the uptake of spiked mercury, while the lack of Cu and Zn is to minimize the eventual toxicity in the absence of EDTA in the medium (Wang and Fisher, 1996) and to reduce the competition with mercury for the binding sites on algae (Le Faucheur et al., 2011). A preliminary growth test (without mercury) comparing modified and non-modified BBM medium showed similar densities within one cycle (7 days) on the growth of *Chlorella*, with a final density of 1.0 x 10^7 ± 8.4 x 10^4 cells mL^{-1} in the non-modified medium, and 1.2 x 10^7 ± 3.9 x 10^5 cells mL^{-1} in the modified medium. Cultures were spiked with both ^{200}Hg and Me^{198}Hg at the exponential phase, which corresponds to the third day of *Chlorella* growth. An aliquot of 0.7 mL of each mercury stock solution was added in the culture, with an initial nominal concentration of 280 ng L^{-1} for ^{200}Hg and 70 ng L^{-1} for Me^{198}Hg. The uptake of spiked mercury by *Chlorella* was monitored by following the concentrations of both ^{200}Hg and Me^{198}Hg in culture water and algae for four days until reaching the stationary phase. Samples for this investigation were taken with triplicates from three different cultures at 15 min, 1 h, 3 h, 6 h, 24 h, 48 h, 96 h, and 120 h after the spiking. The Hg-contaminated *Chlorella* used for the grazing experiment was collected on the seventh day of growth when the stationary phase was reached. A subsample of *Chlorella* was collected at the same time to analyze the background concentrations of inorganic ^{200}Hg and Me^{198}Hg in Hg-contaminated algae. Due to the required minimal biomass for total Hg and MeHg analysis, no other analysis (e.g., ICP MS/MS for other trace metals) was carried out on *Chlorella*. The remaining cultures were centrifuged (Sorvall ST 16 Centrifuge, ThermoFisher Sci.) for 5 min under 23 ^{o}C with a radical centrifugal acceleration of 4000 *g*. This process has been repeated threefold, during which algae were rinsed twice with filtered lake water (0.2 µm mesh size, Alphonse Lake, La Mauricie National Park of Canada) to remove aqueous mercury.

Zooplankton

Copepods were collected ten days before the experiments from Alphonse Lake in La Mauricie National Park of Canada (Shawinigan, Québec) during the summer of 2018. The lake had a pH of about 6.2 and a concentration of dissolved organic carbon around 4.1 mg L^{-1} at the time of collection. Zooplankton were collected at the deepest location (46 ° 45'46.8"N, 72 ° 59'47.5"W) by using a 30 L Schindler-Patalas trap (63 µm mesh size). Lake water was collected at the same time by using a 2 L Van Dorn bottle. Only calanoid copepods were kept after identification with a binocular microscope in the laboratory. *Daphnia magna* monoclonal cultures were established in the laboratory for more than one year. The original cultures came from CEAEQ (Centre d'Expertise en Analyse Environnementale du Québec, Québec City, Canada). All zooplankton cultures were kept in filtered lake water (63 µm mesh size) under room temperature (21 ºC) with a photoperiod simulating local summer light cycles (16 h light: 8 h dark), and pH was measured once a week. They were fed on *Chlorella* with a cell density of 10^6 mL^{-1} per day. The water of cultures was renewed twice a week manually, with 1/3 of culture water replaced with freshly filtered lake water. The calculated size ratios between zooplankton and *Chlorella* were around 110 for calanoids/*Chlorella*, and 340 for *Daphnia*/*Chlorella.*

Experimental design

The randomized experiment included two zooplankton grazing treatments and a control with only Hg-contaminated algae followed in time (15 microcosms in each treatment). In order to avoid pseudoreplication (Hurlbert, 1984), each treatment had independent triplicates for each time step. Therefore, each microcosm was sampled only once. This design allowed us to compare the effects of two different types of grazers (see below) on metal release over a 3 h period (Quinn and Keough, 2012a). All experiments were performed in dark conditions. Before the experiment, the lake water was filtered with a mesh size of 0.2 µm (MilliporeSigma™ Isopore™ polycarbonate membrane filters) to remove some colloids and most bacteria. Microcosms were first filled with 380 mL of filtered lake water, then Hg-contaminated algae were added with a final cell density of about 2.5 x 10^5 mL^{-1} following Lampert (2011). All microcosms were kept in the dark for

3 hours of equilibrium after adding Hg-contaminated algae (He and Wang 2006). Three extra microcosms were sampled at the end of this period and were presented as time 0 before adding zooplankton. Zooplankters were individually picked up from the culture water, washed in clean filtered lake water in a 50 mL acid-washed plastic container, then transferred to a bottle filled with 70 mL fresh filtered lake water. They were left without food for 3 hours and then added to the microcosms. Zooplankton density was adjusted to those observed in the sampled lakes (1 zooplankton versus 10 to 15 mL water). Water samples were taken at the time of 30, 60, 90, 120, and 180 min after adding zooplankton. The first sampling time of 30 min corresponds to the time used for the food to pass through the digestive system of *Daphnia* (Lampert, 2011). For calanoids, some researchers found this period was 20 min for large marine calanoids (*Calanus spp*., Møller et al., 2003), while a period of 30 min has also been reported for other marine calanoids (*Acartia tonsa, A. hudsonica,* and *Temora longicornis*, Reinfelder and Fisher, 1991). Therefore, the first sampling event was considered to capture almost only sloppy feeding effects without the influence of excretion/egestion. The subsequent samplings, extending up to 3 h, represented the combined effects of grazing and excretion/egestion of zooplankton on elements release in water. *Daphnia* was picked out individually from the microcosms before each sampling by using an acid-washed plastic pipette. In contrast, it has not been possible to collect calanoids individually from the microcosm due to their relatively smaller body size and fast mobility in response towards the pipette. They were visually checked in the microcosms and were collected by the filter (see below) during the water sampling and were stored with filters together in the freezer at -20 ºC. No zooplankton mortality was observed during the experiment. At each sampling time, the water was transferred from the microcosms to a 500 mL acid-washed glass beaker. Then, 120 mL unfiltered water was collected for total ^{200}Hg and total $Me^{198}Hg$ analysis, and 50 mL was transferred in a plastic bottle for pH and temperature measurement. The rest of the water was filtered at a mesh size of 0.4 μm (MilliporeSigma™ Isopore™ polycarbonate membrane filters) with the help of a central vacuum system (vacuum pressure was less than 4.87 psi). The filter holder was washed with ultrapure water and dried with kimwipes between each sampling. 120 mL filtered water was collected for dissolved ^{200}Hg and dissolved $Me^{198}Hg$ analysis, 30 mL for dissolved organic carbon,

15 mL for cations, and 15 mL for anions. Mercury water samples were preserved with 0.5 mL high purity HCl (Hydrochloric acid 32–35%, OmniTrace Ultra™ for trace metal analysis, VWR), while dissolved organic carbon water samples were preserved with 30 µL high purity HCl. Cation samples were preserved with 0.3 mL high purity HNO_3 (Nitric acid 67–70%, OmniTrace Ultra™ for trace metal analysis, VWR). All water samples were stocked in a cold chamber at 4 °C until chemical analysis.

Chemical analysis of mercury

Total mercury

Samples were analyzed according to the method EPA 1631 (Environmental Protection Agency, USA). For total Hg in aqueous samples, a 20 mL water sample was placed in an analysis tube. Then, 100 µL BrCl (full strength 100%) was added to the tube and mixed well for digestion overnight. The following day, 25 µL hydroxylamine hydrochloride (30% m/v), 25 µL isopropanol, and 60 µL $SnCl_2$ (20% m/v) were sequentially added to the analysis tube, then mixed well before being quantified with a Tekran 2600 Automated Sample Analysis System cold vapour atomic fluorescence spectrometer (Tekran® Instrument Corp. Canada). A total of 50 analysis tubes were prepared and separated into 5 sample sets during the quantification. The quality control of the analysis was carried out by intercalibrations with the Canadian Association for Laboratory Accreditation (CALA, Ottawa, Canada) using certified inorganic Hg solution (SPC Sciences, Montreal, Canada) with a recovery > 90%. The concentrations of ^{200}Hg isotopes were obtained by coupling the Tekran 2600 with an inductively coupled plasma mass spectrometer (8900 Triple Quadrupole ICP-MS/MS, Agilent, USA). The final results of spiked ^{200}Hg concentrations were obtained with a matrix calculation based on the concentrations of three detected mercury isotopes (^{198}Hg, ^{200}Hg, and ^{202}Hg), where the detected concentration of ^{202}Hg was used as an environmental baseline (Hintelmann and Ogrinc, 2003).

Samples of *Chlorella* for Hg analysis were collected with glass fiber filters. The samples were lyophilized overnight in a freeze dryer (Labconco™ FreeZone Freeze

Dry System, USA), then they were weighed before chemical digestion for total Hg quantification. The weighed sample was firstly added in a Teflon tube with 3 mL high purity HNO_3, then heated in a microwave oven (CEM Corporation MARS 5 Digestion Microwave System, USA) for 10 min at 170 ºC for the digestion. Subsequently, 1 mL of high purity HCl was added into the digestion Teflon tube and left alone for 30 min reaction. The final solution was collected in a metal-free tube (Metal-Free Centrifuge Tubes, Polypropylene, Sterile, VWR®). The volume of the collected solution was adjusted to 15 mL with ultrapure water, then 1 mL of adjusted solution was diluted in 19 mL ultrapure water in an analysis tube. Afterward, 25 µL hydroxylamine hydrochloride, 25 µL isopropanol, and 60 µL $SnCl_2$ were sequentially added, mixed well before the quantification of total Hg and ^{200}Hg by Tekran 2600 coupled with triple quadrupole ICP-MS/MS. Intercalibrations with CALA were used for the quality control of the analysis (see above).

Methylmercury

Samples were analyzed according to the method EPA 1630 (Environmental Protection Agency, USA). For aqueous samples, a 45 mL water sample with 5 mL ultrapure water was added in a Teflon tube, then placed in the heater of a distillation module and heated to 130 ºC for about 3 hours until the recipient Teflon tube in the chiller part recovered 45 mL of vaporized sample water. Next, 30 µL of ascorbic acid was added to the recipient Teflon tube, mixed well, and left for 5 min for the chemical reaction. Subsequently, 30 mL of sample water was transferred to an analysis tube. Afterward, 0.25 mL acetate buffer and 40 µL $NaB(Et)_4$ solution (4% m/v) were sequentially added to the analysis tube and mixed well. Then it was left aside for 15 min and allowed the derivatization reaction to take place before the quantification. In total, 28 water samples were prepared together with 1 blank and 1 certified sample (Tort-2, 152 ng g^{-1} MeHg, National Research Council of Canada) for each quantification with a Tekran 2700 Automated Methyl Mercury Analysis System (Tekran® Instrument Corp. Canada). The quality control of the analysis was carried out by the recovery of certified sample (> 90%). The detection of $Me^{198}Hg$ isotopes was performed by coupling the Tekran 2700

with triple quadrupole ICP-MS/MS. The final concentrations of spiked $Me^{198}Hg$ were calculated by using the same matrix calculation as for ^{200}Hg, with the $Me^{202}Hg$ concentration served as the environmental baseline.

Lyophilized *Chlorella* sample was used for MeHg analysis. After weighing, the sample was placed in a Teflon tube with 5 mL high purity HNO_3 and put in an oven at 65 ºC overnight. The following day, the solution was collected in a metal-free tube and adjusted to 15 mL with ultrapure water. An aliquot of 50 µL of the final solution was diluted with 30 mL ultrapure water in an analysis tube, then 20 µL of ascorbic acid, 0.25 mL acetate buffer and, 40 µL $NaB(Et)_4$ solution were successively added to the analysis tube and mixed well before the quantification by Tekran 2700 coupled with triple quadrupole ICP-MS/MS. Certified samples were used for the quality control of the analysis (see above).

The methods (EPA 1630, 1631) used to measure IHg and MeHg in the particulate phase did not extract all Hg internalized in undamaged *Chlorella* cells. Rather, it extracted Hg species loosely bound to particles (likely including Hg adsorbed to undamaged algal surfaces or organelles from broken cells). Therefore, here this loosely bound fraction was considered as composed mainly by easily exchangeable Hg species. It likely represents the fraction of particulate Hg that could be accessible for uptake by zooplankton, since it has been shown that zooplankton only accesses soluble Hg and not Hg strongly bound to the membrane, during algal uptake (Morel et al. 1998). The concentration of particulate IHg and MeHg was calculated by the difference between the analyzed concentrations of total and dissolved phase.

Finally, the percentages of IHg and MeHg in water liberated by zooplankton sloppy feeding were estimated as following:

$$Hg\% = ((B-C) / A)*100$$

where A is the average amount (in ng) of IHg or MeHg introduced into the microcosm by Hg-contaminated algae, B is the quantity of the same elements in the water of each

zooplankton microcosm (both *Daphnia* and calanoids treatments) after 30 min and C is their average quantity in the water of the control after 30 min.

Statistical analysis

Given that true replicates were set to follow the different treatments over time, a two-way ANOVA has been performed with the statistical computing software R to analyze the effects of grazer type, sampling time, and their interaction (independent variables) on selected chemical variables, such as the concentrations of IHg, MeHg (both dissolved and particulate forms), anions, cations, and DOC (dependent variables). Time 0 was not included in the statistical analysis since only a sub-sample of the microcosms was measured at that time based on the assumption that no effect of grazing was possible before the introduction of the zooplankton. The goal of this analysis is to explain the variation in the dependent variable that can be attributed to the variation in the explanatory variables and to quantify the strength of the relationship between these two types of variables. Sampling time was modeled as either continuous ($time_{cnt}$) or categorical ($time_{cat}$) to potentially account, respectively, for linear or eventual non-linear temporal effects. To assess if adding the interaction term and if treating time as categorical improved the fit of the models, the fit of different established models was compared *a priori*. Therefore, for each dependent variable, the following models were built:

1) Additive models

   M1: $treatment + time_{cnt} + \varepsilon$
   M2: $treatment + time_{cat} + \varepsilon$

2) Interactive models

   M3: $treatment + time_{cnt} + treatment*time_{cnt} + \varepsilon$
   M4: $treatment + time_{cat} + treatment*time_{cat} + \varepsilon$

where ε is a general error term. For each dependent variable, the models *M1-M4* were built and their fit was compared to select the best model. Model selection was based on the Akaike information criterion (AIC) with the smallest AIC value representing the best

model among a given set of models (Quinn and Keough, 2002b). When the difference between two competing models was smaller than 2 ($\Delta AIC = AIC_{observed} - AIC_{smallest} < 2$), indicating that the two models are near equivalents in terms of fit, a parsimony criterion was used in the selection of the best model, by retaining the model with fewer parameters. Planned contrasts between pairs of treatments (control versus calanoids, control versus *Daphnia*, calanoids versus *Daphnia*) were applied after the model selection with post-hoc pairwise comparisons to assess the treatment effects at each step of sampling time. In the results section, the model selection were presented firstly for each variable, and subsequently, the details about the selected model were given, and finally the comparison of the treatments at each step of sampling time was offered. To assess the statistical significance of the models, an overall alpha level of 0.05 was used, and the Holm-Bonferroni correction was used for multiple testing in the case of planned contrasts.

Principal component analysis (PCA) was used to summarize the relationship between treatments and the main variables (Hg species). Given that some extra variables were also taken into account here (see above), PCA was used to summarize their relationship with treatments and the main variables.

Results

Hg uptake by Chlorella vulgaris

Fast uptake of both inorganic ^{200}Hg and $Me^{198}Hg$ by *Chlorella* was detected during the first 15 min after spiking, with an increase of concentrations in algae cells from nearly 0 to 1750 ng g^{-1} for inorganic ^{200}Hg, and 0 to 800 ng g^{-1} for $Me^{198}Hg$ (Fig. S1). The concentration of inorganic ^{200}Hg in *Chlorella* cells reached a peak at 3250 ng g^{-1} after 3 h, whereas the highest concentration of $Me^{198}Hg$ likely appeared between 6 h and 24 h at about 1000 ng g^{-1}. After this period, a decrease was observed in the concentrations of both inorganic ^{200}Hg and $Me^{198}Hg$. At 15 min, only 36 ± 12% of spiked inorganic ^{200}Hg was accumulated in *Chlorella*, while about 59 ± 6% of spiked $Me^{198}Hg$ was accumulated at the same time. When the stationary phase was reached, 55 ± 8% of spiked

inorganic ^{200}Hg was present in algae cells, whereas about 70 ± 3% of spiked $Me^{198}Hg$ was accumulated in *Chlorella*. The quantity of inorganic ^{200}Hg and $Me^{198}Hg$ introduced by harvested *Chlorella* into the grazing experiment was 3.14 ± 0.26 ng and 1.09 ± 0.03 ng per microcosm, respectively (Fig. S1).

Inorganic Hg and MeHg

Particulate portion

To evaluate the effects of zooplankton grazing on the particulate portion of inorganic ^{200}Hg, the selected model included the interaction term between treatment and time (treated as categorical) (*M4*, Tables S1). The selected model was significant (*p-value* < 0.05) and explained 63% of the variation in the data (Table 1). In this model, time was not significantly related to the dependent variable, whereas the effects of both treatments and their interactions with time were significant. Post-hoc comparisons showed significant differences between pairs of treatments at both 30 and 60 min, but not afterward (Table S2). More precisely, i) at 30 min, the calanoids treatment resulted in significantly higher concentrations of particulate inorganic ^{200}Hg than both *Daphnia* and the control, but no significant difference was found between *Daphnia* and the control, whereas ii) at 60 min, though only the calanoids treatment demonstrated significant effects on the dependant variable with higher concentrations than the control, treatments of the calanoids and *Daphnia* were not significantly different one from the other (Table S2, Fig. 1A). The concentrations of particulate inorganic ^{200}Hg peaked at 30 min in the calanoids treatment and 60 min in *Daphnia* treatment, and then both gradually decreased to a level similar to the concentrations in the control treatment (Fig. 1A).

For the particulate portion of $Me^{198}Hg$, the selected model included the interaction term between treatment and time (treated as continuous) (*M3*, Table S1). The selected model was significant (*p-value* < 0.05) and explained 37% of the variation in the data (Table 1). In this model, time was not significantly related to the dependent variable, whereas treatment and its interaction with time were significant. More precisely, as showed by post-hoc comparisons, i) at 30 min, both zooplankton treatments showed

significantly higher concentrations of particulate $Me^{198}Hg$ compared to the control; ii) at 60 min, only the calanoids treatment demonstrated significant effects with higher concentrations compared to the control, whereas no significant difference was found between *Daphnia* and the control (Table S2); iii) the concentration of particulate $Me^{198}Hg$ peaked at 30 min for both zooplankton treatments, and then both decreased gradually, with no significant differences among the treatments between 90 and 120 min (Fig. 1B); iv) at 180 min, *Daphnia* showed significant effects on the particulate $Me^{198}Hg$ with lower concentrations compared to the calanoids and the control treatments, but no significant difference was found between the calanoids treatment and the control (Fig. 1B, Table S2).

The estimated percentages of particulate portion of inorganic ^{200}Hg liberated after 30 min were 8.5 ± 0.4% and 2.1 ± 0.4% for the calanoids and *Daphnia* treatments, respectively. The estimated percentages of particulate portion of $Me^{198}Hg$ liberated after 30 min were 2.3 ± 0.6% and 3.8 ± 0.8% for the calanoids and *Daphnia* treatments, respectively.

Dissolved portion

To assess the impact of zooplankton grazing on dissolved inorganic ^{200}Hg concentrations, the selected model included only additive terms with time treated as continuous (*M1*, Table S1). The model was significant (*p-value* < 0.05) and explained 25% of the variation in the data (Table 1). In this model, whereas time was not significantly related to the dependent variable, the treatment effect was significant. More specifically, *Daphnia* showed a consistent impact throughout the whole duration of the experiment, as shown by post-hoc comparisons, with higher concentrations of dissolved inorganic ^{200}Hg compared to the control treatment (Table S2). In contrast, no difference was observed between the calanoids treatment and the control (Fig. 1C, Table S2).

For dissolved $Me^{198}Hg$, the same model as for dissolved ^{200}Hg was selected as the best but was not significant (*M1*, Fig. 1D, Table 1; S1). No effect of zooplankton grazing was detected.

The estimated percentages of dissolved portion of inorganic ^{200}Hg liberated after 30 min were 0% and 1.9 ± 0.7% for the calanoids and *Daphnia* treatments, respectively. The estimated percentages of dissolved portion of $Me^{198}Hg$ liberated after 30 min were 0% for both the calanoids and *Daphnia* treatments.

Additional water variables

DOC and pH

For DOC, the selected model included the interaction term between treatment and time (treated as categorical) (*M4*, Table S1). This model was significant (*p-value* < 0.05) and explained 63% of the variation in the data, with all the terms included being significant (Table 1.1). Post-hoc comparisons showed significant differences between treatments only at 30 min (Table S2; Fig. 2). More precisely, at 30 min, though only *Daphnia* showed significant effect on the dependant variable, the concentration of DOC in both zooplankton treatments was lower compared to the control, with the lowest value found in *Daphnia* followed by the calanoids treatment. After 30 min, all the treatments showed similar levels (Fig. 2, Table S2).

For pH, the model included only additive terms with time treated as continuous was selected as the best but was not significant (*M1*, Fig. 2, Table 1; S1).

Major anion, cations, and rare-earth elements

The effects of zooplankton grazing were varied depending on the ions in the dissolved phase. For SO_4^{2-} ($R^2_{adj} = 0.73$), Fe ($R^2_{adj} = 0.94$) and Zn ($R^2_{adj} = 0.70$), the model including the interaction term between treatment and time (treated as categorical) has been selected (*M4*, Table S1). The selected models were significant (*p-value* < 0.05) in all cases

and explained from 70% to 94% of the variation in the data depending on the dependent variable, with all the terms included being significant (Table 1). More precisely, at 30 min, the concentrations were significantly higher in both zooplankton treatments compared to the control in all cases, with the highest values found in *Daphnia* followed by the calanoids treatment, as shown by post-hoc comparisons (Fig. 2, Table S2). In the following samplings, the differences between the zooplankton treatments and the control were reduced, with some differences depending on the analyzed variable: i) for SO_4^{2-}, only *Daphnia* showed significant effect with higher concentrations compared to the control at 90 min and 120 min, but no difference was found between the calanoids treatment and the control at the same time (Fig. 2, Table S2). In contrast, ii) for Fe, both zooplankton treatments showed significant effects with higher concentrations compared to the control at 90 min (Fig. 2, Table S2); and iii) no significant differences were found in paired treatments in the following sampling for Zn (Fig. 2, Table S2).

For Cu, the selected model included only additive terms with time treated as categorical (*M2*, Table S1). The selected model was significant (*p-value* < 0.05) and explained 43% variation in the data (Table 1). In this model, time was not significantly related to the dependent variable, whereas treatment resulted to be significant. More precisely, *Daphnia* showed a consistent impact throughout the whole duration of the experiment, as showed by post-hoc comparisons, with higher concentrations of Cu compared to the control treatment, whereas no difference was observed between the calanoids treatment and the control (Fig. 2, Table S2).

Different treatments effects have been observed for rare earth elements in dissolved phase. For ΣREE (calculated as the sum of Y, Eu, La, Pr, Nd and Yb, based on the validated detection of triple quadrupole ICP-MS/MS), the selected model included the interaction term between treatment and time (treated as categorical). The model was significant (*p-value* < 0.05) and explained 59% of the variation in the data, with all the terms included being significant (Table 1). At 30 min, significantly higher concentrations were found in *Daphnia* treatment followed by the calanoids treatment compared to the control. No significant variation was found between zooplankton treatments and control

in the following samplings, as shown by post-hoc comparisons (Fig. 2, Table S2). In contrast, For Ce, the selected model included only additive terms with time treated as continuous (*M1*, Table S1). The model was significant (*p-value* < 0.05) and explained 32% of the variation in the data (Table 1). In this model, time was not significantly related to the dependent variable, whereas treatment resulted to be significant. Both zooplankton treatments showed significant effects with lower concentrations compared to the control, as shown by post-hoc comparisons (Table S2). Whereas no significant effect of time was found for Ce, its concentration in *Daphnia* treatment showed a monotonical tendency to decrease, whereas in the calanoids treatment the concentration peaked at 120 min (Fig. 2).

Multivariate relationships between water chemistry and zooplankton activities

The summarized relationship between zooplankton treatments and the concentrations of IHg and MeHg in different phases in water is presented as Fig. 3A. The first two axes of the PCA with only Hg variables explained together 83.5% variation (66.3% and 17.2% by Axis 1 and 2, respectively) in the data (Fig. 3A). On the ordination biplot, Axis 1 roughly separated the two zooplankton treatments, whereas Axis 2 separated samples of both zooplankton treatments from the control (Fig. 3A). More precisely, samples from the *Daphnia* treatment clustered towards the right side of the first axis, whereas samples from the calanoids treatment clustered on its left side (Fig. 3A). Both dissolved forms of Hg (inorganic ^{200}Hg and Me^{198}Hg) clustered on the upper right side of the graph and correlated with the grouping of samples from *Daphnia* treatment. In contrast, both particulate forms of Hg clustered on the upper left side of the biplot and correlated with the calanoids treatment. Among the four Hg variables, both dissolved forms (inorganic ^{200}Hg and Me^{198}Hg) contributed the most to the explained variation in the data and the separation of samples by zooplankton taxa (Fig. 3A). In contrast, dissolved and particulate inorganic ^{200}Hg contributed the most to the separation of samples between zooplankton and control treatments (Fig. 3A).

When the other measured variables were included in the analysis, the first two axes of the PCA explained together 51.7% variation (35.6% and 16.1%, respectively)

in the data (Fig. 3B). The ordination biplot showed that Axis 1 roughly separated the zooplankton treatments from the control, whereas Axis 2 better separated the two zooplankton treatments (Fig. 3B). More precisely, samples from *Daphnia* treatment clustered in the lower right part of the graph, whereas most samples from the treatment of calanoids clustered in the upper left side of the graphic. Most variables (including the four Hg variables) were found on the right side of the graph and correlated with most zooplankton samples (Fig. 3B). Among these variables, those from filtered samples (dissolved elements; including all anions, most cations, REE, and dissolved inorganic ^{200}Hg and $Me^{198}Hg$) correlated with *Daphnia* treatment and contributed the most to the explained variation in the data. In contrast, all variables from non-filtered samples (particulate inorganic ^{200}Hg and $Me^{198}Hg$) correlated more with either the calanoids treatment or the control, as both treatments clustered closely (Fig. 3B).

Discussion

Grazing effects on the elemental release

The results of this study show clearly that zooplankton grazing is a potential driver for the concentration of Hg in freshwater, but that its impact depends on both zooplankton taxon and Hg species with *Daphnia* having in some cases unexpected stronger effects than calanoids. For example, higher concentrations of dissolved IHg were associated with *Daphnia* relatively to both the calanoids and the control treatments, whereas calanoids were associated with short-term increases in both particulate IHg and MeHg. In addition, the results show that zooplankton grazing could affect the concentration of other trace metals, either via sloppy feeding or via excretion/egestion, with potential consequences on the functioning of freshwater ecosystems.

In contrast with most of the trace metals, the results of DOC from the experiments did not support the predictions based on the sloppy feeding hypothesis, as it was expected an increase of DOC concentrations in zooplankton treatments due to the grazing. The concentrations at 30 min were significantly lower in zooplankton treatments

compared to the control, which rules out the effects of the metabolism of the living organisms on DOC release in the experiments. This unexpected finding is probably due to a more efficient grazing by zooplankton than expected during the first 30 min that resulted in fewer algae presented in water and less release of DOC, especially after a long period of fasting (Enright, 1977; Lampert, 2011). On the other side, the results about calanoids are in accordance with the observations from previous studies that suggested that a predator/prey size ratio threshold lower than 55 is necessary for copepods to have a significant impact on DOC in water (Moller 2005), which is much smaller than the ratio used in the experiment (i.e., 110). The concentrations in the control treatments decreased after 30 min and thereafter were maintained as a lower plateau during the following period of the experiments. Although the DOC concentration has been stabilized for 3 h in microcosms before the grazing experiments, the newly added 70 mL filtered lake water at the end of this period may trigger a short period of equilibrium (He and Wang, 2006). The addition of zooplankton likely helped to shorten the equilibrium period for the concentrations of DOC to less than 30 min.

Whereas the results on DOC did not support that sloppy feeding hypothesis, the findings on trace metals suggested that there was indeed sloppy feeding occurring during the experiments. First of all, for both particulate IHg and MeHg, higher concentrations were observed in zooplankton treatments compared to the control, especially at 30 min when the effect of sloppy feeding was not yet confounded by zooplankton excretion/egestion. The release of particulate IHg was more efficient in the calanoids than in *Daphnia* treatment probably due to its feeding behavior. The lack of effect of *Daphnia* on particulate IHg is unsurprising given by the feeding mode of this taxon because most of this element entered the dissolved phase (see discussion below). Higher concentrations of particulate MeHg in *Daphnia* compared to the calanoids treatment at 30 min are probably related to the different sizes of individuals used in the experiments, with *Daphnia* being about three-fold larger than calanoids. After 30 min, the observed decrease of the concentrations of particulate IHg and MeHg in both zooplankton treatments was possibly due to the re-ingestion of the particulate organic matter (POM) bound with IHg or MeHg generated during zooplankton grazing. Especially

for particulate MeHg, the concentrations were significantly lower in the last sampling of the *Daphnia* treatment compared to the control (Fig. 1B, Table S2). The results on dissolved IHg were in accordance with the initial hypothesis since higher concentrations have been observed in zooplankton treatment compared to the control. However, the *Daphnia* treatment showed higher concentrations of IHg compared to the calanoids treatment during the complete duration of the experiments, which is in contrast to the initial hypothesis, as it was expected a stronger release by calanoids due to the presence of cutting edges with grinding teeth on their mouthparts (Schnack 1989). Whereas this result might be due to the difference in size between the two zooplankton taxa used in the experiment, it could also be explained by different feeding behaviors. Furthermore, the sloppy feeding effect was expected to decrease over time as the number of algae cells decreased due to zooplankton grazing in the microcosms. However, the constant higher concentrations of dissolved IHg in *Daphnia* treatment indicated a significant contribution of excretion/egestion after 30 min and contributed to the observed pattern of this variable (Fig. 1C). Moreover, it is well known that calanoids can potentially tear off the food particles due to the grinding teeth on the mandibles, but IHg may still be attached to the produced detritus and not entered the dissolved phase. The findings on dissolved MeHg were not in accordance with the initial sloppy feeding hypothesis based on zooplankton feeding mode, as no variation was observed between zooplankton treatments and the control. As there was no control for the re-uptake or re-adsorption of dissolved Hg species during the feeding trials, it cannot exclude that this unexpected result might be due to the high absorption of dissolved MeHg in water by living organisms (e.g., algae/bacteria), or the fast adsorption on POM generated during the grazing, especially the POM with the strong affinity function group thiol (-SH). Indeed, it was observed in the *Chlorella* culture that nearly 60% of spiked dissolved MeHg has been uptake within 15 min after the spiking (Fig. S1B; Moye et al., 2002, Gorski et al., 2006). However, zooplankton might not contribute as significantly as algae to uptake dissolved MeHg directly from water, as Tsui et al. (2004) demonstrated that the uptake of MeHg by *Daphnia* was proportional to the ambient concentrations, especially under the concentrations in the experiments that are close to the environmentally realistic conditions (Lange et al., 1993; Harris et al., 2007; Simonin et al., 2008; Emmerton et al., 2018). In contrast, the reabsorption by

algal/bacteria of dissolved IHg in zooplankton treatments was not expected to have greatly affected the conclusions, at least for *Daphnia*. In the presence of this taxon, significantly more dissolved IHg concentrations was in fact observed than in the control, meaning that the grazing effect on this variable was stronger than the eventual effects of reabsorption by algae/bacteria, if any. In the case of calanoids, it cannot exclude that this mechanism might mask the effects of grazing, since no significant difference between this treatment and the control for the concentrations of dissolved IHg. In conclusion, whereas it cannot estimate the contribution of this mechanism in the outcome of the experiments, it can assume that the results are conservative and show a clear pattern for at least one taxon.

Evidence to support the sloppy feeding hypothesis on metal release has also been found by comparing the analyzed results from the control treatment with the predicted mass of IHg and MeHg introduced into the experiment (Fig. 1; S1). The IHg and MeHg introduced by *Chlorella* into the experiment were considered all in the particulate phase and expected to be analyzed efficiently with the conventional methods for water samples that contain mercury (US EPA 1630 and 1631). However, the extraction efficiency was greatly reduced with the presence of algae in water samples from the control treatment. About 23.8% and 27.1% of IHg and MeHg have been measured, respectively, by using the conventional method compared to the one using a more aggressive sample extraction. A great portion of IHg and MeHg seems to be internalized in the algae cells and cannot be extracted with the usual methods. Nevertheless, these unexpected results remain informative on the extra/intra cellular partitioning of IHg and MeHg in algae. Conversely, in zooplankton treatments, the grazing likely increased the lysis of algae cells and the extraction of IHg and MeHg from water sample that can have easily exchanged with water. The amounts (in ng) of IHg and total MeHg that were introduced in the experimental flasks when adding Hg-contaminated algae were father compared to those measured in the water at 30 min in the different treatments. Up to 9% more IHg and 4% more MeHg were found in the particulate fraction in treatments with grazers compared to controls.

A very strong pattern was observed for the dissolved phase of SO_4^{2-}, Fe, Zn and Cu with significantly higher concentrations in both zooplankton treatments compared to the

control at 30 min (Fig. 2). Such an effect of grazing on Fe release from algae has been reported before in marine ecosystems (Smetacek et al., 2004). The increased concentration of SO_4^{2-} might also be caused by zooplankton grazing. It was not expected to see a significant increase of Zn concentrations in zooplankton treatments compared to the control due to the fast uptake of released Zn^{2+} by living algae as shown in previous studies, and because the Hg-contaminated *Chlorella* was cultivated in a modified BBM medium on deficient of Zn and Cu (Ting et al., 1991; Sheng et al., 2004). However, the increased concentrations of this micronutrient at 30 min might indicate a much more efficient zooplankton grazing which led to a decreased number of living cells and a decreased uptake of released Zn^{2+} by algae. Similar to Zn, it was expected to see no significant variation in the concentration of Cu in zooplankton treatments, but the results showed that Cu concentrations were constantly higher in *Daphnia* treatment compared to the control during the complete experiments, whereas no difference was found between the calanoids treatment and the control (Fig. 3F). This finding may be caused by the greater effects of grazing of *Daphnia* due to its larger size used in the experiment compared to calanoids. In the experiments, dissolved Cu showed a similar release pattern as dissolved IHg, suggesting that it may be adequate to be used as a non-specific proxy for the effects of zooplankton sloppy feeding if only including *Daphnia* as zooplankton treatment.

For dissolved REE, the increased concentrations of ΣREE at 30 min in zooplankton treatments might be caused by the efficient grazing as discussed about for other ions. In contrast to the other REE, lower concentrations of dissolved Ce were observed in both zooplankton treatments compared to the control during the complete experiments. This finding might have been caused by the adsorption of Ce on the carapace of zooplankton during the experiments.

Overall, even though there was a difference between the size of the two taxa, some similar effects of zooplankton grazing on the elemental release in freshwater has been demonstrated in the experiments. However, the release efficiency was, as expected, species-specific and depends on both the taxonomy of zooplankton and the speciation of Hg in water as shown in the PCA (Fig. 3A). Calanoids showed significant influences on

releasing both IHg and MeHg into the particulate phase due to their feeding behavior, whereas *Daphnia* showed significant impact on releasing IHg into dissolved phase. Although dissolved MeHg was not affected by zooplankton grazing, the data correlated better with *Daphnia* treatment than calanoids as shown in the PCA (Fig. 3A, B). The effect of zooplankton grazing was expected to decrease over time due to the decreasing number of algae cells, and the contribution of excretion/egestion was negligible (i.e., after 30 min) for the concentrations of the particulate portion of both IHg and MeHg. The released particulate portion of both IHg and MeHg can enter the aquatic food web again by zooplankton grazing as discussed above. However, the contribution of excretion/egestion (i.e., after 30 min) seems to be significant to the overall summed effects (grazing + excretion/egestion) for dissolved IHg in *Daphnia* treatment. For additional elements in the dissolved phase, zooplankton grazing effects were observed for SO_4^{2-}, Fe, Zn, Cu and ΣREE, especially for the samples from 30 min with increased concentrations compared to the control treatment, and all correlated better with *Daphnia* treatment compared to the calanoids (Fig. 1.3B). However, no overall effects of the sum of grazing and excretion/egestion was found after 30 min, except for Cu, which is the only essential trace metal showing a pattern similar to what was observed for Hg in the experiments. No grazing effects were observed for DOC and Ce during the experiments. The decreased concentrations of those two elements in zooplankton treatments compared to the control may be caused either by more efficient grazing or other mechanism as discussed above.

Role of zooplankton grazing in Hg recycling in aquatic ecosystems

The results of this study clearly indicate that the standing stock of Hg contaminants in primary producers is not fully ingested by consumers due to their feeding behavior. Despite the key role of zooplankton in the trophic transfer of Hg in aquatic food webs, the transfer efficiency is likely less than currently assumed. Such poor trophic transfer efficiency may lead to changes in rates of Hg transfer between biota and water, such as the daily perturbation on Hg speciation in the water column as a function of zooplankton diel vertical migration in freshwater ecosystems, for instance. Furthermore, zooplankton grazing may contribute to a greater bioavailability of IHg and MeHg to organisms in lower

trophic levels. As discussed by Branfireum et al. (2020), the finding of increased concentration of dissolved IHg in water may lead to an enhanced production of MeHg in shallow lakes by periphyton, because of an increased availability due to sloppy feeding. Though, different feeding behavior may lead to different bioavailability of Hg contaminants in aquatic ecosystems, as shown by the results on the taxon-specific effects. Despite these observed taxon-specific difference in the grazing experiments, it may expect a higher concentration of total Hg in water layers of lakes with high density of zooplankton, Although, this availability of Hg species due to zooplankton grazing may be affected by other environmental factors (e.g., water pH, nutrient load etc.) and be limited in intensity in time and in space, such as the observed seasonal change of zooplankton community over time in lakes (Ahangar et al., 2012; Prakash, 2016; Sharma and Kumari, 2018).

Conclusion

This study contributes to the understanding of Hg dynamics between primary producers and primary consumers and to the current knowledge of Hg recycling in aquatic ecosystems. Though field data are still needed to assess its importance at the ecosystem scale, the results of this study highlight a neglected potential pathway for IHg and MeHg in the water column for aquatic organisms, which at our knowledge has not been demonstrated in previous studies. As shown in the experiments, up to 9% and 4% of introduced IHg and MeHg, respectively, have been released into the water in the particulate form during the first 30 min. The results of this study also give a new perspective about the role of zooplankton grazing on the bioavailability of trace metal pollutants in aquatic ecosystems in relationship to the different feeding behavior of consumers. This implies for example that the temperature-driven changes in the composition of the zooplankton communities may have important consequences on the bioavailability of trace metal pollutants in lakes. Under the current global warming scenarios, zooplankton may thus enhance their grazing activity in the water column because of increased metabolism, and consequently affect the distribution and speciation

of Hg and MeHg along with other elements in aquatic systems and their transfer in aquatic food webs.

Acknowledgments

We would like to thank our field and laboratory assistants, namely, Caroline Macarez, Francis Sévigny, Stéphanie L'Italien Simard, Laurie Fortin, Alexis Baribeau Rondeau, and Judith Pichon. Also, to thank Valérie Godbout, Joanie Guay and Elois Veilleux from CEAEQ for their generous help with the free source of *D. magna*. A great thanks to the technician team from the Chemistry department at the University of Quebec in Trois-Rivieres, namely Francis Lafontaine, Jocelyn Bouchard, and Vickie Beaupré, for their plentiful help with experimental equipment. A special thanks to Dominic Bélanger for the supervision of laboratory analysis. We would also like to thank four anonymous reviewers who gave constructive insights on a previous version of this work.

Funding

The funds for this study were provided by the Fonds Québécois de la recherche sur la nature et les technologies (FQRNT) (Grant No. 2016-PR-189982) to AB and MA, and the scolarship programs of Groupe de recherche interuniversitaire en limnologie et en environnement aquatique (GRIL) and Centre de Recherche sur les Interactions Bassins Versants – Ecosystèmes Aquatiques (RIVE).

References

Ahangar, I. A., D. N. Saksena, and M. F. Mir, 2012. Seasonal Variation in Zooplankton Community Structure of Anchar lake, Kashmir. *Univers. J. Environ. Res. Technol. 2*(4): 305-310.

Ajitha, V., C. P. Sreevidya, M. Sarasan, J. C. Park, A. Mohandas, I. S. B. Singh, J. Puthumana, and J. S. Lee, 2021. Effects of zinc and mercury on ROS-mediated oxidative stress-induced physiological impairments and antioxidant responses in the microalga Chlorella vulgaris. *Environ. Sci. Pollut. Res. 28*(25): 32475-32492. https://doi.org/10.1007/s11356-021-12950-6

Al-Majed, N. B., and M. R. Preston, 2000. An assessment of the total and methyl mercury content of zooplankton and fish tissue collected from Kuwait territorial waters. *Mar. Pollut. Bull. 40*(4): 298-307. https://doi.org/10.1016/S0025-326X(99)00217

Bess, Z., S. Chandra, E. Suenaga, S. Kelson, and A. Heyvaert, 2021. Zooplankton influences on phytoplankton, water clarity, and nutrients in Lake Tahoe. *Aquat. Sci*. *83*(2): 1-15. https://doi.org/10.1007/s00027-020-00772-6

Bischoff, H. W., and H. C. Bold, 1963. Some algae from Enchanted Rock and related algal species. *Phycological studies. University of Texas*. IV. Austin 68.

Bourdeau, N., 2016. Élaboration d'un milieu de culture à base d'eaux usées industrielles pour la production d'un consortium d'algues-bactéries à des fins énergétiques. Ph.D thesis. Univ. of Québec in Trois-Rivières.

Branfireun, B. A., C. Cosio, A. J. Poulain, G. Riise, and A. G. Bravo, 2020. Mercury cycling in freshwater systems-An updated conceptual model. *Sci. Total Environ.* 745: 140906. https://doi.org/10.1016/j.scitotenv.2020.140906

Choi, S. C., T. Chase, and R. Bartha, 1994. Enzymatic catalysis of mercury methylation by Desulfovibrio desulfuricans LS. *Appl. Environ. Microbiol*. 60(4): 1342-1346. https://doi.org/10.1128/aem.60.4.1342-1346.1994

Darchambeau, F., 2005. Filtration and digestion responses of an elementally homeostatic consumer to changes in food quality: a predictive model. *Oikos*. *111*(2): 322-336. https://doi.org/10.1111/j.0030-1299.2005.13497.x

Deb, S. C., and T. Fukushima, 1999. Metals in aquatic ecosystems: mechanisms of uptake, accumulation and release-Ecotoxicological perspectives. *Int. J. Environ. Stud. 56*(3): 385-417. https://doi.org/10.1080/00207239908711212

Ekstrom, E. B., F. M. Morel, and J. M. Benoit, 2003. Mercury methylation independent of the acetyl-coenzyme A pathway in sulfate-reducing bacteria. *Appl. Environ. Microbiol.* 69(9): 5414-5422. https://doi.org/10.1128/AEM.69.9.5414-5422.2003

Emmerton, C. A., C. A. Cooke, G. R. Wentworth, J. A. Graydon, A. Ryjkov, and A. Dastoor, 2018. Total mercury and methylmercury in lake water of Canada's oil sands region. *Environ. Sci. Technol. 52*(19): 10946-10955. https://doi.org/10.1021/acs.est.8b01680

Enright, J. T., 1977. Diurnal vertical migration: Adaptive significance and timing. Part 1. Selective advantage: A metabolic model 1. *Limnol. Oceanogr.* 22(5): 856-872. https://doi.org/10.4319/lo.1977.22.5.0856

Fleming, E. J., E. E. Mack, P. G. Green, and D. C. Nelson, 2006. Mercury methylation from unexpected sources: molybdate-inhibited freshwater sediments and an iron-reducing bacterium. Appl. *Environ. Microbiol.* 72(1): 457-464. https://doi.org/10.1128/AEM.72.1.457-464.2006

Gladilovich, D. B., V. Kubáň, and L. Sommer, 1988. Determination of the sum of rare-earth elements by flow-injection analysis with Arsenazo III, 4-(2-pyridylazo) resorcinol, Chrome Azurol S and 5-bromo-2-(2-pyridylazo)-5-diethylaminophenol spectrophotometric reagents. *Talanta*, 35(4): 259-265. https://doi.org/10.1016/0039-9140(88)80082-1

Gorski, P. R., D. E. Armstrong, J. P. Hurley, and M. M. Shafer, 2006. Speciation of aqueous methylmercury influences uptake by a freshwater alga (Selenastrum capricornutum). *Environ. Toxicol.* Chem. 25(2): 534-540. https://doi.org/10.1897/04-530R.1

Harris, R. C., J. W. M. Rudd, M. Amyot, C. L. Babiarz, K. G. Beaty, P. J. Blanchfield, R. A. Bodaly, B. A. Branfireun, C. C. Gilmour, J. A. Graydon, A. Heyes, H. Hintelmann, J. P. Hurley, C. A. Kelly, D. P. Krabbenhoft, S. E. Lindberg, R. P. Mason, M. J. Paterson, C. L. Podemski, A. Robinson, K. A. Sandilands, G. R. Southworth, V. L. St. Louis, and M T. Tate, 2007. Whole-ecosystem study shows rapid fish-mercury response to changes in mercury deposition. *Proc. Natl. Acad. Sci. U. S. A. 104*(42): 16586-16591. https://doi.org/10.1073/pnas.0704186104

He, X., and W. X. Wang, 2006. Relative importance of inefficient feeding and consumer excretion to organic carbon flux from Daphnia. *Freshwater Biol.* 51(10): 1911-1923. https://doi.org/10.1111/j.1365-2427.2006.01631.x

Hintelmann, H.; and N. Ogrinc, 2003. Determination of Stable Mercury Isotopes by ICP/MS and Their Application in Environmental Studies. Biogeochemistry of Environmentally Important Trace Elements, *ACS Symp. Ser*. 835: 321-338. https://doi.org/10.1021/bk-2003-0835.ch021

Hodson, P. V., 1988. The effect of metal metabolism on uptake, disposition and toxicity in fish. *Aquat. Toxicol*, *11*(1-2): 3-18. https://doi.org/10.1016/0166-445X(88)90003-3

Hurlbert, S. H., 1984. Pseudoreplication and the design of ecological field experiments. *Ecol. Monogr.* 54(2): 187-211. https://doi.org/10.2307/1942661

Hutchins, D. A., G. R. DiTullio, and K. W. Burland, 1993. Iron and regenerated production: Evidence for biological iron recycling in two marine environments. *Limnol. Oceanogr*. 38(6): 1242-1255. https://doi.org/10.4319/lo.1993.38.6.1242

Hutchins, D. A., and K. W. Bruland, 1994. Grazer-mediated regeneration and assimilation of Fe, Zn and Mn from planktonic prey. *Mar. Ecol.: Prog. Ser.* 110: 259-269. https://doi.org/10.3354/meps110259

Hutchins, D. A., W. X. Wang, and N. S. Fisher, 1995. Copepod grazing and the biogeochemical fate of diatom iron. *Limnol. Oceanogr.* 40(5): 989-994. https://doi.org/10.4319/lo.1995.40.5.0989

Hygum, B. H., J. W. Petersen, and M. Søndergaard, 1997. Dissolved organic carbon released by zooplankton grazing activity-a high-quality substrate pool for bacteria. *J. Plankton Res.* 19(1): 97-111. https://doi.org/10.1093/plankt/19.1.97

Jitaru, P., and F. Adams, 2004. Toxicity, sources and biogeochemical cycle of mercury. *J. Phys. IV*. 121: 185-193. https://doi.org/10.1051/jp4:2004121012

Kamjunke, N., and R. F. Zehrer, 1999. Direct and indirect effects of strong grazing by Daphnia galeata on bacterial production in an enclosure experiment. *J. Plankton Res.* 21(6): 1175-1182. https://doi.org/10.1093/plankt/21.6.1175

Lampert, W., 1978. Release of dissolved organic carbon by grazing zooplankton. *Limnol. Oceanogr. 23*(4): 831-834. https://doi.org/10.4319/lo.1978.23.4.0831

Lampert, W., 2011. Daphnia: Development of a Model Organism in Ecology and Evolution. In O. Kinne [eds], Series: Excellence in Ecology. *International Ecology Institute.*

Lange, T. R., H. E. Royals, and L. L. Connor, 1993. Influence of water chemistry on mercury concentration in largemouth bass from Florida lakes. *Trans. Am. Fish. Soc. 122*(1): 74-84. https://doi.org/10.1577/1548-8659(1993)122<0074:IOWCOM>2.3.CO;2

Le Faucheur, S., Y. Tremblay, C. Fortin, and P. G. Campbell, 2011. Acidification increases mercury uptake by a freshwater alga, Chlamydomonas reinhardtii. *Environ. Chem.* 8(6): 612-622. https://doi.org/10.1071/EN11006

Le Faucheur, S., P. G. Campbell, C. Fortin, and V. I. Slaveykova, 2014. Interactions between mercury and phytoplankton: speciation, bioavailability, and internal handling. *Environ. Toxicol. Chem.* 33(6): 1211-1224. https://doi.org/10.1002/etc.2424

Liu, C., M. Yuan, W. S. Liu, M. N. Guo, H. Huot, Y. T. Tang, B. Laubie, M. O. Simonnot, J. L. Morel, R. L. Qiu, 2018. Element case studies: rare earth elements, p. 471-483. In A. Van der Ent, G. Echevarria, A. J. Baker, M. O. Sinommot, and J. L. Morel [eds], Agromining: farming for metals. *Springer, Cham. Switzerland*.

Mason, R. P., J. R. Reinfelder, and F. M. Morel, 1996. Uptake, toxicity, and trophic transfer of mercury in a coastal diatom. *Environ. Sci. Technol.* 30(6): 1835-1845. https://doi.org/10.1021/es950373d

Møller, E. F., P. Thor, and T. G. Nielsen, 2003. Production of DOC by Calanus finmarchicus, C. glacialis and C. hyperboreus through sloppy feeding and leakage from fecal pellets. *Mar. Ecol.: Prog. Ser.* 262: 185-191. https://doi.org/10.3354/meps262185

Møller, E. F., 2005. Sloppy feeding in marine copepods: prey-size-dependent production of dissolved organic carbon. *J. Plankton Res. 27*(1): 27-35. https://doi.org/10.1093/plankt/fbh147

Morel, F. M., A. M. Kraepiel, and M. Amyot, 1998. The chemical cycle and bioaccumulation of mercury. *Annu. Rev. Ecol. Syst.* 29(1): 543-566. https://doi.org/10.1146/annurev.ecolsys.29.1.543

Mountouris, A., E. Voutsas, and D. Tassios, 2002. Bioconcentration of heavy metals in aquatic environments: the importance of bioavailability. *Mar. Pollut. Bull. 44*(10): 1136-1141. https://doi.org/10.1016/S0025-326X(02)00168-6

Moye, H. A., C. J. Miles, E. J. Phlips, B. Sargent, and K. K. Merritt, 2002. Kinetics and uptake mechanisms for monomethylmercury between freshwater algae and water. *Environ. Sci. Technol.* 36(16): 3550-3555. https://doi.org/10.1021/es011421z

Oremland, R. S., C. W. Culbertson, and M. R. Winfrey, 1991. Methylmercury decomposition in sediments and bacterial cultures: involvement of methanogens and sulfate reducers in oxidative demethylation. *Appl. Environ. Microbiol.* 57(1): 130-137. https://doi.org/10.1128/aem.57.1.130-137.1991

Perhar, G., G. B. Arhonditsis, and M. T. Brett, 2013. Modeling zooplankton growth in Lake Washington: A mechanistic approach to physiology in a eutrophication model. *Ecol. Modell*. 258: 101-121. https://doi.org/10.1016/j.ecolmodel.2013.02.024

Pickhardt, P. C., C. L. Folt, C. Y. Chen, B. Klaue, and J. D. Blum, 2005. Impacts of zooplankton composition and algal enrichment on the accumulation of mercury in an experimental freshwater food web. *Sci. tOTAL eNVIRON. 339*(1-3): 89-101. https://doi.org/10.1016/j.scitotenv.2004.07.025

Prakash, S., 2016. Seasonal variation of Zooplankton and zoobenthos population in Alwara lake of district Kaushambi Uttar Pradesh India. *Journal of Zoology Studies*, *2*(5), 18-21. https://doi.org/10.13140/RG.2.2.14029.67043

Quinn, G. P., and M. J Keough, M. J. 2002a. Chapter 7. Design and power analysis. p. 155-172. In Quinn, G. P., and M. J Keough [eds]. Experimental design and data analysis for biologists. *Cambridge university press.*

Quinn, G. P., and M. J Keough, M. J. 2002b. Chapter 6. Multiple and complex regression. p. 111-143. In Quinn, G. P., and M. J Keough [eds]. Experimental design and data analysis for biologists. *Cambridge university press.*

Reinfelder, J. R., and N. S. Fisher, 1991. The assimilation of elements ingested by marine copepods. *Science*, 251(4995): 794-796. https://doi.org/10.1126/science.251.4995.794

Schnack, S. B., 1989. Functional morphology of feeding appendages in calanoid copepods. pp. 137-151. In Thistle, A. B., and L. Watling [eds]. Functional Morphology of Feeding and Grooming in Crustacea. *CRC Press*. https://doi.org/10.1201/9781003079354-9

Sharma, R. C., and R. Kumari, 2018. Seasonal variation in zooplankton community and environmental variables of sacred Lake Prashar Himachal Pradesh, India. *International Journal of Fisheries and Aquatic Studies*, *6*(2): 207-213.

Sheng, P. X., Y. P. Ting, J. P. Chen, and L. Hong, 2004. Sorption of lead, copper, cadmium, zinc, and nickel by marine algal biomass: characterization of biosorptive capacity and investigation of mechanisms. *J. Colloid Interface Sci.* 275(1): 131-141. https://doi.org/10.1016/j.jcis.2004.01.036

Simonin, H. A., J. J. Loukmas, L. C. Skinner, and K. M. Roy, 2008. Lake variability: key factors controlling mercury concentrations in New York State fish. *Environ. Pollut. 154*(1): 107-115. https://doi.org/10.1016/j.envpol.2007.12.032

Smetacek, V., P. Assmy, and J. Henjes, 2004. The role of grazing in structuring Southern Ocean pelagic ecosystems and biogeochemical cycles. *Antarctic Science,* 16(4): 541-558. https://doi.org/10.1017/S0954102004002317

Sommer, U., F. Sommer, B. Santer, C. Jamieson, M. Boersma, C. Becker, and T. Hansen, 2001. Complementary impact of copepods and cladocerans on phytoplankton. *Ecology letters,* 4(6): 545-550. https://doi.org/10.1046/j.1461-0248.2001.00263.x

Stein, E. D., Y. Cohen, and A. M. Winer, 1996. Environmental distribution and transformation of mercury compounds. Crit. Rev. *Environ. Sci. Technol.* 26(1): 1-43. https://doi.org/10.1080/10643389609388485

Tang, K. W., V. Turk, V., and H. P. Grossart, 2010. Linkage between crustacean zooplankton and aquatic bacteria. *Aquat. Microb. Ecol*. *61*(3): 261-277. https://doi.org/10.3354/ame01424

Thorp, J. H., and A. P. Covich, [eds] 2009. Ecology and classification of North American freshwater invertebrates. *Academic press.* https://doi.org/10.1016/B978-0-12-690647-9.X5000-5

Ting, Y. P., I. G. Prince, and F. Lawson, 1991. Uptake of cadmium and zinc by the alga Chlorella vulgaris: II. Multi-ion situation. *Biotechnol. Bioeng*. 37(5): 445-455. https://doi.org/10.1002/bit.260370506

Tsui, M. T., and W. X. Wang, 2004. Uptake and elimination routes of inorganic mercury and methylmercury in Daphnia magna. *Environ. Sci. Technol*. 38(3): 808-816. https://doi.org/10.1021/es034638x

Twiss, M. R., P. G. Campbell, and J. C. Auclair, 1996. Regeneration, recycling, and trophic transfer of trace metals by microbial food-web organisms in the pelagic surface waters of Lake Erie. *Limnol. Oceanogr.* 41(7): 1425-1437. https://doi.org/10.4319/lo.1996.41.7.1425

Ullrich, S. M., T. W. Tanton, and S. A. Abdrashitova, 2001. Mercury in the aquatic environment: a review of factors affecting methylation. *Crit. Rev. Environ. Sci. Technol.* 31(3): 241-293. https://doi.org/10.1080/20016491089226

Wang, W. X., and N. S. Fisher, 1996. Assimilation of trace elements and carbon by the mussel Mytilus edulis: effects of food composition. *Limnol. Oceanogr.* 41(2): 197-207. https://doi.org/10.4319/lo.1996.41.2.0197

Wang, W. X., and N. S. Fisher, 1998. Excretion of trace elements by marine copepods and their bioavailability to diatoms. *J. Mar. Res.* 56(3): 713-729. https://doi.org/10.1357/002224098765213649

Watras, C. J., and N. S. Bloom, 1992. Mercury and methylmercury, in individual zooplankton: Implications for bioaccumulation. *Limnol. Oceanogr. 37*(6): 1313-1318. https://doi.org/10.4319/lo.1992.37.6.1313

Westcott, K., and J. Kalff, 1996. Environmental factors affecting methyl mercury accumulation in zooplankton. *Can. J. Fish. Aquat. Sci. 53*(10): 2221-2228. https://doi.org/10.1139/f96-178

Williamson, C. E., H. J. De Lange, and D. M. Leech, 2007. Do zooplankton contribute to an ultraviolet clear-water phase in lakes? *Limnol. Oceanogr. 52*(2): 662-667. https://doi.org/10.4319/lo.2007.52.2.0662

Wu, Y., and W. X. Wang, 2011. Accumulation, subcellular distribution and toxicity of inorganic mercury and methylmercury in marine phytoplankton. *Environ. Pollut.* 159(10): 3097-3105. https://doi.org/10.1016/j.envpol.2011.04.012

Xu, Y., and W. X. Wang, 2003. Fates of diatom carbon and trace elements by the grazing of a marine copepod. *Mar. Ecol.: Prog. Ser.* 254: 225-238. https://doi.org/10.3354/meps254225

Tables

Table 1. Results of the selected models for each chemical variable, with the detected effects of independents terms. Significant terms at the alpha level 0.05 (*p-value* < 0.05) are in bold.

Chemical variables (concentrations)	*Selected Model*	R_{adj}^2	*p-value*
^{200}***Hg (particulate)***	*M4*: **treatment** + $time_{cat}$ + **treatment*$time_{cat}$** + ε	0.63	< 0.001
Me^{198}***Hg (particulate)***	*M3*: **treatment** + $time_{cnt}$ + **treatment*$time_{cnt}$** + ε	0.37	< 0.001
^{200}***Hg (dissolved)***	*M1*: **treatment** + $time_{cnt}$ + ε	0.25	< 0.01
Me^{198}***Hg (dissolved)***	*M1*: treatment + $time_{cnt}$ + ε	0	0.735
DOC	*M4*: **treatment** + **$time_{cat}$** + **treatment*$time_{cat}$** + ε	0.63	< 0.001
pH	*M1*: treatment + $time_{cnt}$ + ε	0	0.383
Fe	*M4*: **treatment** + **$time_{cat}$** + **treatment*$time_{cat}$** + ε	0.94	< 0.001
Zn	*M4*: **treatment** + **$time_{cat}$** + **treatment*$time_{cat}$** + ε	0.70	< 0.001
SO_4^{2-}	*M4*: **treatment** + **$time_{cat}$** + **treatment*$time_{cat}$** + ε	0.73	< 0.001
REE	*M4*: **treatment** + **$time_{cat}$** + **treatment*$time_{cat}$** + ε	0.59	< 0.001
Cu	*M2*: **treatment** + $time_{cat}$ + ε	0.43	< 0.001
Ce	*M1*: **treatment** + $time_{cnt}$ + ε	0.32	< 0.001

Figures

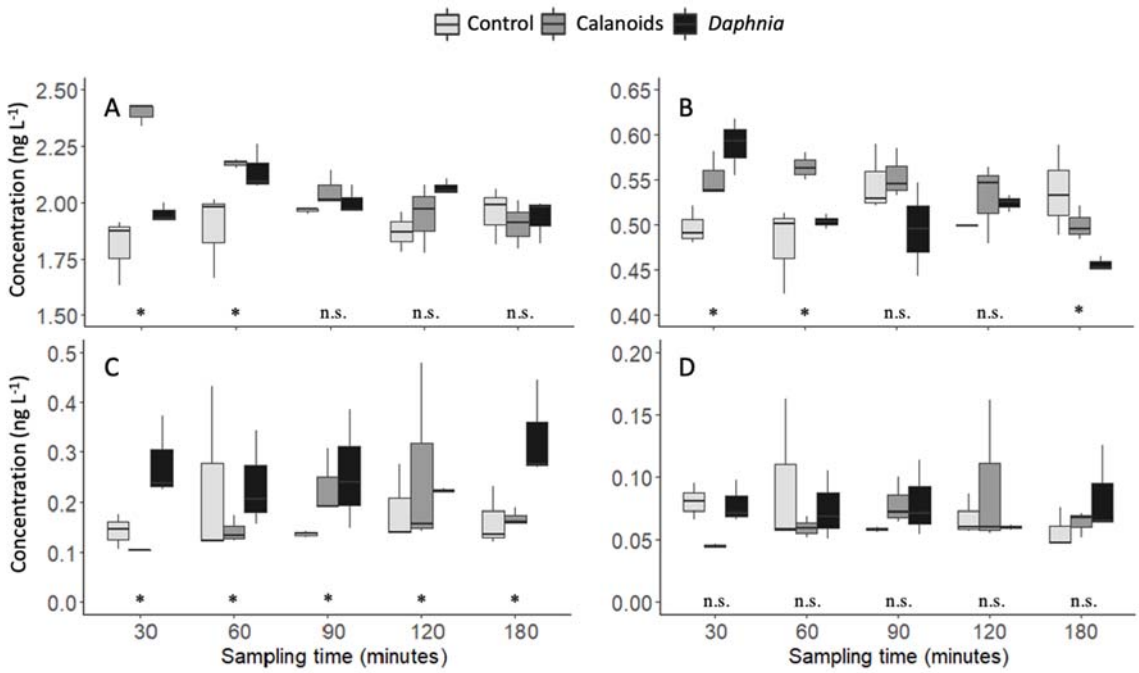

Fig. 1. Time course of the concentrations of particulate and dissolved inorganic ^{200}Hg and $Me^{198}Hg$ in the water of incubators in the three different treatments during the experiment. A) [particulate ^{200}Hg]; B) [particulate $Me^{198}Hg$]; C) [dissolved ^{200}Hg]; D) [dissolved $Me^{198}Hg$]. Light gray = control; dark gray = calanoid copepods; blacks = *D. magna*. Treatment effect is shown with * or n.s. for the significance.

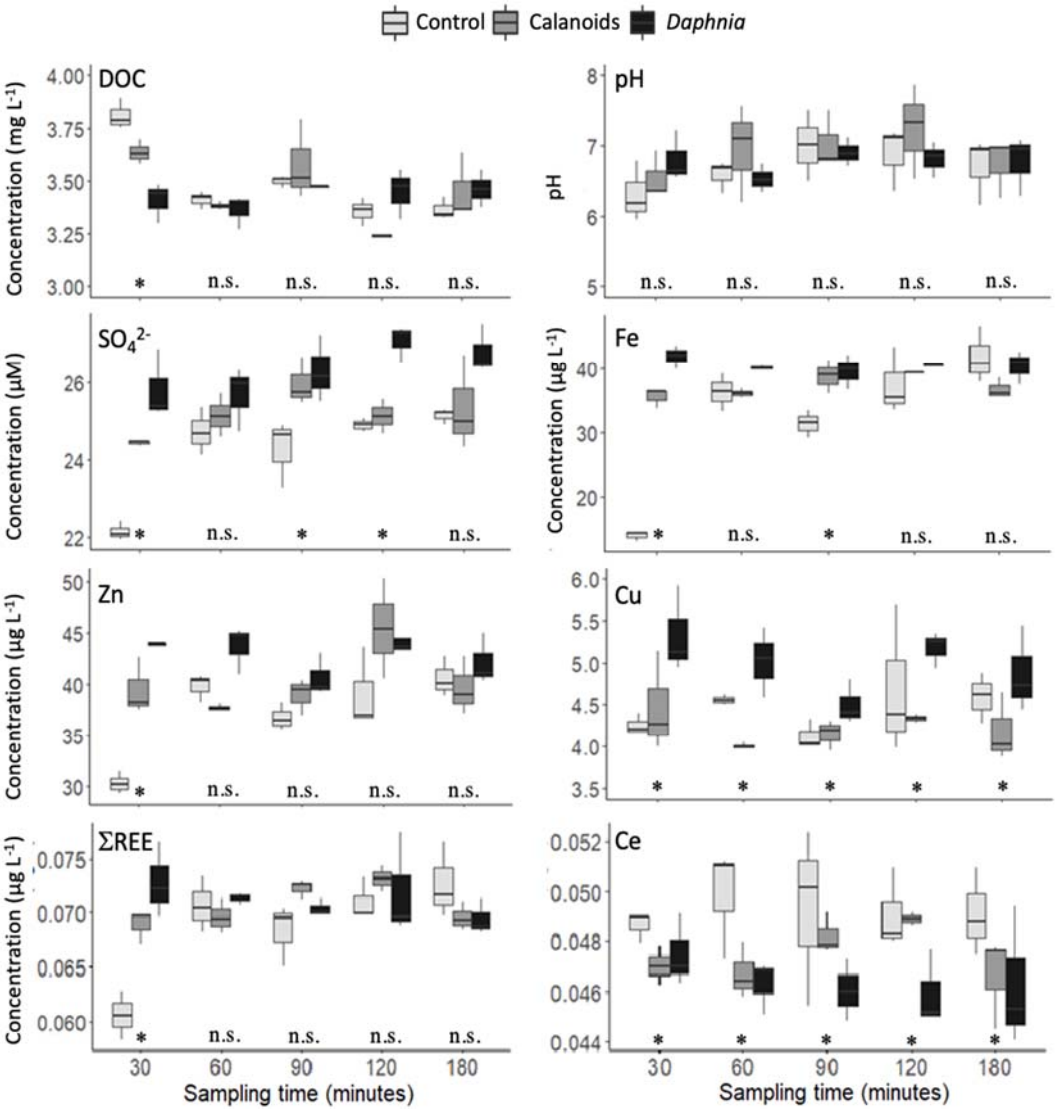

Fig. 2. Time course of the concentrations of DOC (A), pH (B), SO_4^{2-} (C), Fe (D), Zn (E), Cu (F), ΣREE (G), and Ce (H) in the water of incubator in the three different treatments during the experiment. Treatments: Light gray box = control; dark gray box = calanoid copepods; black box = *D. magna*. Significant treatment effect is noted with *, or n.s. for non-significant treatment effect.

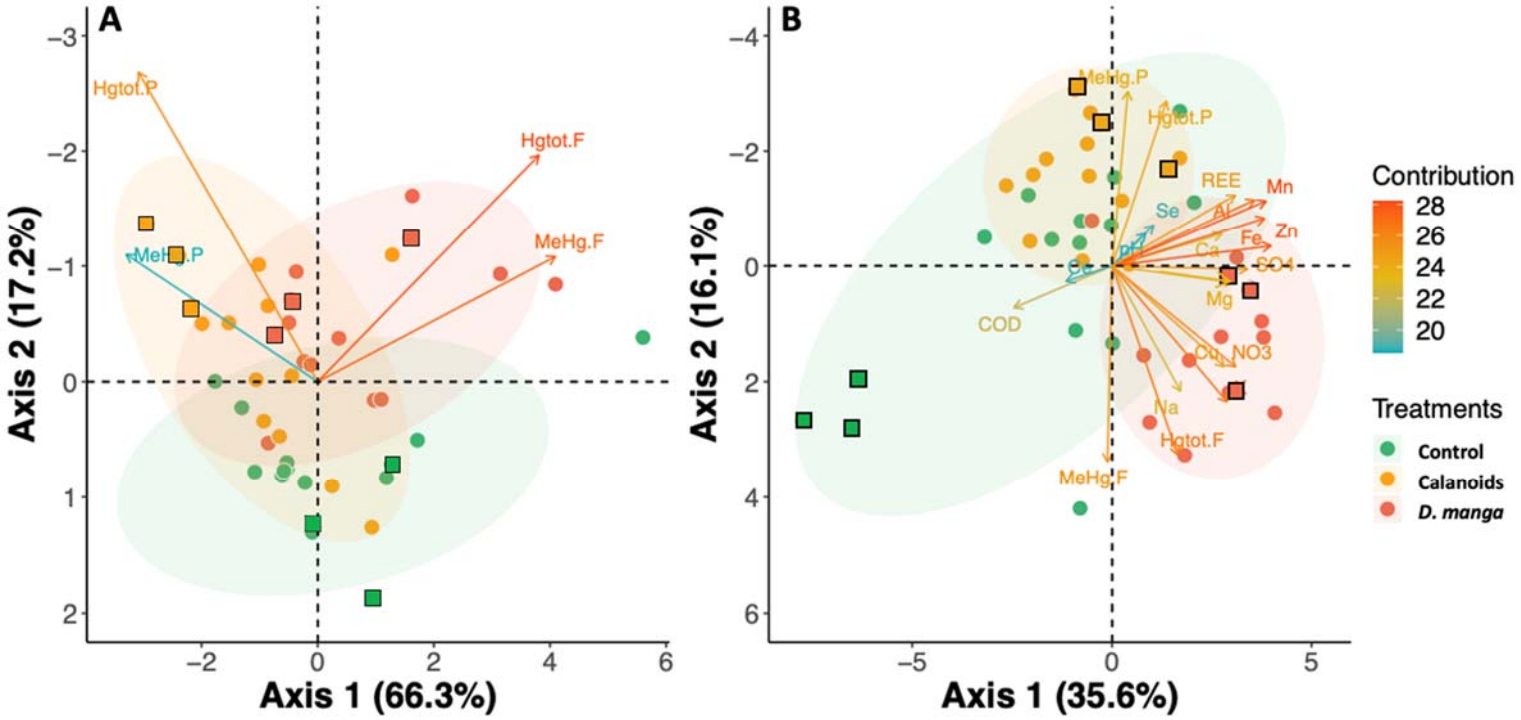

Fig. 3. Principal component analysis with treatments grouped by ellipses and chemical variables by colored arrows. A: PCA with only four mercury variables; B: PCA with all analyzed chemical variables (MeHg.P: particulate $Me^{198}Hg$; Hgtot.P: particulate inorganic ^{200}Hg; MeHg.F: dissolved $Me^{198}Hg$; Hgtot.F: dissolved inorganic ^{200}Hg; REE = ΣREE). Contributions of analyzed chemical variables to establish the x-y graphic are represented by the gradient color from sky blue (less contribution) to coral red (strong contribution). Samples from the first sampling at 30 min were presented by filled square; samples from the extended period were presented by filled circle.

Supplementary Tables and Figures

Table S1. Results of model selection for each chemical variable. Selected models are in bold.

Chemical variables	*Model*	*AIC*	*DAIC*	*Degree of freedom*
^{200}Hg (particulate)	*M1*	-42.5	21.6	5
	M2	-37.3	26.8	8
	M3	-61.3	2.9	7
	M4	**-64.2**	**0.0**	**16**
Me^{198}Hg (particulate)	*M1*	-93.4	13.6	5
	M2	-89.5	17.6	8
	M3	**-105.4**	**1.7**	**7**
	M4	-107.1	0.0	16
^{200}Hg (dissolved)	***M1***	**42.5**	**0.0**	**5**
	M2	47.6	5.1	8
	M3	45.0	2.5	7
	M4	50.6	8.1	16
Me^{198}Hg (dissolved)	***M1***	**29.6**	**1.2**	**5**
	M2	35.1	6.7	8
	M3	28.3	0.0	7
	M4	36.1	7.7	16
DOC	*M1*	-151.2	32.9	5
	M2	-163.3	20.9	8
	M3	-157.4	26.7	7
	M4	**-184.1**	**0.0**	**16**
pH	***M1***	**55.4**	**1.1**	**5**
	M2	54.3	0.0	8
	M3	58.9	4.6	7
	M4	64.9	10.6	16
SO_4^{2-}	*M1*	113.8	10.7	5
	M2	110.7	7.6	8
	M3	113.3	10.2	7
	M4	**103.2**	**0.0**	**16**
Fe	*M1*	-1.4	99.7	5
	M2	-3.7	97.5	8
	M3	-21.5	79.6	7
	M4	**-101.1**	**0.0**	**16**
Zn	*M1*	-86.1	25.9	5
	M2	-87.3	24.8	8
	M3	-92.1	19.9	7
	M4	**-112.0**	**0.0**	**16**
REE	*M1*	-133.7	25.6	5
	M2	-134.0	25.3	8
	M3	-146.3	13.0	7
	M4	**-159.3**	**0.0**	**16**
Cu	*M1*	-84.4	2.6	5
	M2	**-87.0**	**0.0**	**8**
	M3	-82.6	4.4	7
	M4	-80.2	6.7	16
Ce	***M1***	**-167.2**	**0.0**	**5**
	M2	-161.7	5.5	8
	M3	-163.8	3.4	7
	M4	-152.9	14.4	16

Table S2. Post-hoc contrast comparison of treatments in the selected model for each dependant variable. (con = control treatment; cop = calanoid copepods treatment; dap = *Daphnia* treatment; CL = Confidence level). Confidence level and p-value were adjusted with Holm–Bonferroni method for all tests within one variable. Confidence level used: 0.95.

Variables	*Selected model*	*Degree of freedom*	*Sampling time*	*Contrast*	*Mean difference*	*lower. CL*	*upper. CL*	*t.ratio*	*p-value*
^{200}Hg (particulate)	*M4*	30	T1	con - cop	-0.592	-0.857	-0.327	-7.124	< 0.05
				con - dap	-0.146	-0.411	0.119	-1.753	1.000
				cop - dap	0.446	0.181	0.711	5.371	< 0.05
			T2	con - cop	-0.289	-0.554	-0.024	-3.472	< 0.05
				con - dap	-0.256	-0.521	0.009	-3.076	0.067
				cop - dap	0.033	-0.232	0.298	0.395	1.000
			T3	con - cop	-0.091	-0.356	0.174	-1.093	1.000
				con - dap	-0.039	-0.304	0.226	-0.474	1.000
				cop - dap	0.051	-0.214	0.316	0.619	1.000
			T4	con - cop	-0.072	-0.337	0.193	-0.866	1.000
				con - dap	-0.196	-0.461	0.069	-2.361	0.373
				cop - dap	-0.124	-0.389	0.141	-1.495	1.000
			T5	con - cop	0.050	-0.215	0.315	0.604	1.000
				con - dap	0.023	-0.242	0.288	0.275	1.000
				cop - dap	-0.027	-0.292	0.238	-0.329	1.000
Me^{198}Hg (particulate)	*M3*	38	30 min	con - cop	-0.140	-0.265	-0.016	-3.533	< 0.05
				con - dap	-0.132	-0.260	-0.005	-3.249	< 0.05
				cop - dap	0.008	-0.119	0.136	0.198	1.000
			60 min	con - cop	-0.102	-0.195	-0.008	-3.403	< 0.05
				con - dap	-0.075	-0.171	0.021	-2.450	0.285
				cop - dap	0.026	-0.070	0.122	0.862	1.000
			90 min	con - cop	-0.063	-0.140	0.015	-2.545	0.227
				con - dap	-0.018	-0.097	0.061	-0.712	1.000
				cop - dap	0.045	-0.034	0.124	1.780	1.000
			120 min	con - cop	-0.024	-0.108	0.061	-0.885	1.000
				con - dap	0.039	-0.046	0.124	1.445	1.000
				cop - dap	0.063	-0.022	0.148	2.324	0.384
			180 min	con - cop	0.054	-0.093	0.200	1.150	1.000
				con - dap	0.154	0.007	0.300	3.286	< 0.05
				cop - dap	0.100	-0.047	0.246	2.137	0.587

Variables	*Selected model*	*Degree of freedom*	*Sampling time*	*Contrast*	*Mean difference*	*lower. CL*	*upper. CL*	*t.ratio*	*p-value*
^{200}***Hg (dissolved)***	*M1*	41		con - cop	-0.048	-0.379	0.284	-0.360	0.721
				con - dap	-0.472	-0.803	-0.140	-3.552	< 0.05
				cop - dap	-0.424	-0.755	-0.092	-3.192	< 0.05
DOC	*M4*	29	T1	con - cop	0.047	-0.019	0.114	2.267	0.466
				con - dap	0.112	0.045	0.179	5.362	< 0.05
				cop - dap	0.065	-0.002	0.131	3.096	0.065
			T2	con - cop	0.008	-0.059	0.075	0.393	1.000
				con - dap	0.015	-0.052	0.081	0.704	1.000
				cop - dap	0.006	-0.060	0.073	0.310	1.000
			T3	con - cop	-0.022	-0.088	0.045	-1.036	1.000
				con - dap	0.007	-0.060	0.074	0.333	1.000
				cop - dap	0.029	-0.038	0.095	1.369	1.000
			T4	con - cop	0.035	-0.040	0.110	1.501	1.000
				con - dap	-0.027	-0.094	0.040	-1.296	1.000
				cop - dap	-0.062	-0.137	0.013	-2.660	0.189
			T5	con - cop	-0.025	-0.092	0.042	-1.204	1.000
				con - dap	-0.029	-0.095	0.038	-1.371	1.000
				cop - dap	-0.003	-0.070	0.063	-0.167	1.000
SO_4^{2-}	*M4*	29	T1	con - cop	-2.295	-4.040	-0.548	-4.201	< 0.05
				con - dap	-3.681	-5.430	-1.933	-6.738	< 0.05
				cop - dap	-1.386	-3.130	0.361	-2.537	0.252
			T2	con - cop	-0.427	-2.170	1.320	-0.782	1.000
				con - dap	-0.958	-2.710	0.789	-1.754	1.000
				cop - dap	-0.531	-2.280	1.216	-0.973	1.000
			T3	con - cop	-1.694	-3.440	0.053	-3.100	0.064
				con - dap	-2.031	-3.780	-0.284	-3.718	< 0.05
				cop - dap	-0.337	-2.080	1.410	-0.617	1.000
			T4	con - cop	-0.227	-2.180	1.727	-0.371	1.000
				con - dap	-2.180	-3.930	-0.433	-3.990	< 0.05
				cop - dap	-1.953	-3.910	0.000	-3.198	0.051
			T5	con - cop	-0.216	-1.960	1.532	-0.395	1.000
				con - dap	-1.661	-3.410	0.086	-3.040	0.075
				cop - dap	-1.445	-3.190	0.302	-2.645	0.196

Variables		*Selected model*	*Degree of freedom*	*Sampling time*	*Contrast*	*Mean difference*	*lower. CL*	*upper. CL*	*t.ratio*	*p-value*
	Fe	*M4*	29	T1	con - cop	-0.923	-1.095	-0.752	-17.225	< 0.05
					con - dap	-1.087	-1.258	-0.915	-20.271	< 0.05
					cop - dap	-0.163	-0.335	0.008	-3.046	0.074
				T2	con - cop	0.003	-0.168	0.175	0.062	1.000
					con - dap	-0.102	-0.274	0.069	-1.905	1.000
					cop - dap	-0.105	-0.277	0.066	-1.967	0.882
				T3	con - cop	-0.211	-0.383	-0.040	-3.937	< 0.05
					con - dap	-0.230	-0.402	-0.059	-4.298	< 0.05
					cop - dap	-0.019	-0.191	0.152	-0.360	1.000
				T4	con - cop	-0.056	-0.248	0.136	-0.935	1.000
					con - dap	-0.084	-0.256	0.087	-1.576	1.000
					cop - dap	-0.028	-0.220	0.163	-0.474	1.000
				T5	con - cop	0.124	-0.047	0.296	2.314	0.419
					con - dap	0.034	-0.138	0.205	0.629	1.000
					cop - dap	-0.090	-0.262	0.081	-1.686	1.000
	Zn	*M4*	29	T1	con - cop	-0.264	-0.415	-0.112	-5.566	< 0.05
					con - dap	-0.371	-0.523	-0.220	-7.842	< 0.05
					cop - dap	-0.108	-0.259	0.044	-2.275	0.457
				T2	con - cop	0.053	-0.099	0.204	1.110	1.000
					con - dap	-0.092	-0.244	0.059	-1.951	0.911
					cop - dap	-0.145	-0.296	0.006	-3.062	0.071
				T3	con - cop	-0.058	-0.210	0.093	-1.228	1.000
					con - dap	-0.101	-0.253	0.050	-2.138	0.616
					cop - dap	-0.043	-0.195	0.108	-0.910	1.000
				T4	con - cop	-0.149	-0.318	0.020	-2.812	0.131
					con - dap	-0.124	-0.275	0.028	-2.617	0.209
					cop - dap	0.025	-0.144	0.194	0.471	1.000
				T5	con - cop	0.025	-0.127	0.176	0.520	1.000
					con - dap	-0.037	-0.189	0.114	-0.786	1.000
					cop - dap	-0.062	-0.213	0.090	-1.306	1.000

Variables	*Selected model*	*Degree of freedom*	*Sampling time*	*Contrast*	*Mean difference*	*lower. CL*	*upper. CL*	*t.ratio*	*p-value*
REE	*M4*	29	T1	con - cop	-0.129	-0.218	-0.041	-4.665	< 0.05
				con - dap	-0.184	-0.272	-0.095	-6.637	< 0.05
				cop - dap	-0.055	-0.143	0.034	-1.972	0.873
			T2	con - cop	0.015	-0.073	0.104	0.548	1.000
				con - dap	-0.010	-0.098	0.079	-0.344	1.000
				cop - dap	-0.025	-0.113	0.064	-0.892	1.000
			T3	con - cop	-0.058	-0.146	0.031	-2.080	0.697
				con - dap	-0.031	-0.120	0.057	-1.127	1.000
				cop - dap	0.026	-0.062	0.115	0.953	1.000
			T4	con - cop	-0.030	-0.129	0.069	-0.978	1.000
				con - dap	-0.012	-0.100	0.077	-0.425	1.000
				cop - dap	0.019	-0.081	0.118	0.598	1.000
			T5	con - cop	0.043	-0.046	0.131	1.542	1.000
				con - dap	0.045	-0.044	0.133	1.616	1.000
				cop - dap	0.002	-0.087	0.091	0.074	1.000
Cu	*M2*	37		con - cop	0.048	-0.029	0.124	1.561	0.381
				con - dap	-0.114	-0.189	-0.039	-3.802	< 0.05
				cop - dap	-0.161	-0.238	-0.085	-5.290	< 0.05
Ce	*M1*	40		con - cop	0.037	0.006	0.069	2.944	< 0.05
				con - dap	0.058	0.027	0.089	4.710	< 0.05
				cop - dap	0.021	-0.010	0.053	1.684	0.100

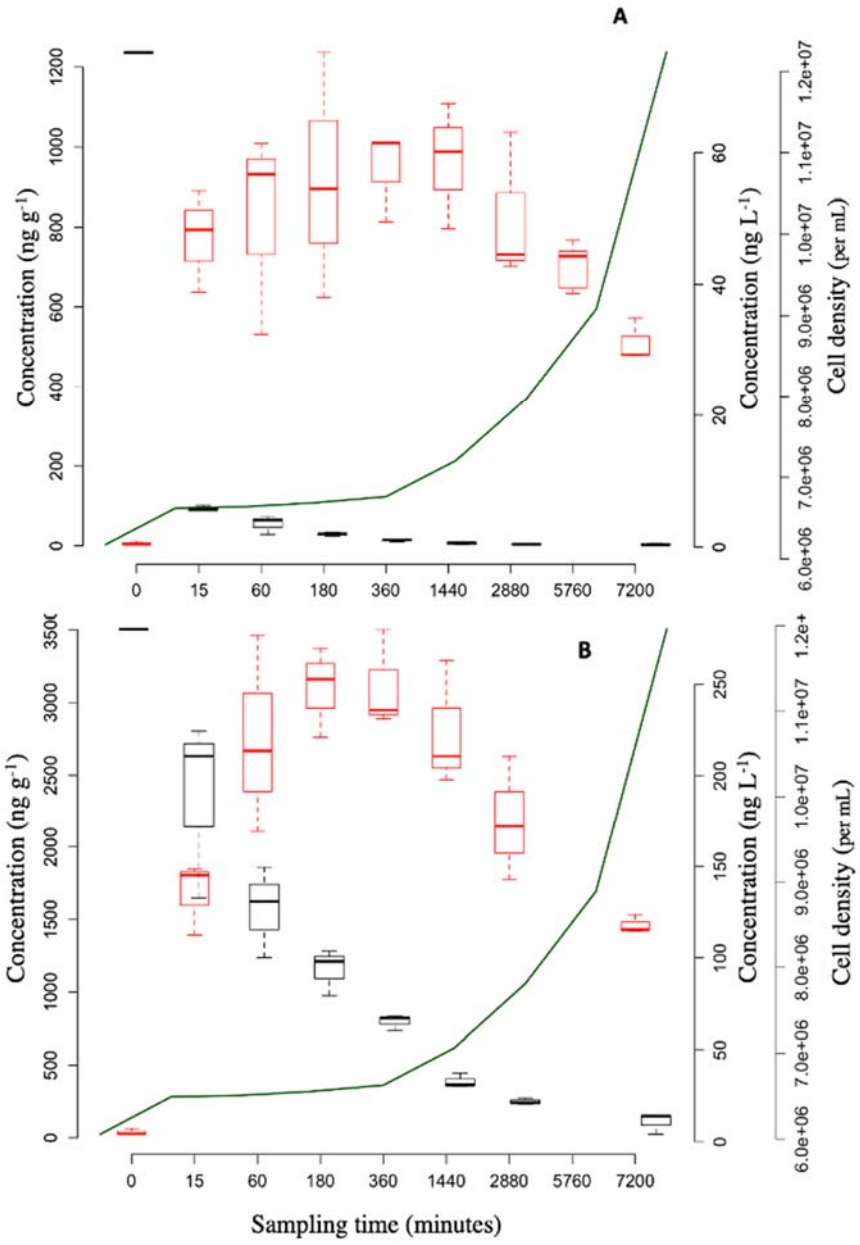

Fig. S1. Time course of inorganic 200Hg (A) and Me198Hg (B) uptake by Chlorella vulgaris. A) Red boxplots represent the 200Hg concentrations (ng g-1) in Chlorella vulgaris, and black boxplots represent the 200Hg concentrations (ng L-1) in water. B) Same symbols as in panel A, but for Me198Hg. Green curve line represents the growth of Chlorella vulgaris during the four days following the spiking. No water samples were taken from day 7 (correspond to 5760 min).

CHAPITRE II

EFFECTS OF OSCILLATING TEMPERATURE ON TRACE METAL ACCUMULATION IN *DAPHNIA MAGNA*

Cet article a été soumis au périodique ACS *omega*

Fan Qin[1,2*], Marc Amyot[2,3] and Andrea Bertolo[1,2]

[1] Centre de recherche sur les interactions bassins versants – écosystèmes aquatiques (RIVE) and Département des sciences de l'environnement, Université du Québec in Trois-Rivières, 3351 Boul. des Forges, C.P. 500, Trois-Rivières QC, G8Z 4M3, Canada

[2] Groupe de Recherche Interuniversitaire en Limnologie (GRIL), Université de Montréal, Campus MIL, C.P. 6128, Succ. Centre-ville, Montréal QC H3C 3J7, Canada

[3] Département des sciences biologiques, Université de Montréal, Campus MIL, C.P. 6128, Succ. Centre-ville, Montréal QC H3C 3J7, Canada

*Corresponding author email: fan.qin@uqtr.ca

Abstract

Whereas many aquatic species experience daily temperature changes, it is still unclear whether oscillating temperature can affect the accumulation of trace metal independently from changes in mean temperature. Here, the impact of oscillating temperature (MT_{osc}: 7/23 ºC, 24 /cycle) on the accumulation of inorganic Hg (IHg) and monomethylmercury (MeHg) in *Daphnia* was investigated, by comparing it to a constant temperature treatment with the same average temperature (MT_{const}: 15 ºC). The effects of mean temperature were tested by comparing this latter to a similar treatment with higher temperature (HT_{const}: 23 ºC). Both trophic and water pathways were estimated by using *Chlorella* labeled with stable Hg isotopes and by directly spiking Hg isotope solutions into the microcosm, respectively. The concentrations of IHg were decreased in *Daphnia* under oscillating temperature for both food and water pathways by at least 42% and 25%, respectively, compared to MT_{const} treatment. In contrast, the accumulation of MeHg was reduced in the trophic pathway but was enhanced in water pathway. Patterns similar to IHg were observed for Fe, Zn, and Cu in the trophic pathway, but only for Cu in the water pathway. This study sheds new light on trace metal accumulation in a near realistic temperature condition.

Keywords**:** mercury, monomethylmercury, trophic transfers, bioconcentration, oscillating temperature, zooplankton, freshwater

Synopsis**:** Minimal research exists on trace metal accumulation under temperature oscillation. This study reports that trace metal bioaccumulation in a keystone aquatic species differs between oscillating temperature vs. equivalent mean stable temperatures with implications for climate change research in ecotoxicology.

Introduction

Aquatic organisms are often found in habitats exposed to great temperature variation, not only at the long-term (e.g., seasonal) but also at the short-term scale (e.g., daily). For example, species living in the intertidal zone (e.g., mussels) are potentially exposed to daily, monthly (lunar phase), and seasonal changes in temperature. Similarly, it is also common to observe organisms exposed to large daily temperature variations in freshwater ecosystems. For instance, zooplankton performing diel vertical migration (DVM) in stratified lakes can experience huge variations in temperature over the 24 h cycle[1]. The physiological and behavioral constraints associated with varying thermal conditions are still poorly known, but the fluctuating temperature has the potential to alter numerous metabolic pathways in aquatic ectotherms, like the capacity to uptake and to accumulate various pollutants, such as mercury (Hg)[2].

It has been demonstrated that constant warm temperatures can increase the concentrations and enhance the toxicity of several metallic contaminants such as Hg components, particularly monomethylmercury (MeHg), in aquatic ectotherms compared to constant cooler temperatures[3-6]. However, it might be misleading to use the results obtained from laboratory experiments under constant temperature conditions to predict, for example, the risk of Hg contamination under field conditions where the temperature fluctuates rapidly[7]. In addition to the overall trend toward higher mean temperatures observed in many regions of the world due to global warming[8-9], recent studies suggest that the diurnal temperature range could also be affected by climate change[10]. Thus, it is crucial to assess the responses to changes in both the mean temperature and its variation in time, since these factors could affect the metabolism in living organisms independently and/or synergistically[11]. In the case of the potential interactions between climate change and contaminants (e.g., increased exposure to contaminants due to global warming, and increased susceptibility to temperature variation due to contaminant exposure), taking into account the temperature variations might change the predictions based on scenarios of climate change which consider only increases in mean temperatures[12-13].

To our knowledge, only a few studies focused on the metal accumulation in aquatic ectotherms under fluctuating temperature, with a nearly complete lack of research since the 1990s. The studies performed by Watkins and Simkiss (1988a, b)[14,15], for example, showed a higher accumulation of essential trace metal elements, such as zinc (Zn), in *Mytilus edulis* exposed to oscillating temperatures compared to the constant upper limit temperature of the oscillating treatment. In contrast, a more recent *in situ* study[2] conducted in boreal lakes reported a reduced accumulation of MeHg in two migrating *Chaoborus* species (*C. trivittatus* and *C. punctipennis*; diptera), which experienced daily temperature changes, compared to sedentary species (*C. americanus*), which used only the warm surface layers during the summer. In addition to this scant and contradictory information, it is unclear whether fluctuating temperature conditions could affect differently the uptake of inorganic vs. organometallic pollutants (e.g., inorganic Hg and MeHg). Furthermore, it is also uncertain whether fluctuating temperature conditions would have similar effects on the different pathways of metal contaminant uptake, such as the trophic and water ones[16].

This study experimentally tested the effects of oscillating temperature on the accumulation of both inorganic Hg (IHg) and MeHg in *Daphnia magna* (hereafter *D. magna*) via either the trophic or the water pathways separately. In addition, the concentrations of other trace metals in *D. magna* were also measured as potential tracers of the accumulation under the oscillating temperature conditions, such as some micronutrients (i.e., Fe, Zn, Cu) and other data-poor trace elements (i.e., rare earth elements, REE), whose recycling potential in freshwater ecosystems is poorly known. Because of the distinctive redox chemistry of cerium (Ce), the results for this REE were presented separately from the sum of all the other REE (hereafter ΣREE) well detected by ICP MS/MS (namely lanthanum (La), yttrium (Y), praseodymium (Pr), and neodymium (Nd)), which usually have similar chemical behavior in aquatic systems[17-18]. Based on the results of previous studies, it was expected that in the experiments (i) the accumulation of IHg, MeHg, and other trace elements in *D. magna* is affected by the oscillating temperature independently from changes in mean temperatures. In addition, based on the existing, albeit limited knowledge[14,15,19], it was expected that (ii) individuals exposed to

oscillating temperature conditions would have an enhanced accumulation of both Hg forms and other trace elements compared to the highest temperature of the oscillating treatment. Finally, given the lack of previous work on this topic, this study explored different pathways of accumulation and make the working hypothesis that (iii) *D. magna* will show similar uptake and accumulation patterns of IHg, MeHg, and other trace elements through both food and water pathways.

Material and methods

Study design summary

A laboratory experiment was conducted under controlled conditions to study the effects of oscillating temperature on the accumulation of IHg and MeHg in *D. magna* by using Hg solutions enriched with stable isotopes ($^{200}HgCl_2$ or $Me^{198}HgCl$) (see SI for experimental condition). Two sets of experiments were established to examine the effects of oscillating temperature on metal accumulation via either the trophic or the water pathways separately. Three temperature treatments were used in the experiments including an oscillating temperature treatment (MT_{osc}: 7/23 ºC) and a constant medium and high one (MT_{const}: 15 ºC; and HT_{const}: 23 ºC, respectively). The upper (23 ºC) and the lower (7 ºC) bounds of the oscillating temperature treatment corresponded roughly to the temperatures normally observed in the epilimnion and hypolimnion of boreal lakes in southern Quebec (Canada) during the summer, respectively. The effect of oscillating temperature was assessed by a direct comparison between the MT_{const} treatment and the MT_{osc} treatment which had an average temperature of 15 ºC. The upper constant temperature treatment (HT_{const}) was chosen in order to match the maximum temperature used in the oscillating temperature treatment[14,15,19], and allowed to follow the effect of mean temperature by directly comparing to the MT_{const} treatment. In contrast, it was not possible to set a treatment for the lowest bound (i.e., 7 ºC) of the oscillating temperature treatment due to logistical constraints. The switch of temperature was controlled within 1 h for the oscillating temperature treatment with a thermostated chiller and a submersible aquarium heater (Fig. S2). The trophic pathway experiment was conducted during 3 days

with *D. magna* sampled once per day, whereas the water pathway experiment was conducted for a period of 24 h with *D. magna* sampled at each 8 h.

Experimental design

One-week-old *D. magna* were divided equally into three aquaria and were acclimated under each of the three temperature treatments, respectively, for one week before the exposition to IHg and MeHg (Fig. S2). They were fed with uncontaminated *Chlorella* with a density of 10^6 cells mL^{-1} per day. The temperature oscillation cycle for MT_{osc} treatment was synchronized with the local summer light cycle (8 h at 23 ºC/dark: 16 h at 7 ºC/light). Because all the experiments were performed in the dark, the duration of the photoperiod for the acclimatization of *D. magna* was adapted by setting an 8 h/16 h light/dark cycle.

The trophic pathway experiment was conducted during a three-day period under dark condition in order to avoid potential photochemical effects on Hg species in water[20]. A sub-sample of *D. magna* was taken before the exposition to obtain the background concentration of IHg and MeHg. Three treatments with or without Hg spiking (inorganic ^{200}Hg, $Me^{198}Hg$, and control, respectively) were prepared with four replicates for each temperature treatment. Acclimatized *D. magna* were distributed into acid-washed glass incubators used as microcosms with a final density of 10 to 15 individuals mL^{-1}. This density corresponded roughly to the field observation in boreal lakes during the summer from previous studies in our laboratory[21]. The starting temperature was 7 ºC for the MT_{osc} treatment. Prepared algae with or without the Hg contamination (inorganic ^{200}Hg, $Me^{198}Hg$, and control, respectively) were added to the microcosm 8 h after the beginning of the experiment with a final density of 2.5 x 10^5 cells mL^{-1}.[22] Water was heated to 23 ºC at the same time in the MT_{osc} treatment, then was cooled down to 7 ºC 8 h later. The average temperature of the MT_{osc} treatment was about 14.4 ºC (Fig. S2). The first sampling was carried out 24 hours after the experiments began. During the sampling, *D. magna* was picked out individually, put into an acid-washed plastic container filled with clean water, and fed with uncontaminated algae for 30 min to clean out the

undigested Hg-contaminated algae. Then, they were transferred to an acid-washed Petri dish and washed twice with ultrapure water for 5 min before being collected (Fig. S3). The collected *D. magna* were stored at -20 ºC until further analysis. Two more samplings were carried out in the next two days. No mortality was observed during the first sampling, but a few individuals were found dead in the last two samplings. No molting was observed during the first two samplings but a few exuviae were observed in the last sampling (Table S1). No reproduction was observed during the 3-days experiments.

The water pathway experiment was conducted for 24 h under dark condition. A minor portion (15% and 0%, respectively) of spiked inorganic ^{200}Hg and $Me^{198}Hg$ was adsorbed on the wall of glass incubators after 24 h according to the preparation tests with the same concentrations used in the experiments (240 ng L^{-1} and 64.6 ng L^{-1}, respectively). These concentrations, which are well below the lethal levels, aim to compensate some of the spiked Hg lost during the manipulation (e.g., IHg) and to facilitate the monitoring of Hg dynamics during the experiment. After background sampling, acclimated *D. magna* were kept in the microcosms for a 3 h fasting after the last feeding cycle. The density of *D. magna* in the microcosms was similar to those used in the trophic pathway experiment. The MT_{osc} treatment started at 23 ºC at the beginning of the experiments. At the same time, 300 µL of isotopic ^{200}Hg or $Me^{198}Hg$ stock solutions were spiked into four microcosms from each temperature treatment taken randomly. The first sampling was carried out 8 h after the first spiking. During the sampling, *D. magna* was sorted out individually and washed in ultrapure water for 5 min before being collected. After the sampling, additional spiking was added into the microcosms that have been spiked previously with either inorganic ^{200}Hg or $Me^{198}Hg$ to prevent decreasing concentrations of Hg components due to the uptake by *D. magna*. Water was then cooled down to 7 ºC in the MT_{osc} treatment. After the second sampling was carried out (i.e., 8 h after the second spiking), water was heated to 23 ºC in the MT_{osc} treatment, and microcosms were spiked again with either inorganic ^{200}Hg or $Me^{198}Hg$. The last sampling was carried out at 24 h (Fig. S4). All samples were conserved at -20 ºC until further analysis. The observed mean temperature in the oscillating treatment was equal to 15.0 ºC (Fig. S2). No mortality was observed during the 24 h experiments. Whereas only a few

molts were observed at the end of the experiment in the control treatment, many were found in both the inorganic ^{200}Hg and $Me^{198}Hg$ treatments (Table S1). No reproduction was observed during the 24 h experiment.

Inorganic ^{200}Hg and $Me^{198}Hg$ analysis

Lyophilized *D. magna* samples for the quantification of total Hg were firstly digested with 0.6 mL ultra-trace HNO_3 (Nitric acid 67–70%, OmniTrace Ultra™ for trace metal analysis, VWR) in a pressure cooker under 15 to 20 psi for 3 h. Then, 0.25 mL hydrogen peroxide solution (≥30%, for trace metal analysis) and 0.15 mL ultra-trace HCl (Hydrochloric acid 32–35%, OmniTrace Ultra™ for trace metal analysis, VWR) were sequentially added to the sample and well mixed to complete the digestion overnight. On the following day, the digested sample was prepared following the method EPA 1631 (U.S. Environmental Protection Agency) before being quantified with Tekran 2600 Automated Sample Analysis System cold vapour atomic fluorescence spectrometer (Tekran® Instrument Corp. Canada) coupled with an inductively coupled plasma mass spectrometry (8900 Triple Quadrupole ICP-MS/MS, Agilent, USA). The quality control of the analysis was carried out by intercalibrations with the Canadian Association for Laboratory Accreditation (CALA, Ottawa, Canada) using certified inorganic Hg solution (SPC Sciences, Montreal, Canada) and reference samples made with certified reference material (DORM-4, #MEF-25, 410 ng g^{-1} total Hg, National Research Council of Canada) with a recovery > 90%. Isotopic dilution method was applied to analyze the concentration of spiked inorganic ^{200}Hg in *D. magna*[23]. 0.1 ng L^{-1} inorganic ^{201}Hg solution was added to all samples including the quality control in order to unbalance all the isotopic ratios to allow to quantify the spiked inorganic ^{200}Hg from the experiments. The final results of spiked inorganic ^{200}Hg concentration in *D. magna* were obtained with a matrix calculation based on two detected mercury isotopes (^{200}Hg and ^{201}Hg)[24].

Lyophilized *D. magna* sample for MeHg quantification was digested with HNO_3 (4M) overnight in an oven at 60 ºC. The next day, digested samples were prepared following the method EPA1630 (U.S. Environmental Protection Agency) and was

analyzed with Tekran 2700 Automated Methyl Mercury Analysis System (Tekran® Instrument Corp. Canada) coupled with triple quadrupole ICP-MS/MS. The quality control of the analysis was carried out by the recovery of certified sample (> 90%, Tort-2, 152 ng g^{-1} MeHg, National Research Council of Canada). Isotopic dilution method was applied during the analysis by adding 0.1 ng L^{-1} $Me^{201}Hg$ in all samples including certified samples to quantify the concentration of spiked $Me^{198}Hg$ in *D. magna*. The final results of the concentration of spiked $Me^{198}Hg$ in *D. magna* were obtained with a matrix calculation based on two detected mercury isotopes ($Me^{198}Hg$ and $Me^{201}Hg$).

Statistical analysis

A linear mixed modeling approach was used (with the statistical language R) to take into account both fixed (time and temperature treatment) and random (incubator) effects (alpha = 0.05). Four models were established:

1) Additive models

   M1: treatment+ time + incubator

   M2: treatment + $time_{cat}$ + incubator

2) Interactive models

   M3: treatment + time + treatment *time + incubator

   M4: treatment + $time_{cat}$ + treatment*$time_{cat}$ + incubator

where time was modelled either as continuous (time) or categorical ($time_{cat}$) in order to take into account, respectively, either linear or non-linear effects. Model selection for dependent variables was based on Akaike information criterion (AIC). The selected model possessed the smallest AIC value[25]. Post-hoc contrast analysis was applied on the selected model to highlight differences between paired temperature treatments to assess the temperature effects at each step of sampling time. In the result section, the model selection was presented first for each dependent variable to demonstrate how well the selected models support the hypotheses. Then, the details about the explanatory variables included in the selected model were given. Finally, the details about post-hoc comparison at each

step of sampling time were explained. The Holm-Bonferroni correction was applied for multiple testing using post-hoc comparisons.

Results

Trophic pathway

The model selected to evaluate the effect of oscillating temperature on IHg accumulation in *D. magna* in food pathway included the interactive term between treatment and sampling time (treated as categorical) (model *M4*; Tables 1 and S2). Fixed effects explained 92.3% variation in data with all terms contributing significantly to explain the dependent variable (Table 1). A clear pattern was observed in the data, with the MT_{osc} treatment having lower concentrations of IHg in *D. magna* compared to the two treatments with constant temperatures, as showed by post-hoc tests (Fig. 1A; Table S3). Only at day 1 the HT_{const} treatment was not significantly different from the MT_{osc} treatment (Fig. 1A). In this case, the significant interaction term between treatment and sampling time is mostly related to the fact that the differences between the MT_{osc} treatment and the other two treatments increased with time. Therefore, for IHg bioaccumulation, a clear negative effect of oscillating temperature was found but not of mean temperature.

For MeHg, the selected model included only additive terms with sampling time treated as categorical (*M2*; Table 1 and S2). Fixed effects explained 84% variation in data with all terms being significant (Table 1). A different bioaccumulation pattern was observed in *D. magna* relatively to IHg, with significantly higher concentrations in the HT_{const} treatment compared to the other two treatments during the entire experiment, as shown by post-hoc comparisons (Fig. 1C; Table S3). However, the concentrations of MeHg in *D. magna* were not significantly different between the MT_{osc} and the MT_{const} treatments in this case. Therefore, for MeHg bioaccumulation, a clear positive effect of mean temperature was observed but not of oscillating temperature.

For Fe and Zn, the selected model included only additive terms with sampling time treated as categorical (*M2*; Table 1 and S2). Fixed effects explained 57.4% and 56.9% variation in data, respectively, with all terms being significant (Table 1). For both Fe and Zn, the concentrations in *D. magna* were significantly lower in the MT_{osc} treatment compared to the two treatments with constant temperatures (Fig. 2A, C, Table S3). However, the pattern was somewhat different between these two elements, as shown by post-hoc comparisons: i) for Fe, higher concentrations were observed in the HT_{const} treatment compared to MT_{const} treatment, whereas ii) for Zn, no significant difference was observed between these two treatments (Table S3). Therefore, whereas for Zn bioaccumulation, only a clear negative effect of oscillating temperature was observed, for Fe a positive effect of mean temperature was also found.

The selected model for Cu included only additive terms with sampling time treated as continuous (*M1*; Table 1 and S2). Fixed effects explained 28% variation in data with only treatment being significant (Table 1). This metal showed a pattern similar to Zn, with lower concentrations observed in *D. magna* in the MT_{osc} treatment compared to the HT_{const} and the MT_{const} treatments, whereas no difference was found between the two constant temperature treatments, as showed by post-hoc tests (Fig. 2E; Table S3). Therefore, for Cu bioaccumulation, a clear negative effect of oscillating temperature was observed but not for mean temperature.

The selected model for ΣREE included only additive terms with sampling time treated as categorical (*M2*; Table 1 and S2). Fixed effects explained 45.5% variation in data with all terms being significant (Table 1). For ΣREE, a less clear pattern was found, with the MT_{osc} treatment having significantly lower concentrations in *D. magna* compared to the HT_{const} treatment, but the MT_{const} treatment being not significantly different from the other two treatments (Fig. 2G; Table S3).

The selected model for Ce, included only additive terms and sampling time treated as continuous (*M1*; Table 1 and S1). Fixed effects explained 16.4% variation in data with

only time being significant. The concentrations of Ce in *D. magna* were not impacted by any of the temperature treatments. (Fig. 2I; Table S3).

Water pathway

The model selected to assess the impact of oscillating temperature on the uptake of IHg directly from water by *D. magna* included the interactive term between treatment and sampling time (treated as categorical) (*M4*; Table 1 and S2). Fixed effects explained 92.1% variation in data with all terms being significant (Table 1). A pattern relatively similar to what found for IHg in the trophic pathway was observed here, with the MT_{osc} treatment having lower concentrations in *D. magna* compared to the other two treatments with constant temperatures. However, as shown by post-hoc comparisons: i) in the first sampling, the temperature effects were not significantly different on the uptake of IHg in *D. magna* among the three treatments, and ii) in the last sampling, the effect of the MT_{osc} treatment was not significantly different from the HT_{const} treatment (Fig. 1B; Table S3). Despite some discrepancies, this pattern showed a clear negative effect of oscillating temperature on IHg bioconcentration via the water pathway after the first sampling, but no effects of mean temperature.

For MeHg, the selected model included the interactive term between treatment and sampling time (treated as categorical) (*M4*; Table 1 and S2). Fixed effects explained 95% variation in data with all terms being significant (Table 1). Whereas this pattern was not very clear-cut, it was in general the inverse of what observed for IHg. Higher concentrations of MeHg were in fact found in *D. magna* in the MT_{osc} treatment compared to the MT_{const} at least 8 and 24 h, whereas the HT_{const} treatment was never significantly different from the other two treatments (Fig. 1D; Table S3). Globally, these results show only a positive effect of oscillating temperature on the bioconcentration of MeHg in *D. magna*.

For Fe and Zn, the selected model included the interactive term between treatment and sampling time (treated as categorical) (*M4*; Table 1 and S2). Fixed effects explained

39.1% and 34.2% variation in data, respectively. The interactive term was significant for both Fe and Zn, with sampling time being significant only for Fe and treatment being significant only for Zn (Table 1). Temperature effects were not significantly different on the accumulation of both metals in *D. magna* at 8 h and 24 h among the three treatments. However, as shown by post-hoc comparisons, in the second sampling at 16 h the MT_{osc} treatment had lower concentrations of both metals in *D. magna* compared to the two treatments with constant temperatures (Fig. 2B, D).

For Cu, the same model as for Fe and Zn was selected (*M4*; Table 1; S2). Fixed effects explained 81% variation in data with treatment and interactive term being significant (Table 1). For this metal, a pattern partly similar to what was observed in the trophic pathway was observed, with the MT_{osc} treatment having lower concentrations in *D. magna* compared to the two treatments with constant temperatures (excluded for the first sampling). However, a sharp contrast was also found between the two treatments with constant temperature, with higher Cu concentrations in the warmer treatment (Fig. 2F; Table S3). Therefore, for Cu in the water pathways clear-cut effects of both mean temperature ($HT_{const} > MT_{const}$) and of temperature oscillations ($MT_{const} > MT_{osc}$) were observed.

The selected model for both variables of rare earth elements (ΣREE and Ce) included the interactive term between treatment and sampling time (treated as categorical) (*M4*; Table 1 and S2). Fixed effects explained 28.8% and 25.5% variation in data, respectively (Table 1). The interactive term was significant for both variables, but treatment was also significant only for ΣREE. No temperature effects were found on the accumulation of rare earth elements via water pathway in our experiments (Fig. 2I, J; Table S3).

Discussion

Temperature oscillation alters bioaccumulation of Hg and other trace metals

The results of this study showed clearly that temperature oscillations have the potential to affect dramatically the accumulation of Hg species independently from the effects of mean temperature. Moreover, the observed accumulation patterns vary not only between IHg and MeHg but also between the trophic and the water pathways for MeHg, suggesting that temperature oscillations can have complex (and sometimes opposing) effects on living organisms. More precisely, the trophic pathway experiment showed clearly that i) IHg responded only to oscillations in temperature and not to changes in its mean value: oscillating temperature decreased in fact the concentrations of IHg in *D. magna* compared to the two treatments with constant temperature, whereas ii) MeHg responded only to changes in average temperature and not to its oscillations: the warmer treatment (HT_{const}) showed higher concentrations than both colder treatments (i.e., LT_{const} and MT_{osc}) independently of their temporal variation in temperature.

In the water pathway, whereas IHg displayed a pattern relatively similar (albeit less clear) to what was found for the trophic pathway, MeHg showed a distinct pattern with a significant effect of oscillating temperature observed only at the beginning (8 h) and at the end of the experiment (24 h), and no effect of neither average nor oscillating temperature for the second sampling (16 h). Surprisingly, these effects of oscillating temperature treatment showed an opposite pattern to what was found in the trophic pathway experiment, with higher concentrations of MeHg in *D. magna* compared to the two treatments with constant temperature. Despite being different from essential trace metals like Zn (class A metal), this latter observation on MeHg (class B metal) is similar to the finding from the laboratory studies performed by Watkins and Simkiss (1988a, b)[14,15], where the authors observed an increased concentration of spiked ^{65}Zn in the soft tissues of *Mytilus edulis* under an oscillating temperature treatment compared to a control with constant warmer temperature via a water pathway.

The accumulation patterns were also different between trophic and water pathways for the other metals. Similar to what was observed for IHg, the oscillating temperature significantly decreased the concentrations of non-spiked Fe, Zn, and Cu in *D. magna* via the trophic pathway compared to both treatments with constant temperatures. Among these metals, only Cu showed a clear negative effect of oscillating temperature also via the water pathway ($MT_{const} > MT_{osc}$). In addition, this metal responded also to mean temperature by increasing its concentration at higher temperature ($HT_{const} > MT_{const}$). These interesting results on Cu not only confirm that temperature oscillations can affect metal accumulation independently from the variation in mean temperature, but also that these two factors can have opposite effects. For Fe, we observed a negative effect of oscillating temperature on bioaccumulation via the water pathways, but only for one of the samplings (i.e., 16 h; Fig. 2B), and no effect of mean temperature. For Zn we observed a very similar pattern, but in this case the MT_{osc} treatment only differed from the HT_{const} treatment, and no strong conclusion could be drawn, since a proper comparison of the effects of oscillating temperature could only be accomplished by comparing MT_{osc} to MT_{const}. Whereas it is difficult to explain the observed temporal patterns for both Fe and Zn in the water pathways, it is clear that these results contrasted with those obtained via the trophic pathway. For rare earth elements, the oscillating temperature decreased the concentrations of ΣREE (albeit the temporal pattern is less clear relatively to the other elements) but showed no effect on Ce via the trophic pathway. No effect of temperature was not found via the water pathway for neither ΣREE nor Ce.

Integrating temperature oscillation in metal biodynamic model

Metal bioaccumulation can be greatly affected by temperature via its effects on multiple biological variables[26]. From a biodynamical modelling framework perspective[27], the parameters that facilitate metal bioaccumulation under constant temperatures include food ingestion rate (IR), assimilation efficiency (AE) and uptake directly from water, whereas the parameters hindering bioaccumulation include growth and excretion. Warmer temperatures could in fact boost certain metabolic processes in aquatic ectotherms including IR, AE, and the excretion of several trace metal pollutants, such as IHg and

MeHg, leading to overall increased bioaccumulation[6,12,13,28]. However, the results of this study showed that warmer temperature (HT_{const}) did not significantly increase the bioaccumulation of IHg and Zn in *D. magna* in both trophic and water pathways compared to the cooler temperature (MT_{const}), as well as for MeHg in the water pathway and Cu in the trophic pathway. This finding may be due to opposite effects of uptake and elimination rates neutralizing each other out for these trace metals under constant temperatures. On the other hand, clear effects of constant warmer temperature were observed in other cases, such as for MeHg and Fe in the trophic pathway and Cu in the water pathway. This might suggest that increasing temperature promotes more bioaccumulation than elimination processes for these trace metals, especially for MeHg, for which it is well known that the rate of excretion can be low in some species[6,29]. In this study the effects of growth on the overall bioaccumulation can be considered trivial since the *D. magna* individuals used here have already reached their maximal size (life cycle 14 days from neonate to reproductive adults) and no reproduction was observed for both experiments.

The comparisons of the results obtained under similar mean temperature but differing for the oscillating temperature pattern suggest that conceptual models such as the biodynamic model should consider daily changes in temperature, rather than the mean. In the trophic pathway experiment, only MeHg showed a similar bioaccumulation pattern between the two treatments with similar mean temperature but different oscillation regime (i.e., MT_{const} vs. MT_{osc}), whereas an increased accumulation was found in the water pathway under the oscillating temperature for this variable. In addition, a significantly decreased accumulation was found under the oscillating temperature for IHg and Cu in both trophic and water pathways, and for Fe and Zn in the trophic pathway. In these cases, it is reasonable to think that in addition to the constraints of the biodynamic model, additional biochemical changes can be important and differ between treatments with constant and oscillating temperatures. For example, Watkins and Simkiss (1988)[15] observed an increase of low molecular weight cytoplasmic protein (c. 3 kDa) and a decrease of high molecular weight ones (c. 70 kDa) in the digestive gland of *M. edulis* under oscillating temperature. Thus, it is possible that changes of intracellular ligand could be found in *D. magna* under oscillating temperature conditions, which may be responsible

for the observed accumulation pattern in the experiments. However, it is still unclear how the biomolecules of different molecular weight are distributed into the different subcellular fractions related to metal accumulation under oscillating temperature[30,31]. Moreover, the experimental design used by Watkins and Simkiss[14,15,19] did not allow to properly test the effects of oscillating temperature independently of the effects of mean temperature, since the mean temperature of the oscillating treatment differed from that of the other treatments, hindering to disentangle the effects of each source of variation. Additional studies should be undertaken on these metals vs pathways pairs, by comparing the biochemical changes and subcellular partitioning under mean versus oscillating temperature condition separately.

Implications for a changing environment

Living in a fluctuating environment may provide some advantage to some aquatic organisms to cope with environment pollution. For example, Gama-Flores et al. (2013)[32] and Hallman and Brooks (2015)[33] have reported increased tolerance of trace metal pollutants in rotifer and amphibian, respectively, by comparing individuals from oscillating temperature treatment to constant one, suggesting that some adaptative mechanisms could counteract the increased metal accumulation under a regime of oscillating temperature. The study performed by Watkins and Simkiss (1988b)[15] may provide one of the possible mechanisms to explain such enhanced tolerance, where the authors observed an increase in granular metal and a decrease in the cytosol fraction in *M. edulis*, which could lead to an induced detoxification. However, since they dealt with essential metals, mechanisms like homeostasis and hemocyanin production might have played a role in the accumulation of those metals. Thus, more studies like those of Watkins and Simkiss[14,15,19] and ours are needed to see how temperature fluctuations can affect essential vs non-essential metals (with active transport, for example) accumulation in aquatic ectotherms in a changing environment.

Several researchers have pointed out that the ecological effects expected under oscillating temperature conditions are distinct from those expected under constant

temperature ones[7,11,34]. It has been suggested that the temporal variation in environmental conditions can affect biological patterns and processes differently from the average condition (i.e., the so-called Jensen's inequality)[35]. However, there is still a lack of knowledge on the many biological processes of aquatic organism facing daily temperature changes, such as intertidal organisms or zooplankton performing diel vertical migration. Under the current global warming scenario, the temperature change and contaminant accumulation have been predicted to be of great importance for the future of aquatic food webs[12,13]. As showed by theoretical approaches, an increase of protein-binding pollutants such as MeHg is expected in aquatic food webs, whereas fat-soluble persistent organic pollutants, such as PCBs (polychlorinated biphenyls), are expected to decrease[12,13,36]. As discussed above, the mechanisms behind those modeling need to be carefully evaluated by taking into account the effects of temperature fluctuations.

Whereas our study contributed to fill a research gap, there is still a lack of knowledge on many biological processes concerning metal uptake and accumulation in aquatic ectotherms under realistic environmental temperature conditions. For example, it is still unclear whether the defense strategies of *Daphnia* against trace metal pollutants would be changed under natural conditions of temperature fluctuations. Whereas it is well documented that crustaceans can deposit trace metals in the carapace during the molt as a mechanism of detoxication[37,38,39], it is still unknown whether the natural temperature fluctuations would affect differently the frequency, the mortality risk due to molting, as well as the deposited quantity and quality of trace metal in the carapace. Reproduction is another important mechanism for *Daphnia* allowing to eliminate trace metal pollutants, such as inorganic Hg and MeHg under constant experimental temperatures[6]. However, the importance of reproduction on the elimination of trace metal pollutants may be affected not only by changes in average temperature, but also by changes in its temporal variance as expected in natural conditions under a warming climate scenario, and we hope that future studies will address these questions.

By showing that trace metal pollutant accumulation in zooplankton is affected by diel variations in water temperature via different pathways, our findings contributed to

bridge an important research gap in the literature. Our results show clearly, and for the first time, that not only temperature oscillations can affect metal accumulation in aquatic ectotherms independently from the variation in mean temperature, but also that these two factors can have opposite effects. Our findings corroborate the view that the ecological effects of oscillating temperature cannot be predicted based on observations conducted under constant temperatures by expanding the idea to metal contamination. We thus support the idea that it could be misleading to use the findings obtained at constant temperatures to explain the natural phenomena in conditions of oscillating temperature[7,34]. Although the study on the effects of fluctuating temperature on metal accumulation in aquatic organisms begun decades ago[14,15,19], this topic has not drawn enough attention from researchers and is still an under-explored research area. With climate change, both the amplitude and the average of the oscillating temperature in the environment may change, and consequently, a change in the accumulation patterns of trace metal pollutants would be expected. A framework is needed in an urge to reevaluate the cycling of trace metal pollutants in a fluctuating environment and to assess its risk to the health of aquatic ecosystems.

Acknowledgments

We would like to thank our laboratory assistants, namely, Caroline Macarez, Stéphanie L'Italien Simard. Also, to thank Valérie Godbout, Joanie Guay and Elois Veilleux from CEAEQ for their generous help with the free source of *D. magna*. A special thanks to Dominic Bélanger, Kathy St-Fort, and Maria Chrifi Alaoui for the sample analysis during the pandemic. We acknowledge funding from the Fonds Québécois de la recherche sur la nature et les technologies (FQRNT) (Grant No. 2016-PR-189982), Groupe de recherche interuniversitaire en limnologie et en environnement aquatique (GRIL), Centre de Recherche sur les Interactions Bassins Versants – Ecosystèmes Aquatiques (RIVE), the Canadian Foundation for Innovation and the Canada Research Chair Program.

References

(1) Ringelberg, J. (2009). Diel vertical migration of zooplankton in lakes and oceans: causal explanations and adaptive significances. *Springer Science & Business Media.*

(2) Le Jeune, A. H., Bourdiol, F., Aldamman, L., Perron, T., Amyot, M., Pinel-Alloul, B. (2012). Factors affecting methylmercury biomagnification by a widespread aquatic invertebrate predator, the phantom midge larvae *Chaoborus*. *Environ. Pollut*. *165*, 100-108. DOI: 10.1016/j.envpol.2012.02.003

(3) Odin, M., Ribeyre, F., Boudou, A. (1996). Temperature and pH effects on cadmium and methylmercury bioaccumulation by nymphs of the burrowing mayfly *Hexagenia rigida*, from water column or sediment source. *Arch. Environ. Contam. Toxicol. 31*(3), 339-349. DOI: 10.1007/BF00212672

(4) Inza, B., Ribeyre, F., Boudou, A. (1998). Dynamics of cadmium and mercury compounds (inorganic mercury or methylmercury): uptake and depuration in *Corbicula fluminea*. Effects of temperature and pH. *Aquat. Toxicol*. *43*(4), 273-285. DOI: 10.1016/S0166-445X(98)00055-1

(5) Rathore, R. S., Khangarot, B. S. (2002). Effects of temperature on the sensitivity of sludge worm *Tubifex tubifex* Müller to selected heavy metals. *Ecotoxicol. Environ. Saf*. *53*(1), 27-36. DOI: 10.1006/eesa.2001.2100

(6) Tsui, M. T., Wang, W. X. (2004). Temperature influences on the accumulation and elimination of mercury in a freshwater cladoceran, *Daphnia magna*. *Aquat Toxicol*. *70*(3), 245-256. DOI: 10.1016/j.aquatox.2004.09.006

(7) Hagstrum, D. W., Hagstrum, W. R. (1970). A simple device for producing fluctuating temperatures, with an evaluation of the ecological significance of fluctuating temperatures. *Ann. Entomol. Soc. Am*. *63*(5), 1385-1389. DOI: 10.1093/aesa/63.5.1385

(8) Karl, T. R., Kukla, G., Razuvayev, V. N., Changery, M. J., Quayle, R. G., Heim Jr, R. R., Easterling, D. R., Fu, C. B. (1991). Global warming: Evidence for asymmetric diurnal temperature change. *Geophys. Res. Lett*. *18*(12), 2253-2256. DOI: 10.1029/91GL02900

(9) Braganza, K., Karoly, D. J., Arblaster, J. M. (2004). Diurnal temperature range as an index of global climate change during the twentieth century. *Geophys. Res. Lett*. *31*(13). DOI: 10.1029/2004GL019998

(10) Vinnarasi, R., Dhanya, C. T., Chakravorty, A., AghaKouchak, A. (2017). Unravelling diurnal asymmetry of surface temperature in different climate zones. *Sci. Rep*. *7*(1), 1-8. DOI: 10.1038/s41598-017-07627-5

(11) Vasseur, D. A., DeLong, J. P., Gilbert, B., Greig, H. S., Harley, C. D., McCann, K. S., Savage, V., Tunney, T. D., O'Connor, M. I. (2014). Increased temperature variation poses a greater risk to species than climate warming. *Proc. R. Soc. B*. *281*(1779), 20132612. DOI: 10.1098/rspb.2013.2612

(12) Alava, J. J., Cheung, W. W., Ross, P. S., Sumaila, U. R. (2017). Climate change–contaminant interactions in marine food webs: Toward a conceptual framework. *Global change biology*. *23*(10), 3984-4001. DOI: 10.1111/gcb.13667

(13) Alava, J. J., Cisneros-Montemayor, A. M., Sumaila, U. R., Cheung, W. W. (2018). Projected amplification of food web bioaccumulation of MeHg and PCBs under climate change in the Northeastern Pacific. *Sci. Rep*. *8*(1), 1-12. DOI: 10.1038/s41598-018-31824-5

(14) Watkins, B., Simkiss, K. (1988a). The effect of oscillating temperatures on the metal ion metabolism of Mytilus edulis. *J. Mar. Biol. Assoc. U. K. 68*(1), 93-100. DOI: 10.1017/S0025315400050128

(15) Watkins, B., Simkiss, K. (1988b). Effects of temperature oscillations on the distribution of ^{65}Zn on cytoplasmic proteins. *Comp. Biochem. Physiol., Part C: Toxicol. Pharmacol. 89*(1), 53-55. DOI: 10.1016/0742-8413(88)90144-2

(16) Kainz, M. J., A. T. Fisk. (2009). Chapiter 5. Integrating Lipids and Contaminants in Aquatic Ecology and Ecotoxicology. In: Kainz, M. J., M. T. Brett, & M. T. Arts., (eds). Lipids in aquatic ecosystems (pp. 94-113). New York: *Springer-Verlag.*

(17) Amyot, M., Clayden, M. G., MacMillan, G. A., Perron, T., Arscott-Gauvin, A. (2017). Fate and trophic transfer of rare earth elements in temperate lake food webs. *Environ. Sci. Technol*. *51*(11), 6009-6017. DOI: 10.1021/acs.est.7b00739

(18) Liu, C., Yuan, M., Liu, W. S., Guo, M. N., Zheng, H. X., Huot, H., Jally, B., Tang, Y. T., Laubie, B., Simonnot, M. O., Morel, J. L., Qiu, R. L. (2021). Element case studies: rare earth elements. In: Van der Ent, A., Baker, A. J. M., Echevarria, G., Simonnot, M. O., Morel, J. L. (eds), Agromining: farming for metals (pp. 471-483). Switzerland Cham: *Springer*.

(19) Simkiss, K., Watkins, B. (1988). Metal ion activities in oscillating temperatures. *Mar. Environ. Res*. *24*(1-4), 125-128. DOI: 10.1016/0141-1136(88)90278-4

(20) Poulain, A. J., Amyot, M., Findlay, D., Telor, S., Barkay, T., Hintelmann, H. (2004). Biological and photochemical production of dissolved gaseous mercury in a boreal lake. *Limnol. Oceanogr*. *49*(6), 2265-2275. DOI: 10.4319/lo.2004.49.6.2265

(21) Gignac-Brassard, S. (2020). Les rôles relatifs de la prédation et des ressources sur la distribution verticale du zooplancton à travers un gradient de prédation des poissons dans les lacs boréaux. Master thesis. Univ. of Québec in Trois-Rivières.

(22) Lampert, W. (2011). Daphnia: Development of a Model Organism in Ecology and Evolution: International Ecology Institute. Germany: *Oldendorf/Luhe,*

(23) Perna, L., LaCroix-Fralish, A., Stürup, S. (2005). Determination of inorganic mercury and methylmercury in zooplankton and fish samples by speciated isotopic dilution GC-ICP-MS after alkaline digestion. *J. Anal. At. Spectrom*. *20*(3), 236-238. DOI: 10.1039/B410545A

(24) Hintelmann, H., Ogrinc, N. (2003) Chapiter 21: Determination of Stable Mercury Isotopes by ICP/MS and Their Application in Environmental Studies. In: Cai, Y., Braids, O. C., (eds) Biogeochemistry of Environmentally Important Trace Elements (pp. 321-338). *ACS symposium series Vol. 835.* DOI: 10.1021/bk-2003-0835.ch021

(25) Quinn, G. P., Keough, M. J. (2002). Chapter 6. Multiple and complex regression, 6.1 Multiple linear regression analysis, In: Quinn, G. P., Keough, M. J. (eds) Experimental design and data analysis for biologists (pp. 111-143). *Cambridge university press.*

(26) Wang, W. (2012). Biodynamics understanding of mercury accumulation in marine and freshwater fish. *Adv. Environ. Res*. 1(1), 15-35. DOI: 10.4319/lo.1996.41.2.0197

(27) Luoma, S. N., Rainbow, P. S. (2005). Why is metal bioaccumulation so variable? Biodynamics as a unifying concept. *Environ. Sci. Technol*. *39*(7), 1921-1931. DOI: 10.1021/es048947e

(28) Sokolova, I. M., Lannig, G. (2008). Interactive effects of metal pollution and temperature on metabolism in aquatic ectotherms: implications of global climate change. *Climate Research*. *37*(2-3), 181-201. DOI: doi.org/10.3354/cr00764

(29) Amlund, H., Lundebye, A.K. Berntssen, M.H.G. (2007). Accumulation and elimination of methylmercury in Atlantic cod (*Gadus morhua L*.) following dietary exposure. *Aquat. Toxicol. 83*(4), 323-330. DOI: 10.1016/j.aquatox.2007.05.008

(30) Wu, Y., Wang, W. X. (2011). Accumulation, subcellular distribution and toxicity of inorganic mercury and methylmercury in marine phytoplankton. *Environ. Pollut*. *159*(10), 3097-3105. DOI: 10.1016/j.envpol.2011.04.012

(31) Cardon, P. Y., Triffault-Bouchet, G., Caron, A., Rosabal, M., Fortin, C., Amyot, M. (2019). Toxicity and subcellular fractionation of yttrium in three freshwater organisms: *Daphnia magna*, *Chironomus riparius*, and *Oncorhynchus mykiss*. *ACS omega*. *4*(9), 13747-13755. DOI: 10.1021/acsomega.9b01238

(32) Gama-Flores, J. L., Huidobro-Salas, M. E., Sarma, S. S. S., Nandini, S. (2014). Combined effects of temperature (level and oscillation) and cadmium concentration on the demography of *Brachionus calyciflorus* (Rotifera). *Int. Rev. Hydrobiol*. *99*(1-2), 173-177. DOI: 10.1002/iroh.201301722

(33) Hallman, T. A., Brooks, M. L. (2015). The deal with diel: temperature fluctuations, asymmetrical warming, and ubiquitous metals contaminants. *Environ. Pollut*. *206*, 88-94. DOI: 10.1016/j.envpol.2015.06.005

(34) Niehaus, A. C., Angilletta Jr, M. J., Sears, M. W., Franklin, C. E., Wilson, R. S. (2012). Predicting the physiological performance of ectotherms in fluctuating thermal environments. *J. Exp. Biol*. *215*(4), 694-701. DOI: 10.1242/jeb.058032

(35) Ruel, J. J., Ayres, M. P. (1999). Jensen's inequality predicts effects of environmental variation. *Trends in Ecology & Evolution*. *14*(9), 361-366. DOI: 10.1016/S0169-5347(99)01664-X

(36) Borgå, K., Saloranta, T. M., Ruus, A. (2010). Simulating climate change-induced alterations in bioaccumulation of organic contaminants in an Arctic marine food web. *Environ. Toxicol. Chem*. *29*(6), 1349-1357. DOI: 10.1002/etc.159

(37) Weeks, J. M., Rainbow, P. S., Moore, P. G. (1992). The loss, uptake and tissue distribution of copper and zinc during the moult cycle in an ecological series of talitrid amphipods (Crustacea: Amphipoda). *Hydrobiologia*. *245*(1), 15-25. DOI: 10.1007/BF00008725

(38) Weis, J. S., Cristini, A., Ranga Rao, K. (1992). Effects of pollutants on molting and regeneration in Crustacea. *Am. Zool.*, *32*(3), 495-500. DOI: 10.1093/icb/32.3.495

(39) Factor, J. R. (Ed.). (1995). Biology of the Lobster: Homarus americanus. Academic Press.

Tables

Table 1. Results of the selected linear mixed models for each chemical variable, with the detected effects of independents terms. Only the fixed effects are shown; the random effect (i.e., the incubator) was taken into account in all models. Significant terms (alpha levels = 0.05) are in bold.

Experiment	Chemical variables (Concentrations)	Selected model	Marginal R^2
Trophic pathway	Inorganic ^{200}Hg	*M4*: **treatment** + **$time_{cat}$** + **treatment*$time_{cat}$**	*0.923*
	$Me^{198}Hg$	*M2:* **treatment** + **$time_{cat}$**	0.840
	Fe	*M2:* **treatment** + **$time_{cat}$**	0.574
	Zn	*M2:* **treatment** + **$time_{cat}$**	0.569
	Cu	*M1:* **treatment**+ time	0.280
	ΣREE	*M2:* **treatment** + **$time_{cat}$**	0.455
	Ce	*M1:* treatment+ **time**	0.164
Water pathway	Inorganic ^{200}Hg	*M4:* **treatment** + **$time_{cat}$** + **treatment*$time_{cat}$**	0.921
	$Me^{198}Hg$	*M4:* **treatment** + **$time_{cat}$** + **treatment*$time_{cat}$**	0.950
	Fe	*M4:* treatment + **$time_{cat}$** + **treatment*$time_{cat}$**	0.391
	Zn	*M4:* **treatment** + $time_{cat}$ + **treatment*$time_{cat}$**	0.342
	Cu	*M4:* **treatment** + $time_{cat}$ + **treatment*$time_{cat}$**	0.810
	ΣREE	*M4:* **treatment** + $time_{cat}$ + **treatment*$time_{cat}$**	0.288
	Ce	*M4:* treatment + $time_{cat}$ + **treatment*$time_{cat}$**	0.255

Figures

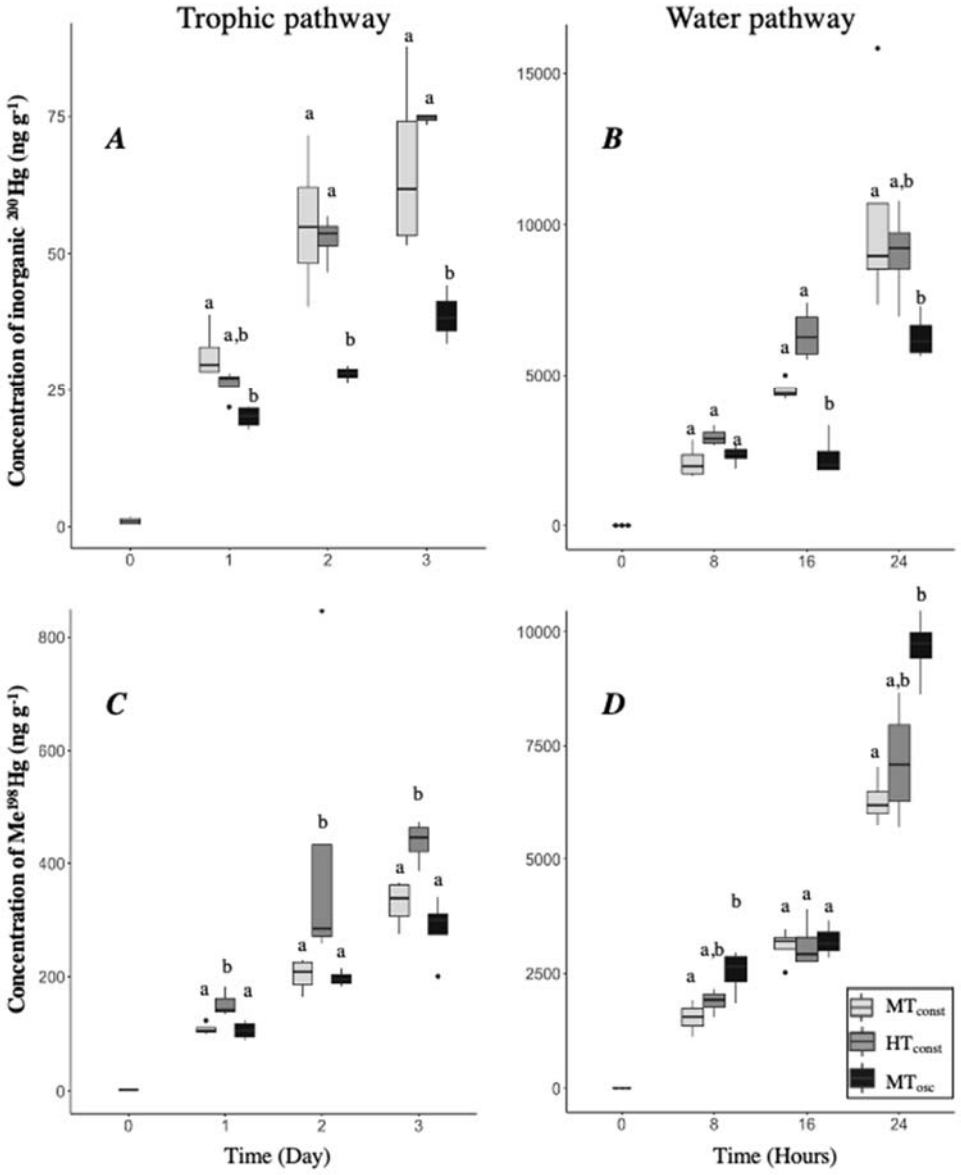

Fig. 1. Concentrations (ng g^{-1}) of inorganic ^{200}Hg (A, B) and Me^{198}Hg (C, D) over time in *Daphnia magna* in different temperature treatments (MT$_{osc}$: 7/23 ºC, HT$_{const}$: 23 ºC, MT$_{const}$: 15 ºC) in trophic pathway (A, C) and in water pathway (B, D). The significance of pairwise comparison is presented with lower-case letters above the boxplots. Note that the values at time 0 were included in the figure only for reference since they were not estimated in all the treatments and thus, they were not used in the analysis.

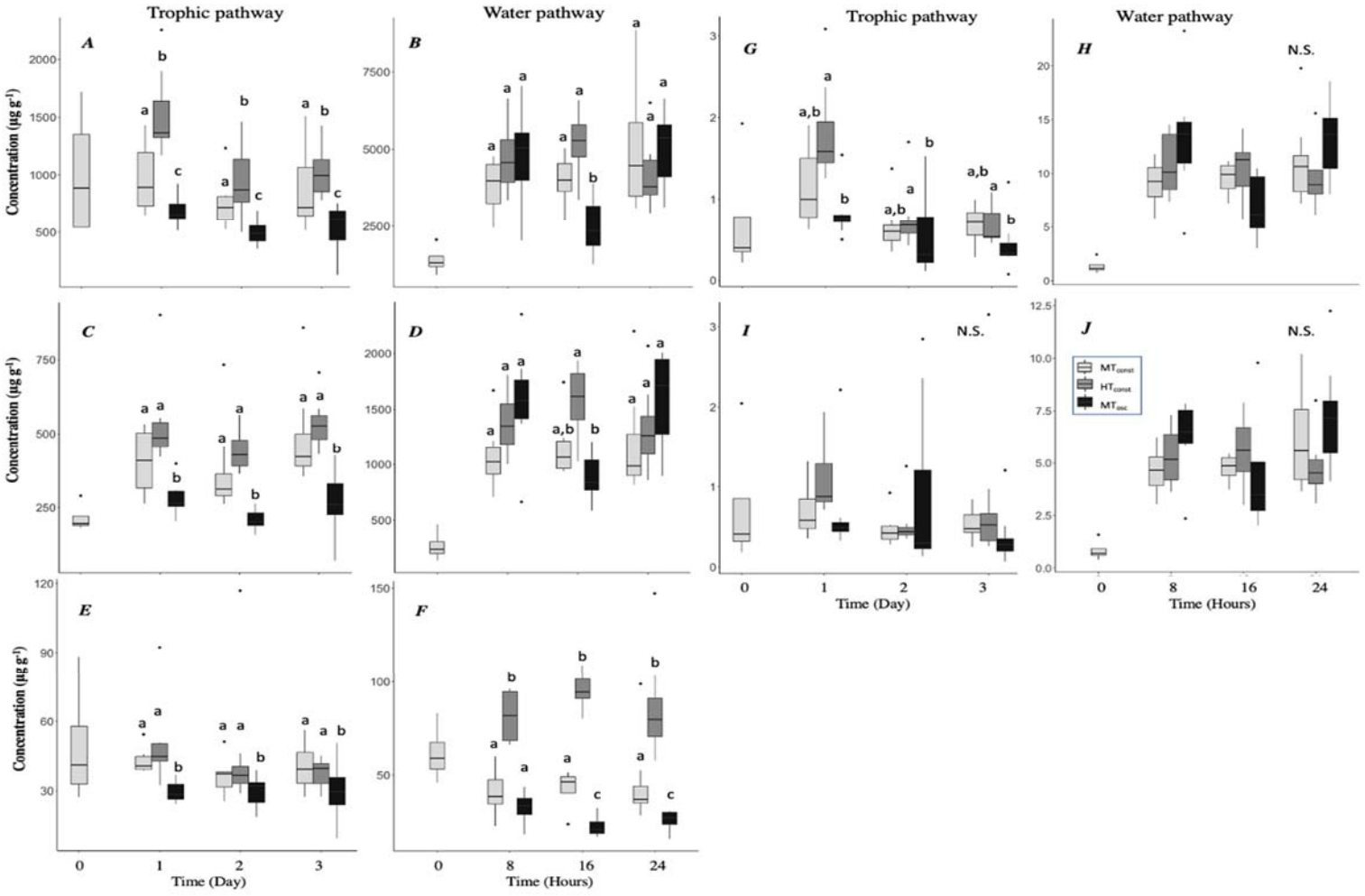

Fig. 2. Concentrations (µg g^{-1}) of Fe (A, B), Zn (C, D), Cu (E, F), ΣREE (G, H), and Ce (I, J) over time in *Daphnia magna* in different temperature treatments (MT_{osc}: 7/23 ºC, HT_{const}: 23 ºC, MT_{const}: 15 ºC) in trophic pathway (A, C, E, G, I) and in water pathway (B, D, F, H, J). See Fig. 1 for details.

Supplementary information

Experimental conditions

D. magna monoclonal culture (neonate) was obtained from the governmental laboratory at Centre d'Expertise en Analyse Environnementale du Québec (CEAEQ, Quebec City, Quebec). The culture was maintained in the prepared culture water (see below) at room temperature (20 ºC) with a photoperiod simulating local summer light cycles (16 h light: 8 h dark). They were fed with uncontaminated *Chlorella vulgaris* at a density of 10^6 cells mL^{-1} per day for one week until the individual grew to a properly large size for the experiments. The culture water was changed twice a week, with 1/3 of the water in the aquaria being replaced manually with freshly prepared water.

Dechloraminated water was used for both the *D. magna* culture and the experiments. Water hardness was adjusted with a solution made of $CaCl_2$ (187.1 g L^{-1}) and $MgCl_2$ (55.8 g L^{-1}) to equal 120 mg L^{-1} $CaCO_3$ (1 mL for 20 L dechloraminated water, É. Veilleux, CEAEQ, pers. comm.), and the pH was adjusted to about 7.3 by adding $NaHCO_3$ solution (18 g L^{-1}) (100 mL for 20 L dechloraminated water). The prepared water was aerated for three days before being used. The background concentration of total Hg and MeHg has been analyzed in water before the experiments.

Enriched inorganic ^{200}Hg and $Me^{198}Hg$ stock solutions ($^{200}HgCl_2$ and $Me^{198}HgCl$, respectively) were prepared in the chemical laboratory at the University of Montreal (Quebec, Canada). The stock solution of inorganic ^{200}Hg with a concentration of about 400 ng mL^{-1} was diluted from a commercial standard solution bought from Trace Sciences International Corp. Canada (#18b, 98.29%). The stock solution of $Me^{198}Hg$ was made by diluting a standard solution bought from the National Research Council of Canada's (NRC) Metrology Research Centre (EMMS-1, 96.45%) with a final concentration of about 107.5 ng mL^{-1}. Both prepared stock solutions were kept at 4 ºC until use.

Chlorella vulgaris was used as the vector of Hg species for food pathway experiments. The strain (CPCC 90 *Chlorella vulgaris*) was brought from Canadian

Phycological Culture Center (CPCC), Toronto. Three cultures of *Chlorella* with a volume of 1 L in each were prepared one week before the food pathway experiments with demineralized water. Only two of the cultures with a modified Bold Basal nutrient Medium (BBM) deficient in EDTA, Zn and Cu were spiked with either inorganic ^{200}Hg or $Me^{198}Hg$, whereas the third one with full nutrients was used for the control treatmen[1]. The lack of EDTA, Zn and Cu in the modified BBM medium aims to maximize the uptake of spiked Hg species by *Chlorella*[2]. The spiking of inorganic ^{200}Hg or $Me^{198}Hg$ was carried out on the third day after starting new *Chlorella* cultures following the same protocol as described in a previous study[3]. The algae were harvested on the seventh day when reaching the stationary phase. 150 mL of culture were filtered with fiberglass filters (pore size 1 μm) for the quantification of the concentrations of inorganic ^{200}Hg or $Me^{198}Hg$ in algae cells. *Chlorella* in the remaining culture was collected by centrifugation during which the cells were washed twice with demineralized water to remove aqueous mercury. The collected algae were divided equally into three portions and were stored in acid-washed centrifuge tubes (Fisherbrand™ Easy Reader™ Conical Polypropylene Centrifuge Tubes, sterile). All collected algae samples were stored at -20 ºC until use.

Table S1. Observed mortality and molts* of *D. magna* during the trophic pathway experiments and the water pathway experiments (MT_{const} =15 ºC; HT_{const} = 23 ºC; MT_{osc} = 7/23 ºC). (*: molts were unable to collected or to count, the quantity of molts was determined by water transparency).

		Sample 1		**Sample 2**		**Sample 3**	
Trophic pathway		**1st day**		**2nd day**		**3rd day**	
		mortality	molts	mortality	molts	mortality	molts
MT_{const}	control	-	-	-	-	7	few
	Inorganic ^{200}Hg	-	-	2	-	8	few
	$Me^{198}Hg$	-	-	-	-	4	few
HT_{const}	control	-	-	3	-	3	few
	Inorganic ^{200}Hg	-	-	-	-	6	few
	$Me^{198}Hg$	-	-	2	-	6	few
MT_{osc}	control	-	-	1	-	7	few
	Inorganic ^{200}Hg	-	-	1	-	4	few
	$Me^{198}Hg$	-	-	-	-	4	few

		8 h		**16 h**		**24 h**	
Water pathway							
		mortality	molts	mortality	molts	mortality	molts
MT_{const}	control	-	-	-	-	-	-
	Inorganic ^{200}Hg	-	-	-	-	1	many
	$Me^{198}Hg$	-	-	-	-	-	many
HT_{const}	control	-	-	-	-	2	-
	Inorganic ^{200}Hg	-	-	-	-	1	many
	$Me^{198}Hg$	-	-	-	-	2	many
MT_{osc}	control	-	-	-	-	-	-
	Inorganic ^{200}Hg	-	-	-	-	1	many
	$Me^{198}Hg$	-	-	-	-	8	many

Table S2. Results of model selection for each chemical variable. Selected models are in bold.

Experiments	Chemical variables	Model	AIC	ΔAIC	Degree of freedom
Trophic pathway	Inorganic ^{200}Hg	*M1*	-15.93	7.22	6
		M2	-18.94	4.21	7
		M3	-19.39	3.76	8
		M4	**-23.15**	**0**	**11**
	$Me^{198}Hg$	*M1*	6.68	4.19	6
		M2	**2.49**	**0**	**7**
		M3	10.05	7.56	8
		M4	6.94	4.45	11
	Zn	*M1*	348.65	9.89	6
		M2	**338.76**	**0**	**7**
		M3	349.87	11.11	8
		M4	343.73	4.97	11
	Fe	*M1*	419.24	7.69	6
		M2	**411.55**	**0**	**7**
		M3	420.11	8.56	8
		M4	414.84	3.29	11
	Cu	***M1***	**31.25**	**0**	**6**
		M2	32.66	1.41	7
		M3	33.99	2.74	8
		M4	38.36	7.11	11
	Ce	***M1***	**144.99**	**0**	**6**
		M2	145.88	0.89	7
		M3	147.95	2.96	8
		M4	149.50	4.51	11
	ΣREE	*M1*	-0.70	4.76	6
		M2	**-5.46**	**0**	**7**
		M3	-0.69	4.77	8
		M4	-3.08	2.38	11
Water pathway	Inorganic ^{200}Hg	*M1*	15.56	19.07	6
		M2	16.06	19.57	7
		M3	13.41	16.92	8
		M4	**-3.51**	**0**	**11**
	$Me^{198}Hg$	*M1*	-8.43	10.07	6
		M2	-15.10	3.4	7
		M3	-4.76	13.74	8
		M4	**-18.50**	**0**	**11**
	Zn	*M1*	44.54	17.76	6
		M2	43.51	16.73	7
		M3	48.06	21.28	8
		M4	**26.78**	**0**	**11**

Experiments	Chemical variables	Model	AIC	ΔAIC	Degree of freedom
	Fe	*M1*	64.86	27.36	6
		M2	61.16	23.66	7
		M3	66.14	28.64	8
		M4	**37.50**	**0**	**11**
	Cu	*M1*	16.22	6.67	6
		M2	18.13	8.58	7
		M3	15.56	6.01	8
		M4	**9.55**	**0**	**11**
	Ce	*M1*	66.02	9.65	6
		M2	63.87	7.5	7
		M3	66.94	10.57	8
		M4	**56.37**	**0**	**11**
	ΣREE	*M1*	69.42	20	6
		M2	63.87	14.45	7
		M3	71.63	22.21	8
		M4	**49.42**	**0**	**11**

Table S3. Post-hoc contrast comparison of temperature treatments in the selected model for each dependant variable with detected significant treatment effects. (MT_{const} =15 ºC; HT_{const} = 23 ºC; MT_{osc} = 7/23 ºC; CL = Confidence level). Confidence level and *p-value* were adjusted with Holm-Bonferroni method for all tests within one variable. Confidence level used: 0.95.

Experiment	*Chemical variables*	*Selected model*	*Sampling time*	*Contrast*	*df*	*lower. CL*	*upper. CL*	*t.ratio*	*p-value*
Food pathway	***Inorganic 2^{00}Hg***	***M4***	Day 1	MT_{const}–HT_{const}	47.1	-0.113	0.492	1.819	0.677
				MT_{const}–MT_{osc}	47.1	0.152	0.757	4.363	< 0.05
				HT_{const}-MT_{osc}	47.1	-0.038	0.568	2.543	0.129
			Day 2	MT_{const}–HT_{const}	47.1	-0.272	0.333	0.293	1.000
				MT_{const}–MT_{osc}	47.1	0.358	0.963	6.342	< 0.05
				HT_{const}-MT_{osc}	47.1	0.327	0.933	6.049	< 0.05
			Day 3	MT_{const}–HT_{const}	47.1	-0.453	0.152	-1.446	1.000
				MT_{const}–MT_{osc}	47.1	0.181	0.842	4.496	< 0.05
				HT_{const}-MT_{osc}	47.1	0.331	0.993	5.820	< 0.05
	Me^{198}Hg	***M2***	Day 1	MT_{const}–HT_{const}	17.7	-0.847	-0.019	-3.300	< 0.05
				MT_{const}–MT_{osc}	17.3	-0.343	0.480	0.527	1.000
				HT_{const}-MT_{osc}	17.7	0.088	0.916	3.822	< 0.05
			Day 2	MT_{const}–HT_{const}	17.7	-0.847	-0.019	-3.300	< 0.05
				MT_{const}–MT_{osc}	17.3	-0.343	0.480	0.527	1.000
				HT_{const}-MT_{osc}	17.7	0.088	0.916	3.822	< 0.05
			Day 3	MT_{const}–HT_{const}	17.7	-0.847	-0.019	-3.300	< 0.05
				MT_{const}–MT_{osc}	17.3	-0.343	0.480	0.527	1.000
				HT_{const}-MT_{osc}	17.7	0.088	0.916	3.822	< 0.05
	Fe	***M2***	Day 1	MT_{const}–HT_{const}	24.7	-8.400	-0.672	-3.566	< 0.05
				MT_{const}–MT_{osc}	24.7	1.590	9.319	4.290	< 0.05
				HT_{const}-MT_{osc}	23.1	6.200	13.783	8.055	< 0.05
			Day 2	MT_{const}–HT_{const}	24.7	-8.400	-0.672	-3.566	< 0.05
				MT_{const}–MT_{osc}	24.7	1.590	9.319	4.290	< 0.05
				HT_{const}-MT_{osc}	23.1	6.200	13.783	8.055	< 0.05

Experiment	*Chemical variables*	*Selected model*	*Sampling time*	*Contrast*	*df*	*lower. CL*	*upper. CL*	*t.ratio*	*p-value*
			Day 3	MT_{const}–HT_{const}	24.7	-8.400	-0.672	-3.566	< 0.05
				MT_{const}–MT_{osc}	24.7	1.590	9.319	4.290	< 0.05
				HT_{const}-MT_{osc}	23.1	6.200	13.783	8.055	< 0.05
	Zn	***M2***	Day 1	MT_{const}–HT_{const}	27.7	-5.150	1.060	-1.981	0.518
				MT_{const}–MT_{osc}	27.7	1.440	7.650	4.402	< 0.05
				HT_{const}-MT_{osc}	26.7	3.510	9.670	6.455	< 0.05
			Day 2	MT_{const}–HT_{const}	27.7	-5.150	1.060	-1.981	0.518
				MT_{const}–MT_{osc}	27.7	1.440	7.650	4.402	< 0.05
				HT_{const}-MT_{osc}	26.7	3.510	9.670	6.455	< 0.05
			Day 3	MT_{const}–HT_{const}	27.7	-5.150	1.060	-1.981	0.518
				MT_{const}–MT_{osc}	27.7	1.440	7.650	4.402	< 0.05
				HT_{const}-MT_{osc}	26.7	3.510	9.670	6.455	< 0.05
	Cu	***M1***		MT_{const}–HT_{const}	27.6	-0.338	0.183	-0.759	1.000
				MT_{const}–MT_{osc}	27.6	0.044	0.564	2.981	< 0.05
				HT_{const}-MT_{osc}	26.6	0.125	0.638	3.800	< 0.05
	ΣREE	***M2***	Day 1	MT_{const}–HT_{const}	25.2	-0.313	0.087	-1.709	0.898
				MT_{const}–MT_{osc}	24.5	-0.047	0.350	2.316	0.263
				HT_{const}-MT_{osc}	22.7	0.069	0.459	4.150	< 0.05
			Day 2	MT_{const}–HT_{const}	25.2	-0.313	0.087	-1.709	0.898
				MT_{const}–MT_{osc}	24.5	-0.047	0.350	2.316	0.263
				HT_{const}-MT_{osc}	22.7	0.069	0.459	4.150	< 0.05
			Day 3	MT_{const}–HT_{const}	25.2	-0.313	0.087	-1.709	0.898
				MT_{const}–MT_{osc}	24.5	-0.047	0.350	2.316	0.263
				HT_{const}-MT_{osc}	22.7	0.069	0.459	4.150	< 0.05
Water pathway	***Inorganic 2^{00}Hg***	***M4***	8 h	MT_{const}–HT_{const}	45.4	-0.762	0.056	-2.512	0.141
				MT_{const}–MT_{osc}	45.4	-5.534	0.284	-0.887	1.000
				HT_{const}-MT_{osc}	45.4	-0.181	0.637	1.625	1.000

Experiment	*Chemical variables*	*Selected model*	*Sampling time*	*Contrast*	*df*	*lower. CL*	*upper. CL*	*t.ratio*	*p-value*
			16 h	MT_{const}–HT_{const}	45.4	-0.752	0.066	-2.441	0.167
				MT_{const}–MT_{osc}	45.4	0.292	1.110	4.994	< 0.05
				HT_{const}-MT_{osc}	45.4	0.635	1.453	7.435	< 0.05
			24 h	MT_{const}–HT_{const}	45.4	-0.313	0.505	0.681	1.000
				MT_{const}–MT_{osc}	45.4	0.042	0.859	3.208	< 0.05
				HT_{const}-MT_{osc}	45.4	-0.054	0.764	2.527	0.136
	$Me^{198}Hg$	***M4***	8 h	MT_{const}–HT_{const}	44.1	-0.548	0.111	-1.933	0.537
				MT_{const}–MT_{osc}	44.1	-0.826	0.167	-4.391	< 0.05
				HT_{const}-MT_{osc}	44.1	-0.607	0.052	-2.458	0.161
			16 h	MT_{const}–HT_{const}	44.1	-0.334	0.325	-0.044	1.000
				MT_{const}–MT_{osc}	45.4	-0.397	0.317	-0.324	1.000
				HT_{const}-MT_{osc}	45.4	-0.392	0.322	-0.283	1.000
			24 h	MT_{const}–HT_{const}	44.1	-0.447	0.212	-1.037	1.000
				MT_{const}–MT_{osc}	44.1	-0.760	-0.101	-3.810	< 0.05
				HT_{const}-MT_{osc}	44.1	-0.643	0.016	-2.773	0.073
	Fe	***M4***	8 h	MT_{const}–HT_{const}	68.7	-0.654	0.209	-1.479	1.000
				MT_{const}–MT_{osc}	68.7	-0.636	0.226	-1.362	1.000
				HT_{const}-MT_{osc}	68.7	-0.414	0.449	0.116	1.000
			16 h	MT_{const}–HT_{const}	68.7	-0.690	0.172	-1.719	0.811
				MT_{const}–MT_{osc}	68.7	0.088	0.950	3.447	< 0.05
				HT_{const}-MT_{osc}	68.7	0.347	1.209	5.166	< 0.05
			24 h	MT_{const}–HT_{const}	68.7	-0.258	0.605	1.152	1.000
				MT_{const}–MT_{osc}	68.7	-0.446	0.416	-0.099	1.000
				HT_{const}-MT_{osc}	68.7	-0.620	0.243	-1.250	1.000
	Zn	***M4***	8 h	MT_{const}–HT_{const}	70.9	-0.671	0.122	-1.980	0.464
				MT_{const}–MT_{osc}	70.9	-0.762	0.031	-2.635	0.093
				HT_{const}-MT_{osc}	70.9	-0.487	0.306	-0.655	1.000

Experiment	*Chemical variables*	*Selected model*	*Sampling time*	*Contrast*	*df*	*lower. CL*	*upper. CL*	*t.ratio*	*p-value*
			16 h	MT_{const}–HT_{const}	70.9	-0.696	0.097	-2.161	0.307
				MT_{const}–MT_{osc}	70.9	-0.134	0.660	1.897	0.557
				HT_{const}-MT_{osc}	70.9	0.166	0.959	4.058	< 0.05
			24 h	MT_{const}–HT_{const}	70.9	-0.528	0.265	-0.951	1.000
				MT_{const}–MT_{osc}	70.9	-0.705	0.088	-2.226	0.263
				HT_{const}-MT_{osc}	70.9	-0.573	0.220	-1.275	1.000
	Cu	***M4***	8 h	MT_{const}–HT_{const}	61.1	-1.096	-0.358	-5.664	< 0.05
				MT_{const}–MT_{osc}	61.1	-0.182	0.555	1.454	1.000
				HT_{const}-MT_{osc}	61.1	0.545	1.282	7.119	< 0.05
			16 h	MT_{const}–HT_{const}	61.1	-1.169	-0.431	-6.235	< 0.05
				MT_{const}–MT_{osc}	61.1	0.266	1.004	4.950	< 0.05
				HT_{const}-MT_{osc}	61.1	1.066	1.804	11.186	< 0.05
			24 h	MT_{const}–HT_{const}	61.1	-1.039	-0.301	-5.224	< 0.05
				MT_{const}–MT_{osc}	61.1	0.123	0.861	3.835	< 0.05
				HT_{const}-MT_{osc}	61.1	0.793	1.531	9.058	< 0.05
	ΣREE	***M4***	8 h	MT_{const}–HT_{const}	66.7	-0.649	0.296	-1.069	1.000
				MT_{const}–MT_{osc}	66.7	-0.802	0.144	-1.996	0.450
				HT_{const}-MT_{osc}	66.7	-0.626	0.320	-0.927	1.000
			16 h	MT_{const}–HT_{const}	69.0	-0.562	0.411	-0.444	1.000
				MT_{const}–MT_{osc}	66.7	-0.075	0.870	2.409	1.169
				HT_{const}-MT_{osc}	69.0	-0.014	0.960	2.782	0.063
			24 h	MT_{const}–HT_{const}	66.7	-0.325	0.621	0.898	1.000
				MT_{const}–MT_{osc}	66.7	-0.653	0.292	-1.093	1.000
				HT_{const}-MT_{osc}	66.7	-0.801	0.144	-1.991	0.455
	Ce	***M4***	8 h	MT_{const}–HT_{const}	70.4	-0.636	0.342	-0.861	1.000
				MT_{const}–MT_{osc}	72.2	-0.789	0.220	-1.613	1.000
				HT_{const}-MT_{osc}	72.2	-0.642	0.367	-0.779	1.000

Experiment	*Chemical variables*	*Selected model*	*Sampling time*	*Contrast*	*df*	*lower. CL*	*upper. CL*	*t.ratio*	*p-value*
			16 h	MT_{const}–HT_{const}	72.2	-0.642	0.368	-0.777	1.000
				MT_{const}–MT_{osc}	70.4	-0.271	0.707	1.273	1.000
				HT_{const}-MT_{osc}	72.2	-0.150	0.860	2.010	0.433
			24 h	MT_{const}–HT_{const}	70.4	-0.241	0.738	1.454	1.000
				MT_{const}–MT_{osc}	70.4	-0.652	0.327	-0.951	1.000
				HT_{const}-MT_{osc}	70.4	-0.900	0.078	-2.405	0.169

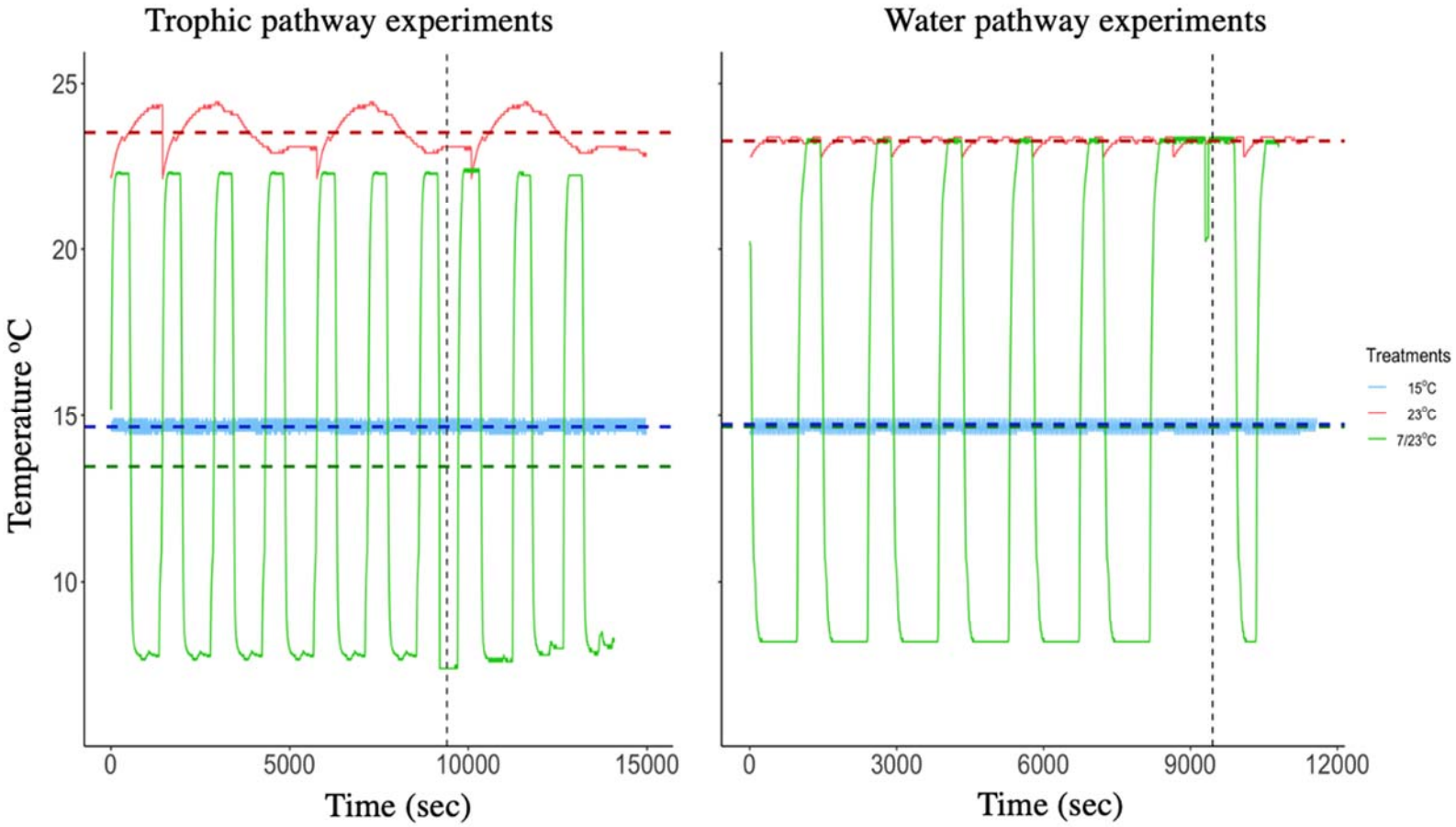

Fig. S1. Temperature recording during the experiments. Room temperature was 18 ºC during the trophic pathway experiments and 21 ºC during the water pathway experiments. Temperature was recorded with a submerged logger in an extra incubator without Daphnia. The vertical dotted line separates the acclimatation period (1 week; left side) and the exposition period (3 days for trophic pathway, 24 h for water pathway; on the right). The horizontal dotted lines correspond to the average temperature for each temperature treatment in each experiment.

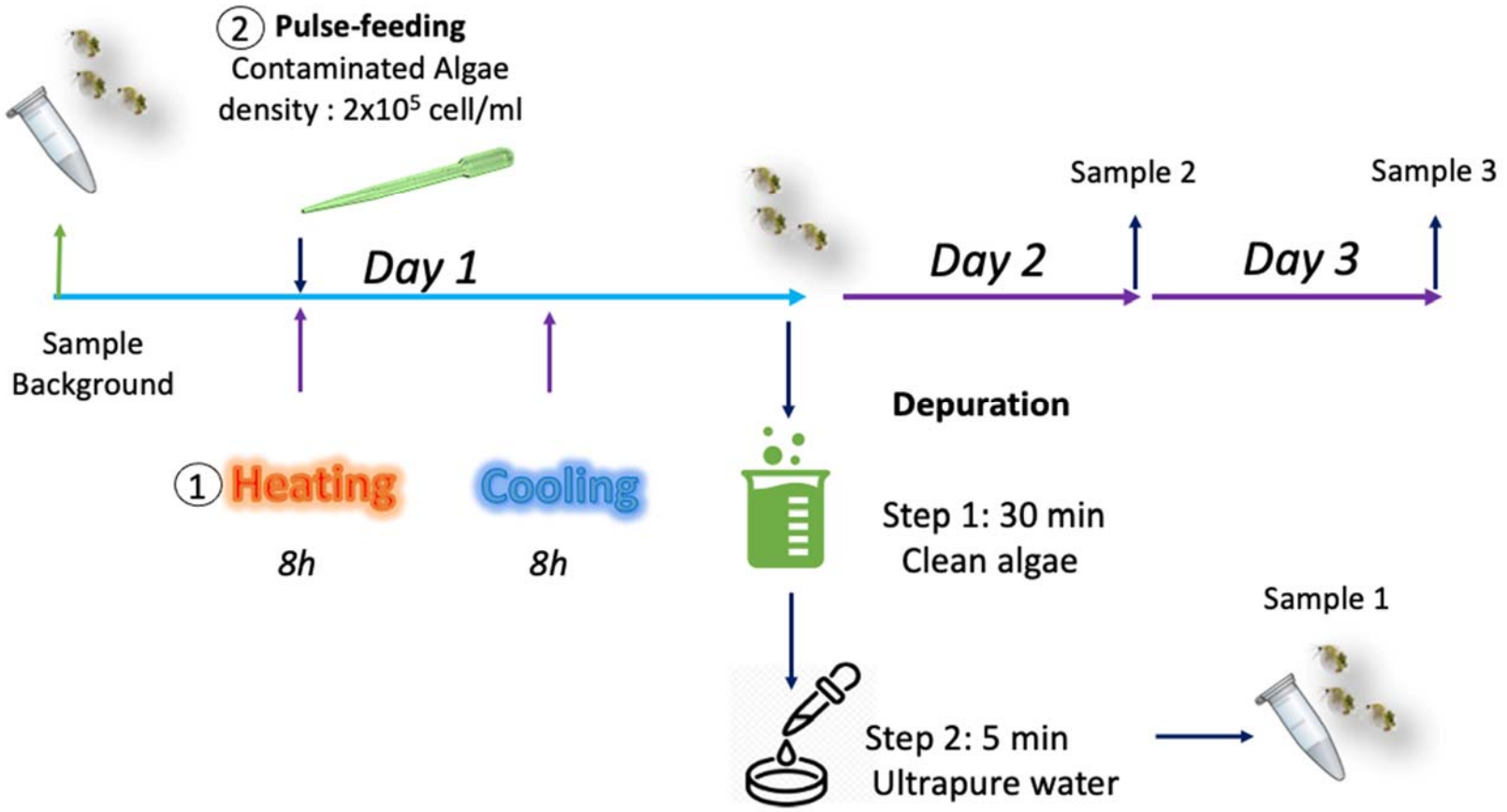

Fig. S2. Sampling schedule for trophic pathway experiments. Operations performed at the same moment were following the order indicated by circled number.

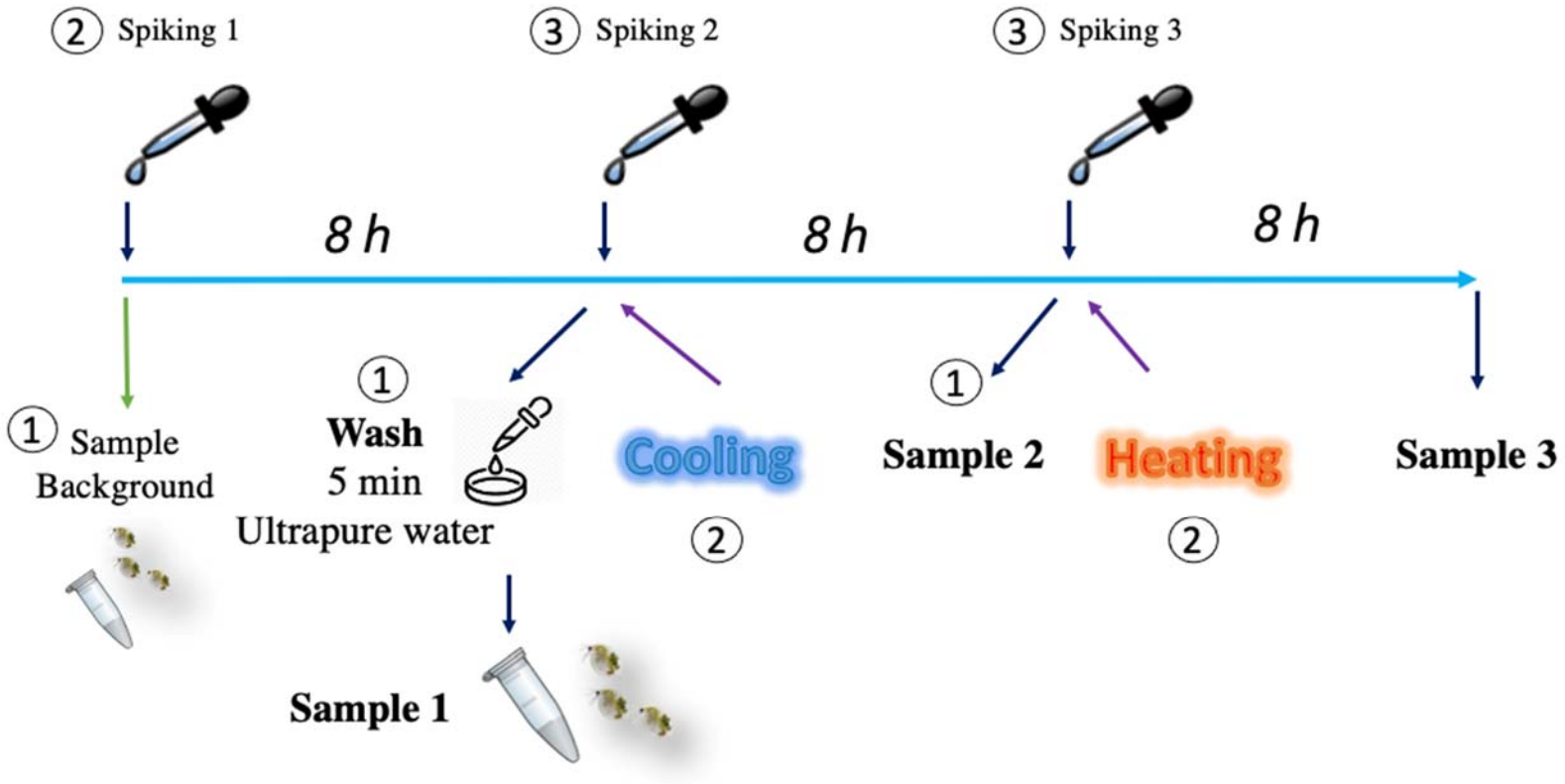

Fig. S3. Sampling schedule for water pathway experiments. Operations performed at the same moment were following the order indicated by circled number.

Reference

(1) Bischoff, H. W., Bold, H. C. (1963). Some algae from Enchanted Rock and related algal species. Phycological studies IV. *Univ. Texas Publ, (6318).*

(2) Wang, W. X., Fisher, N. S. (1996). Assimilation of trace elements and carbon by the mussel *Mytilus edulis*: effects of food composition. *Limnol. Oceanogr*. *41*(2), 197-207. DOI: 10.4319/lo.1996.41.2.0197

(3) Qin, F., Amyot, M., Bertolo, A. (2022). Grazer-mediated regeneration of methylmercury, inorganic mercury, and other metals in freshwater. *Sci. Total Environ*. 154553. DOI: 10.1016/j.scitotenv.2022.154553

CHAPITRE III

THE RELATIONSHIP BETWEEN ZOOPLANKTON VERTICAL DISTRIBUTION AND THE CONCENTRATION OF AQUEOUS HG IN BOREAL LAKES: A COMPARATIVE FIELD STUDY

Cet article est sous presse dans le périodique *Science of the total Environment*.

Fan Qin[1,2], Marc Amyot[2,3], Andrea Bertolo[1,2]

[1] Centre de recherche sur les interactions bassins versants – écosystèmes aquatiques (RIVE) and Département des sciences de l'environnement, Université du Québec à Trois-Rivières, 3351 Boul. des Forges, C.P. 500, Trois-Rivières QC G8Z 4M3, Canada

[2] Groupe de Recherche Interuniversitaire en Limnologie (GRIL), Université de Montréal, Campus MIL, C.P. 6128, Succ. Centre-ville, Montréal QC H3C 3J7, Canada

[3] Département de sciences biologiques, Université de Montréal, Campus MIL, C.P. 6128, Succ. Centre-ville, Montréal QC H3C 3J7, Canada

* corresponding author: fan.qin@uqtr.ca

Abstract

The production of the highly toxic monomethylmercury (MeHg) is heterogenous through the water column. Multiple factors have been identified to significantly affect this process, such as an extended anoxic water layer and a deep-water phytoplankton maximum. However, the role of water column heterogeneity on Hg cycling is still poorly known, especially concerning the role of zooplankton grazers. Here, we sampled four boreal lakes with contrasting characteristics (i.e., transparency and the presence/absence of fish) in order to maximize the heterogeneity in zooplankton abundance both among and within lakes and analyze their potential links with Hg vertical heterogeneity. The results showed that the presence of large copepods and medium-sized cladocerans was significantly associated with a decrease in the concentration of dissolved total Hg (DTHg) in the water at a given depth, whereas the presence of medium copepods significantly associated with the concentration of total Hg (THg). The presence of cladocerans was significantly associated with the ratio between the dissolved MeHg and DTHg. Phytoplankton biomass was directly correlated with the concentration of both dissolved and total MeHg, the methylation potential and the fraction of total MeHg in THg. At the same time, phytoplankton biomass was inversely related to the fraction of DTHg. Diel variations of the concentrations of both DTHg and THg was observed, with night samples significantly higher than day samples. Lower pH and higher concentration of DOC increased the concentrations of both DTHg and THg in the water column. These results highlighted the potential key role of water column heterogeneity, especially the abundance of zooplankton, on the cycling of total Hg and MeHg in boreal lakes.

Keywords: diel vertical migration, mercury, monomethylmercury, fish predation, invertebrate predators, grazing, zooplankton, freshwater lakes.

Introduction

As an ubiquitous trace metal, mercury (Hg) is considered an important pollutant in aquatic ecosystems, mainly due to its high toxicity, acting as a neurotoxin when presents in its organic form (monomethylmercury, MeHg), and its ability to be bioaccumulated and bioamplified in food webs to levels of great concern for human health (Ullrich et al., 2001; Jitaru et al., 2004). In the commonly accepted paradigm of environmental Hg cycling in freshwater ecosystems (Newman, 2009), elemental mercury is oxydized in the atmosphere, transferred on land by wet and dry deposition, and delivered to lake sediments within the landscape where it is methylated by multiple microorganisms possessing adequate gene clusters (e.g., *hgcAB*; Parks et al., 2013) under anoxic condition. However, as pointed out in a recent review on Hg methylation in oxic aquatic environments (Gallorini and Loizeau, 2021), the MeHg produced in the sediments is not necessarily related to the observed increasing concentration of Hg in fish, mainly due to the barrier between sediment and water phases. Thus, in the last two decades several studies have been conducted on other compartments of aquatic systems (e.g., water column) in order to locate other potential sources of MeHg production (Watras and Bloom, 1995; Eckley and Hintelmann, 2006; Guevara et al., 2008), which could potentially affect the Hg concentration in fishes.

Several factors could affect the speciation of Hg in the water column of freshwater lakes, with potential consequences for the production of highly toxic MeHg and its transfer in the aquatic food webs (Ullrich et al., 2001, Branfireun et al., 2020). For example, Ph has a predominant impact on the speciation of Hg in water. Indeed, fish in acidic lakes have been found to have higher Hg concentrations than those found in lakes with higher pH (Grieb et al., 1990; Wiener et al., 1990; Lange et al., 1993; Simonin et al., 2008). This phenomenon is not only explained by the fact that the lower pH conditions increase the bioavailability of Hg species and favors the activities of bacteria methylators, but also by the concomitant relatively high concentration of sulfates, which serve as electron acceptor in the redox reaction occurring during MeHg production (Bravo and Cosio, 2020). Solar radiation can also have a predominant role in the control of the Hg burden in some aquatic systems by the production of Hg(0) via photoreduction (Amyot et al., 1997;

Krabbenhoft et al., 1998; Garcia et al., 2005). In addition, oxic conditions are usually associated to a reduced activity of methylating bacteria in the water column, though some studies have shown possible methylation in the oxic water layer (Gallorini and Loizeau, 2021). Phytoplankton is another key biological factor having an important potential role in the speciation and cycling of Hg in lakes, as emphasized and detailed by Le Faucheur et al. (2014). In contrast, although zooplankton is considered an important biotic compartment in the trophic transfer of Hg in aquatic ecosystems, other potential roles of these organisms on the Hg cycling in the water column are poorly known. More precisely, their potential effects on Hg recycling via its grazing on phytoplankton, as demonstrated in experimental conditions (Qin et al., 2022), have not been taken into account explicitly in the current paradigm describing these cycles. The complex interplay between zooplankton and the above-mentioned factors in determining the speciation and the cycling of Hg is therefore still poorly understood.

Because of the strong heterogeneous and temporally variable distribution of zooplankton within the water column of lakes and oceans, grazing on phytoplankton in the water column probably varies with both space and time. A widely documented phenomenon illustrating such vertical heterogeneity is their diel vertical migration (DVM) behavior, which is represented by an ascent to the surface layers at sunset in lakes and oceans for feeding and a descent to the deep-water layers at sunrise to avoid fish predation and/or UV damage (Ringelberg, 2009). Preliminary field studies suggested that zooplankton grazing have the potential to affect the diel variation of the concentration and the distribution of multiple trace metals in coastal waters (Pinedo-Gonzalez et al., 2014). Laboratory studies confirmed that zooplankton grazing can have significant effects on the release of both inorganic Hg and MeHg in freshwater (Qin et al., 2022). However, very few studies in situ can be found to describe the effects of zooplankton behavior (e.g., grazing) on phenomena such as mercury recycling and speciation in freshwater ecosystems (Lejeune et al. 2012; Le Faucheur et al. 2014). It is therefore of interest to get a more integrated picture of the Hg cycle in freshwater systems by explicitly analyzing the relationship between the vertical distribution of resources, zooplankton behavior and the speciation of Hg.

The aim of this correlative field study is to establish a direct link between the heterogeneity of both abiotic factors (e.g., temperature and pH) and biotic (e.g., phytoplankton and zooplankton) in the water column and the diel variations in Hg profiles in oligotrophic boreal lakes. More specifically, our objective is to fill this knowledge gap by focussing on the potential role of zooplankton in Hg cycling in freshwater ecosystems by analyzing the relationship between the vertical heterogeneity of different forms of Hg in the water column and the distribution of different zooplankton taxa and size classes. Here, we hypothesize that (i) the abundance of zooplankton at a given depth correlates positively with the concentrations of both Hg and MeHg in the water column and affects its speciation in boreal lakes. As zooplankton is supposed to undergo a nocturnal ascent with an accelerated grazing in the epilimnion (Enright, 1977; Lampert, 2011), Hg compounds, either in the cytoplasm of algae or attached to their wall by their exudates (Mason et al. 1996; Wu and Wang, 2011) would thus be released directly by grazing. In addition, we hypothesize (ii) that the diel variation in Hg profile in lakes is a function of the heterogeneity in the water column, both in terms of abiotic (e.g., pH, sulfate, iron, etc.) and biotic factors (e.g., phytoplankton density) (Poulin et al., 2019; Bravo and Cosio, 2020; Gascón Díez et al., 2016), and (iii) that higher potential of Hg methylation would be expected in water layer with higher abundance of phytoplankton and zooplankton due to the increased bioavailability of Hg species because of zooplankton grazing (Coelho-Souza et al., 2006; Gascón Díez et al., 2016; Grégoire and Poulain, 2018; Qin et al., 2022; Yin et al., 2002).

Material and Methods

Study site and field sampling

Four boreal lakes (Fou, Chevaux, Solitaire, and Noir) in La Mauricie National Park of Canada (46°45'50.50"N, 73°1'37.93"W) were selected for the study (Fig. 1). None of the lakes had human development (e.g., cottages) within its watershed. The choice of the lakes was based on their contrasting characteristics, such as the presence versus the absence of fish and water clarity (Table 1; Gignac-Brassard et al 2022), which could have

profound effects on the heterogeneity of zooplankton distribution in the water column (Ringelberg. 2009), thus increasing the range of vertical heterogeneity within and among our study lakes. Otherwise, the lakes were also selected based on their relatively easy access, to optimize the collection and conservation of samples which can only be kept for a short period under summer temperature (see below).

Sampling was carried out between the middle of August and early September 2017. Vertical profiles of different biotic and abiotic variables (see below) were conducted in each lake during the same day at both noon (12:00 am) and midnight (00:00 am) at the deepest location. Vertical profiles included samplings taken at each 1 m depth intervals from 1 m to 9 m depth. Water samples were taken with a Teflon tube connected to a peristaltic pump. Before each sampling, the acid-washed (10% HCl) Teflon tube was rinsed with lake water for 1 min to avoid contamination of the samples or residual traces of acid. Water samples were taken by respecting the "ultraclean sampling principle" with nitrile gloves worn all the time. Unfiltered water samples for the analysis of total Hg and MeHg were collected by filling directly amber glass bottles previously washed with concentrated acid solution (50% HNO_3, 5% HCl, 45% ultrapure H_2O). Filtered water samples were collected by connecting a groundwater sampling capsule to the peristaltic pump (0.45 µm pore size, GWV High-Capacity Groundwater Sampling Capsules, Pall Laboratory, VWR) (Lejeune et al. 2012). For the analysis of dissolved Hg and MeHg, filtered water was collected with acid-washed amber glass bottles. For dissolved organic carbon (DOC), filtered water samples were collected with amber glass bottles previously treated in an oven heated to 550 ^{o}C for 2 hours. For anion sampling, filtered water sample was collected with acid-washed (10% HCl) high-density polyethylene (HDPE) sampling bottles (Thermo Scientific™ Nalgene™ Wide-Mouth HDPE Economy Bottles with Closure). Sterile metal-free tubes (VWR® Metal-Free Centrifuge Tubes, Polypropylene, Sterile) were used to sample filtered water for the analysis of cation. High purity HCl (Hydrochloric acid 32–35%, OmniTrace Ultra™ for trace metal analysis, VWR) was used to preserve the water samples for Hg and MeHg analysis (0.5 mL for 120 mL water sample), and for DOC analysis (30 µL for 15 mL water sample). High purity HNO_3 (Nitric acid 67 – 70%, OmniTrace Ultra™ for trace metal analysis, VWR) was used to preserve

water samples for cation analysis (0.3 mL for 15 mL water sample). All water samples were stocked in a cooler with ice packs for 24 h before being transferred to a cold chamber at 4 ^{o}C until being transported to the chemical laboratory at the University of Montreal for subsequent analysis.

Zooplankton was sampled with a 30 L Schindler-Patalas trap (63 µm mesh size) at the same depth as water samples immediately after water sampling. Zooplankton samples were preserved in a 120 ml plastic jars with 4% sucrose-formaldehyde solution, then were stored at room temperature until further analysis. The physicochemical profiles of the lakes (temperature, pH) were measured with an interval of 0.5 m from the water surface up to 12 m deep or to the bottom (Table 1) of the lake with a YSI multiparameter sonde 55b MPS (Yellow Springs Instruments, Yellow Springs, OH, USA). Chlorophyll-a profiles were measured with a submersible fluoroprobe probe (Submersible Spectrofluorometer for Algae Class and Chlorophyll-a Analysis, bbe Moldaenke GmbH, Germany). For each lake, the whole sampling took a 3 h-period around noon and midnight to be completed.

Sample analysis

Chemical analysis of total Hg and MeHg

Method 1631 EPA was applied for total Hg analysis in water samples. This analysis was performed with Tekran 2600 Automated Sample Analysis System CV-AFS (Tekran® Instrument Corp. Canada). In general, a 20 mL water sample was digested with 100 µl BrCl (full strength 100%) overnight in an analysis tube. Then, 25 µl hydroxylamine hydrochloride (30% m/v), 25 µl isopropanol, and 60 µl $SnCl_2$ (20% m/v) were subsequently added into the analysis tube before being quantified by Tekran 2600. The quality control of the analysis was carried out by intercalibrations with the Canadian Association for Laboratory Accreditation (CALA, Ottawa, Canada) using certified inorganic Hg solution (SPC Sciences, Montreal, Canada) with a recovery > 90%.

Method 1630 EPA was used for MeHg analysis in the water samples. The analysis was performed with Tekran 2700 Automated Methyl Mercury Analysis System (Tekran® Instrument Corp. Canada). Briefly, 45 ml water samples with 5 ml ultrapure water were placed in a Teflon analysis tube; the solution was then placed in the heater of a distillation module with the temperature at about 130 ºC until 45 ml of distilled water sample was recovered in the recipient Teflon tubes in the chiller part. A blank (45 mL ultrapure water) and a certified sample (Tort-2, 152 ng g^{-1} MeHg, National Research Council of Canada) were prepared at the same time. After the distillation, 30 µl ascorbic acid was added to the recipient Teflon tube and left for 5 min of chemical reaction. Subsequently, 30 ml of distilled water sample were transferred to the analysis tube. Before being quantified with Tekran 2700, 0.25 ml acetate buffer and 40 µl $NaB(Et)_4$ solution (4% m/v) were added into the analysis tube for derivatization reaction for about 15 min. The quality control of the analysis was ensured by the recovery of the certified sample (> 90%).

Besides the analyzed concentrations of Hg and MeHg, we have also estimated the following ratios to get a more complete picture of the speciation of Hg in the water column (Table 2):

1) Dissolved fraction of MeHg (DFM) = [dissolved MeHg] / [total MeHg]
2) Methylation ratio (MR) = [dissolved MeHg] / [dissolved Hg]
3) Dissolved fraction of total Hg (DFH) = [dissolved Hg] / [total Hg]
4) Fraction of total MeHg (FTM) = [total MeHg] / [total Hg]

Zooplankton analysis

Zooplankton samples were analyzed with a digital imaging system. They were first scanned with a ZooScan (Zooplankton Scanner V2, Hydroptic Inc. France). Then, the scanned image of each sample was processed with the ZooProcess image analyzer (Version 7.25) which separated the scanned images of each individual zooplankters (hereafter “vignettes”). The vignettes were subsequently uploaded to EcoTaxa (version 2.0, Picheral et al., 2017), a web application dedicated to visually exploring and identifying zooplankton based on a random forest algorithm. Then, a subset

of the automatically identified zooplankton was manually validated by a well-trained user (Gorsky et al. 2010). Based on the detected abundance, only five cladocerans (genus level: *Daphnia, Holopedium, Ceriodaphnia, Diaphanosoma;* family level: *Bosminidae*) and two copepods (subclass level: Calanoida and Cyclopoida) were retained for further analysis to model Hg data. This procedure also allowed to obtain the biometric variables (e.g., body length, surface area, etc.) of each detected particle in the sample. Zooplankton abundance was presented as the number of individuals per cubic meter and their size was estimated as the major axis of the ellipsoid covering at least 95% of the black pixels for each vignette. Three size classes of zooplankton were established based on the inspection of the size-frequency histograms with the pooled data from all the samples (72 samples from 4 lakes): small (< 0.6 mm), medium (0.6 to 1.2 mm) and large (> 1.2 mm) individuals. The invertebrate predator *Chaoborus* sp. (Diptera) larvae were also found in zooplankton samples and analyzed with the digital imaging system as for other zooplankton. The abundance of the invertebrate predator *Chaoborus* was used as an indirect indicator of fish predation on zooplankton distribution in this study because no data on the fish abundance was available for the study lakes.

Statistical modeling approach

A generalized additive modelling (GAM) approach was used to model the data collected from the field. The GAM approach is an extension of the generalized linear model (GLM) framework, in which each of the linear predictors is replaced by a non-parametric smoothing function (Wood, 2006). This approach also allows to combine, as in our case, linear and smoothing predictors in the same model (i.e., a "semi-parametric" model; Quinn and Keough 2002). More specifically, semi-parametric GAM models were built to analyze the relationship between the concentrations of different forms of Hg with depth (which is typically nonlinear based on preliminary inspection of the data), but also with different physicochemical (pH, temperature, the concentration of DOC and sulfate) and biological (Chla-a, zooplankton, and *Chaoborus*) variables to take into account potential non-linearity in the responses (Table 2). The concentration of Fe was also included in the model as a proxy of the

potential bacterial activities and redox potential in the water column, which are potential drivers of MeHg production (Hatch and Leventhal, 1992; Gascon et al., 2016; Bravo et al., 2018). In addition to modeling the concentrations of the four Hg variables, we have modeled the potential relationship between the calculated ratios of Hg data (see above) with the same set of abiotic and biotic variables (Table 3). A random factor for the lake was included in all the models to take into account the non-independency of the data belonging to the same vertical profile.

Some preliminary steps were taken prior to establish the final GAM models. First, for each of the continuous explanatory variables, we established if a linear or a non-linear relationship (i.e., spline) best modeled the relationship with the dependent variables (Table 3). This choice was based on the Akaike information criterion corrected for small samples (AICc) by comparing paired alternative models with or without a smooth function for each explanatory variable. For each comparison, we selected the model with the smaller AICc value (Quinn and Keough., 2002). In all cases, depth was always included in the models with a smooth function in interaction with sampling time (day vs night), which was treated as a categorical variable. Next, once we determined if a given variable was to be modeled with a linear or a smooth function, an automatic model selection (*drege*() function in the MuMin library of the R statistical language) was applied in order to choose a set of models for each of the Hg variables. The available biotic and abiotic variables (including the interaction mentioned above) were used to build all the possible models with a maximum model size of 7 corresponding to a ratio of 1:10 between the number of variables and the number of observations (i.e., 72 here). Among biotic variables, two sets of zooplankton variables (i.e., total vs. small, medium and large individuals) for each group (i.e., cladocerans and copepods) were used in the models, but were never included in the same model during the automatic model selection. Finally, all the models within the 95% confidence were kept in order to calculate model-averaged coefficients and 95% confidence interval for linear terms. The effect of each of the explanatory variables with linear effect on the Hg data in the water column was then determined by verifying the model-averaged coefficients, whereas the significance of the variable was determined by the confidence interval (CI), with those CI

not including the 0-value being considered as significant. For those explanatory variables modeled with a smooth function, it has not been possible to calculate averaged estimates, so their effects were analyzed graphically by plotting GAM predictions. Although it is not possible to determine the averaged estimation for explanatory variables modeled with a spline function in a GAM, the consistency of the results was confirmed by plotting the predictive values for all the alternative GAM models including a given (spline) variable (results not shown). This approach was used to model the variation in the dissolved and the total concentration of both Hg and MeHg in the water column, but also the calculated ratios relative to the Hg speciation in the water column. The % of the variation explained in the data was presented by R_{adj}^2 from the selected best model in the model selection for each dependant variable.

Results

Vertical profiles of Hg, MeHg and physicochemical variables in the water column

Clear differences in the ranges of concentrations for both Hg and MeHg in the water column were observed among lakes. The concentrations of total Hg in lakes Solitaire and Chevaux showed similar (and relatively low) ranges (0.28–0.99 ng L^{-1} and 0.29–0.71 ng L^{-1}, respectively), whereas lakes Fou and Noir showed ranges four- and ten-fold higher, respectively (1.54–2.71 ng L^{-1} and 0.59–6.12 ng L^{-1}, respectively) (Fig. 2). The ranges of MeHg concentrations were even more variable among lakes, with lake Solitaire showing the lowest values, with most samples having concentrations close to the detection limit of ICP-MS/MS (0.01 ng L^{-1}), whereas the highest concentrations of MeHg were found in lake Noir (0.05–1.24 ng L^{-1}) (Fig. 2). Lakes Chevaux and Fou showed intermediate values (0.02–0.11 ng L^{-1} and 0.08–0.19 ng L^{-1}, respectively). The importance of the dissolved Hg fraction also varied among lakes for both Hg and MeHg. More than 80% of Hg was dissolved in three out of four lakes, with the exception of lake Noir, where this fraction was clearly lower (i.e., 46%). Dissolved MeHg represented close to 60% of total Hg in the two clearest lakes (i.e., 60% and 57% for lakes Solitaire and Chevaux, respectively), whereas in the darkest lake, this fraction was close to 80% (i.e., 78% and

87% for lake Fou and Noir, respectively). Clear differences in the shape of the vertical gradients of both Hg and MeHg (both dissolved and total) have also been observed among the four lakes (Fig. 2). More precisely, i) for Hg (both total and dissolved), a strong vertical heterogeneity was observed in all cases, but the shape of the vertical profiles differed among lakes. The concentration of total Hg decreased slightly with depth in both lakes Solitaire and Chevaux, but slightly increased with depth in Lake Fou. Whereas in Lake Noir, the concentration of total Hg increased rapidly below the upper thermocline (2 m). ii) For MeHg (both total and dissolved), a strong vertical heterogeneity was observed only in Lake Chevaux and Lake Noir (Fig. 2). The concentration of MeHg slightly increased with depth in Chevaux but increased rapidly below the upper thermocline (2 m) in Noir, with a pattern similar to total Hg. The concentrations of MeHg remained relatively constant in lakes Solitaire and Fou.

The profiles of physicochemical variables also differed among the four lakes. Water stratification was observed in all lakes at the time of sampling with the epilimnion thickness varying between 2 m (lake Noir) and 6 m (lake Solitaire) (Table 1, Fig. S1). The concentrations of DOC and the pH remained relatively constant in the water column within each lake (Fig. S1). However, a gradient of DOC has been observed among the lakes: Solitaire (mean ± s.d.; 2.89 ± 0.12 mg L^{-1}) < Chevaux (3.73 ± 0.26 mg L^{-1}) < Fou (7.23 ± 0.22 mg L^{-1}) < Noir (11.33 ± 1.34 mg L^{-1}). Whereas in most cases the pH vertical profiles were rather constant, Lake Fou, the most acidic among the study lakes, showed a strong contrast between the surface (1 m, pH = 5.1) and the lower depth (9 m, pH = 3.8). A slight gradient of pH was observed among the other three lakes: Noir (5.4 ± 0.2) < Chevaux (5.7 ± 0.5) < Solitaire (6.2 ± 0.2). The profiles for the concentration of sulfates showed some variability among the lakes (Fig. S1), with relatively constant profiles observed in lakes Solitaire and Fou (20.6 ± 1.0 µmol L^{-1} and 23.8 ± 1.6 µmol L^{-1}, respectively) and strong gradients observed in the other two lakes. More precisely, i) in lake Chevaux, the concentrations of sulfates (24.9 ± 2.7 µmol L^{-1}) increased from the surface towards the thermocline (5 m), ii) whereas in Lake Noir, the concentrations (10.5–25.7 µmol L^{-1}) decreased below the thermocline (2 m). Both the concentrations of Fe and their variability in the water column increased from clear to brown lakes.

Relatively constant profiles of Fe concentrations in the water column have been observed in Lake Solitaire (1.39–5.79 µg L-1), the clearest lake (Fig. S1). A slight increase in Fe concentration has been observed around the thermocline in lakes Chevaux (8.92–75.81 µg L^{-1}) and Fou (96.8–293.6 µg L^{-1}) (Table 1, Fig. S1). Lake Noir, the darkest lake, showed the highest concentrations of Fe in the water column, varying between 50.4 µg L^{-1} (surface water) and 4094.6 µg L^{-1} (9 m depth). Phytoplankton concentrations and vertical profiles also varied clearly among lakes, with all lakes showing a deep chlorophyll maximum (DCM) except lake Solitaire (Fig. S1).

Inter-lake patterns in zooplankton abundance and water chemistry

The first two axes of the PCA on the biotic variables (zooplankton abundances and phytoplankton) explained together 62.7% variation (35.2% and 27.5% by Axes 1 and 2, respectively) in the data (Fig. 3a). The PCA showed a clear difference between fish and fishless lakes, with most samples from fishless lakes clustered towards the upper right side of the biplot, and the samples from fish lakes clustered towards its lower left side. In contrast, despite the fact that the ellipsoids roughly separated the four lakes in the biplot, there was no clear pattern related to water clarity along the first two axes. The first axis of the PCA contrasted Lake Noir from the other three lakes, and also showed that this lake had a stronger vertical gradient relatively to the other lakes (Fig. 3A). Samples from Lake Noir were spread along the positive part of the first axis, which correlated with phytoplankton, cladocerans (small- and medium-sized, and total), copepods (small-sized) and the sum of small zooplankton, whereas the negative part of the first axis correlated partly with the abundance of large cladocerans (Fig. 3A). The second axis correlated with the abundance of the *Chaoborus*, showing that this invertebrate predator was on average more abundant in fishless lakes (i.e., Solitaire and Noir) than in fish ones (i.e., Chevaux and Fou) (Fig. 3A). The negative part of the second axis correlated with cladocerans (large-size), copepods (medium- and large-size, ant total), and the sum of medium- and the sum of large-size zooplankton (Fig. 3A). Among all the sampled lakes, Noir had the highest abundance of small-size zooplankton, whereas Chevaux and Fou have a higher abundance of large-size zooplankton (Fig. S2, S3). The abundance of medium-size

zooplankton was similar among the four lakes. Regarding zooplankton groups, the highest abundance of cladocerans was found in Lake Noir, composed mostly of small- and medium-size, whereas large-size cladocerans was mostly found in lakes Chevaux and Fou (Fig. S3). The highest abundance of copepods was found in Chevaux and Fou (Fig. S2), composed mostly of medium-size copepods. Most abundant small-size copepods were found in Lake Noir, whereas medium-size copepods had similar abundances among sampled lakes (Fig. S2).

When only considering physicochemical variables in the PCA, the first two axes explained together 78.8% variation (56.4% and 23.4% by Axis 1 and 2, respectively) in the data (Fig. 3b). The ordination biplot showed that Axis 1 roughly separated the lakes according to water clarity; indeed, most samples from dark water lakes were on the left side of the biplot, whereas all samples from the clearwater lakes are clustered on the right side of the biplot. MeHg (both dissolved and total) and total Hg correlated closely with samples from Lake Noir, which yielded the highest concentrations among sampled lakes (Figs. 2 and 3B). Dissolved Hg correlated with both lakes Fou and Noir, which showed similar concentrations that were higher than clearwater lakes (Figs. 2 and 3B). DOC and Fe correlated better with samples from dark water lakes, and clustered together with Hg data, indicating positive correlations between these two variables and the concentrations of both Hg and MeHg in the water column. Sulfates correlated with the positive part of Axis 1 and the negative part of Axis 2, being inversely correlated to Ca and Mg concentrations, and, albeit less tightly, to MeHg concentrations (both dissolved and total). The second axis was also characterized by a strong pH gradient (positive part) which was inversely correlated with the concentration of dissolved Hg. The results from the two PCA showed strong a strong heterogeneity in the water column between and within sampled lakes.

Drivers of Hg and MeHg heterogeneity in the water column

Concentrations of Hg and MeHg

The multi-model inference approach to explain the concentration of dissolved Hg retained a total of 61 models that were within the 95%CI limits set of models (Table S1). The best of these models had a relatively low weight ($w_i = 0.154$) but explained 86.8% of the variation in the data. Despite a certain degree of uncertainty (since several models with each a relatively low weight were retained in the 95%CI limits set of models) to explain the variation in the concentration of dissolved Hg in the water column, some clear patterns could be found. More precisely, i) significant effects of DOC, pH, sampling time, sulfates, as well as the abundance of medium-size cladocerans and large-size copepods were found (Table 4). As predicted, ii) the concentration of DOC was directly related to the concentration of dissolved Hg. In contrast, iii) whereas a positive relationship was expected between zooplankton abundance and the concentration of dissolved Hg, an opposite effect was found, with the abundances of both medium-size cladocerans and large-size copepods being inversely related to the concentration of dissolved Hg in the water column (Table 4). iv) A similar effect was observed for pH and sulfates. Contrary to our predictions, v) the abundance of phytoplankton was inversely, albeit nonlinearly, related to the concentration of dissolved Hg in the water column (Fig. 4a). vi). Finally, a significant effect of the time of the day was observed, with on average higher concentrations of dissolved Hg during the night than during the day.

The multi-model inference approach to explain the concentration of total Hg retained a total of two models that were within the 95%CI limits (Table S2). The best of these models explained 96.9% of the variation in the data and had a relatively high weight ($w_i = 0.867$). For total Hg, explanatory variables, such as DOC, pH, and sampling at night showed similar significant effects as for dissolved total Hg. In addition, both total ($w_i = 0.07$) and medium-sized copepods ($w_i = 0.87$) showed a significant negative relationship with total Hg, (Table 4). It is important to note that these two copepod variables never occurred in the same model by construction (see Methods section) and that medium-size copepods were the dominant size class within this zooplankton group

(Fig. S2). The abundance of phytoplankton, albeit nonlinearly, positively related with the concentration of total Hg in the water column (Fig. 4b). Finally, the smoothing term for temperature was inversely related to the concentration of the total Hg, indicating higher concentrations of total Hg at lower and cooler water layers, and lower concentrations in warmer water layers (Fig. 4c).

The multi-model inference approach to explain the concentration of dissolved MeHg retained a total of five models that were within the 95%CI limits (Table S3). The best of these models explained 97.1% of the variation in the data and had a relatively high weight (w_i = 0.853). Only the abundance of phytoplankton showed a significant linear (positive) relationship with dissolved MeHg (Table 4). The concentration of DOC and Fe were positively (albeit nonlinearly) related to the concentration of dissolved MeHg in the water column, although at higher concentration of DOC, the concentration of dissolved MeHg dropped rapidly in the water column (Fig. 4e, 4f). Finally, the concentration of sulfates was inversely related to the concentration of dissolved MeHg in the water column (Fig. 4g).

The multi-model inference approach to explain the concentration of total MeHg retained a total of 84 models that were within the 95%CI limits (Table S4). The best of these models had a relatively low weight (w_i = 0.071) but explained 95.6% of the variation in the data. For total MeHg, both the abundance of phytoplankton and the concentration of DOC showed significant linear positive effects (Table 4). In contrast, the concentration of sulfates and the temperature, albeit nonlinearly, were inversely related to the concentration of total MeHg in the water column (Figs. 4d and 4h).

Hg ratios

The multi-model inference approach to explain the dissolved fraction of MeHg (DFM ratio) retained a total of 1253 models that were within the 95%CI limits (Table S5). The best of these models explained 16.2% of the variation in the data and had a relatively low weight (w_i = 0.013). For DFM ratio, only the concentration of Fe showed significant

positive effect (Table 5). These results show that not only there is a very large degree of uncertainty here (since a very large number of models was retained in the 95%CI limits set of models), but also that the selected models do not explain a large share of the variation in the DFM ratio.

The multi-model inference approach to explain the methylation rate (MR ratio) retained a total of 73 models within the 95%CI set of models (Table S6). The best of these models had a relatively low weight (w_i = 0.249) but explained 97.1% of the variation in the data. The MR ratio was significantly (positive) related with the abundance of phytoplankton and small-size cladocerans (Table 5). In contrast, the pH and the abundance of medium-size cladocerans showed significant relationships and being inversely related to the methylation rate in the water column (Table 5). The concentration of Fe, albeit nonlinearly, was positively related to the methylation rate (Fig. 5a).

The multi-model inference approach to explain the dissolved fraction of total Hg (DFH ratio) retained a total of 1109 models that were within the 95%CI limits (Table S7). The best of these models explained 39.9% of the variation in the data and had a relatively low weight (w_i = 0.015). For DFH ratio, only the abundance of phytoplankton showed significant negative effect (Table 5). These results show that not only there is a very large degree of uncertainty here (since a very large number of models was retained in the 95%CI limits set of models), but also that the selected models do not explain a large share of the variation in the DFH ratio.

The multi-model inference approach to explain the fraction of total MeHg in total Hg (FTM ratio) retained a total of 215 models that were within the 95%CI limits (Table S8). The best of these models had a relatively low weight (w_i = 0.028) but explained 88.5% of the variation in the data. For FTM ratio, the abundance of phytoplankton showed significant positive effect (Table 5). The concentration of sulfates, albeit nonlinearly, inversely related to the fraction of total MeHg (Fig. 5b).

Discussion

Our results show clearly that zooplankton vertical distribution is a relatively good predictor of Hg vertical heterogeneity, but that both zooplankton taxonomy and Hg species are to be taken into account. Indeed, although zooplankton was not significantly related to MeHg (both total and dissolved) our results clearly show that copepods were clearly associated with the concentration of total Hg in the water column. It is noteworthy that at least two of the Hg variables analyzed here (i.e. total Hg and dissolved MeHg) showed low uncertainty in model selection, with very few models retained in the 95% CI set of models. Besides this, the explained variation was not trivial for all the four Hg concentrations analyzed here, with a potential strong relationship also between zooplankton and dissolved Hg. Those results clearly showed that the zooplankton abundance is potentially a significant driver for the concentrations of both dissolved and total Hg in the water column, but not for the respective forms of MeHg. In addition, the impact of zooplankton on Hg likely depends on both the taxonomy and the size of the zooplankton in sampled lakes, with the medium size cladocerans and large copepods having the most impacts on the concentration of dissolved Hg, whereas the medium copepods showed a significant effect on the concentration of total Hg. However, in contrast to our initial hypothesis based on the release of Hg compounds by grazing (Mason et al. 1996), negative correlations were found between the abundance of zooplankton and the concentrations of dissolved and total Hg. On the other hand, these unexpected results are consistent with our previous findings on Hg release due to zooplankton grazing under controlled conditions (Qin et al., 2022), where we observed decreasing concentrations of total Hg in microcosm 30 min after adding copepods. This finding might be due to, at least for total Hg, a more efficient nocturnal grazing (Enright, 1977; Lampert, 2011), which could lead to significant grazing on the particulate portion of Hg (Qin et al., 2022). In the case of dissolved Hg, we could not rule out the uptake directly by the presence of zooplankton in the water column, as suggested by Tsui and Wang (2004a, b). These authors showed indeed that water exposure represents among the most important route for the accumulation of inorganic Hg in zooplankton. Furthermore, the observed diel variation for both dissolved and total Hg, which corresponds to higher concentrations in the water column during the night than during the

day, could also be explained by the nocturnal grazing of zooplankton, which leads to a decreased density of phytoplankton in the water column and, in turn, a weaker uptake of Hg from the aqueous environment (Gorski et al., 2005; Qin et al., 2022). This is supported by our results which showed that low phytoplankton density is associated to a relatively high concentration of dissolved Hg in water (Fig. 4a). Alternatively, if the night increase of total Hg cannot be explained by nocturnal grazing of zooplankton, other mechanisms may be involved. No correlation between zooplankton abundance and the concentrations of MeHg in the water column was found. These results are consistent with our previous observation under controlled conditions, where a high absorption of dissolved MeHg in water by living organisms (e.g., algae/bacteria) or the high adsorption on particle organic matter (POM) generated during the grazing may play important roles.

The potential effects of other factors on the concentrations of Hg and MeHg in the water column are also supported by our results. Significant positive correlations have been found between the density of phytoplankton and the concentrations of both dissolved and total MeHg. This result suggests that primary producers could be an important site for Hg methylation by providing DOC to boost microbial production (Eckley and Hintelmann, 2006; Huguet et al., 2010; Gascón Díez et al., 2016). In addition, primary producers may also provide ligands by exudation that could modify the bioavailability and facilitate the uptake of inorganic Hg for methylating microbes, as proposed in recent studies (Leclerc et al. 2015; Bouchet et al., 2018; Grégoire and Poulain, 2018). As for pH, a lower value corresponding to a high concentration of Hg is consistent with previous studies (Ulrich et al., 2001; Branfireun et al., 2020). The concentration of DOC is positively correlated with the concentration of Hg and MeHg in water, may indicated a transport of total Hg from the watershed and a stimulation of Hg methylation in a given depth in the water column, although the drop of dissolved MeHg concentration in Fig. 4e may suggest a threshold value, over which a great portion of dissolved MeHg may enter the particulate phase. The role of sulfates in the cycling of Hg is also supported by our results. As also shown by the PCA (Fig. 3b), the negative correlation between sulfates and Hg concentrations, especially for both MeHg forms, indicated a lower concentration of sulfates concomitant with a higher Hg methylation in the water column with the likely

involvement of sulfate-reducing bacteria. This observation has been confirmed by GAM models, which showed an inverse relationship between the concentration of sulfates and the concentration of total MeHg (Fig. 4d). The effect of Fe has only been found for MeHg (both dissolved and total), indicating a possible involvement of iron-reducing bacteria and favor redox potential in the production of MeHg (Fig. 4f). O_2 was not included in the modeling, because the calibration was not accurate for the exact values, but the profile in the water column was recorded correctly (Fig. S1) in each sampled lake. We thus explored its relationship with other variables in the PCA (Fig. 3b). The observation from this analysis indicated a favors hypoxia-anoxia condition for Hg methylation in the water column in samples lakes.

Despite a great deal of uncertainty was found in the model selection process for some calculated Hg ratios (> 1000 models were retained in the 95% CI set of models for both DFM and DFH ratio and > 200 for the FTM ratio), a relatively small uncertainty was observed for the MR ratio (73 models were retained in the 95% CI set of models). Thus, some interesting results were obtained also for the four variables expressed as ratios. Firstly, the results suggested a potential effect of zooplankton on the MR ratio (conventionally used as a proxy of methylation), but with mixed support for our hypothesis on Hg speciation (hypothesis (i)), with small- and medium-sized cladocerans showing, respectively, a positive and a negative relationship with this variable (Table 5). These apparently contradictory effects of cladocerans in different size classes suggest either a spurious correlation with some unmeasured variables for one of the size classes, or a possible effect of cladocerans size on grazing, which could potentially affect the MR ratio. Size-related zooplankton grazing effects have already been shown in copepods on DOC regeneration, where Møller, (2005) found a size ratio (predatory/prey) lower than the threshold of 55 is required to have a significant impact on the concentration of DOC. In our case, it is more difficult to explain why different size classes have opposite relationships with this ratio. Future studies are needed to clarify the size-related effects of zooplankton grazing on the partitioning of dissolved MeHg in dissolved total Hg. It is important to note that the relationship between the MR ratio and the potential methylation might differ among our sampled lakes. Indeed, the MR ratio might be a good proxy of

methylation for lakes such as lake Noir, which have a great potential for Hg methylation in the water column (e.g. because of the presence of a extended hypoxia-anoxia hypolimnion), whereas this ratio might only reflect the methylation potential in the surface water (e.g., Lake Solitaire), where other factors may influence the concentration of dissolved MeHg (e.g., photodemethylation) or the concentration of dissolved total Hg (e.g., the contribution from tributaries). However, after modeling the concentration of dissolved MeHg in the sampled lakes (data not shown), no effects of photodemethylation were observed in the first 3 m depth of water.

Other factors have also shown some correlations on the calculated ratios. Despite a certain degree of uncertainty in the results, the density of phytoplankton was associated with higher values of both MR and FTM ratio, which may be related to its potential role in Hg methylation (Huguet et al., 2010; Gascón Díez et al., 2016; Grégoire and Poulain, 2018). We also found that the DFH ratio was directly associated with Chl-a, suggesting a potential link with the observed relationship between the concentration of dissolved Hg and Chl-a, but these results should be taken cautiously given the high uncertainty and low explained variance for this variable. The positive correlation between Fe and the MR ratio (and also for DFM ratio, but with more uncertainty in our model selection process), suggests a possible involvement of iron-reducing bacteria. As for pH, lower value favors the concentration of MeHg in the MR ratio as discussed above. Finally, decreased concentration of sulfates may increase the concentration of total MeHg in the FTM ratio, as discussed above and as shown in Fig. 5b.

Conclusion

Despite its correlative nature, this study supports for the first time a potential important role of zooplankton as a driver for the Hg vertical heterogeneity in boreal lakes and contributes to the current understanding of Hg dynamics in freshwater ecosystems. As shown by our results, the potential effects of zooplankton on Hg concentration in the water column are taxon- and size-dependent, with medium-sized copepods abundance negatively correlated to the concentration of total Hg, and medium-sized cladocerans and

large-sized copepods negatively correlated to the concentration of dissolved Hg. Diel variation of dissolved and total Hg also have been observed, which could be due to the nocturnal grazing by the zooplankton. Unfortunately, introducing explicitly an interaction term between each zooplankton size class and time was not possible due to the reduced sample size, and we hope that future studies will shed light on this pattern. An interesting, albeit puzzling, size-related grazing effect has also been found for cladocerans, with small- and medium-sized cladocerans having opposite relationships with the PMR ratio. Whereas we cannot disentangle the full complexity of the relationships between Hg forms and grazers in natural lakes, our results clearly highlight the importance of the heterogeneity in their distribution in the water column in determining the vertical profiles of this contaminant. Besides confirming some previous findings on the role of physicochemical variables such as DOC and pH, especially the role of phytoplankton in Hg methylation, our results thus shed a new light on the potential role of zooplankton in the speciation of Hg and should open the way to broader in situ studies helping to clarify their full position in the Hg cycle.

Acknowledgments

We would like to thank La Mauricie National Park of Canada for access to the lakes and for helping with field logistics. We are grateful for Catherine Simard Dunn, Joëlle Guitard, Antoine Filion and Matteo Giacomazzo for the precious help in the field. Special thanks to Dominic Bélanger from Université de Montréal for the supervision of chemical analysis of the samples. We acknowledge funding from the Fonds Québécois de la recherche sur la nature et les technologies (FQRNT) (Grant No. 2016-PR-189982), Groupe de recherche interuniversitaire en limnologie et en environnement aquatique (GRIL; Joint Projects Grant Program), Centre de Recherche sur les Interactions Bassins Versants – Ecosystèmes Aquatiques (RIVE), the Canadian Foundation for Innovation and the Canada Research Chair Program.

Reference

Amyot, M., Lean, D., Mierle, G., 1997. Photochemical formation of volatile mercury in high Arctic lakes. *Environ. Toxicol. Chem. 16*(10), 2054-2063. https://doi.org/10.1002/etc.5620161010

Branfireun, B. A., Cosio, C., Poulain, A. J., Riise, G., & Bravo, A. G., 2020. Mercury cycling in freshwater systems-An updated conceptual model. *Sci. Total Environ. 745*, 140906. https://doi.org/10.1016/j.scitotenv.2020.140906

Bouchet, S., Goñi-Urriza, M., Monperrus, M., Guyoneaud, R., Fernandez, P., Heredia, C., Tessier, E., Gassie, C., Point, D., Guédron, S., Achá, D., Amouroux, D., 2018. Linking mi- crobial activities and low-molecular-weight thiols to Hg methylation in biofilms and periphyton from high-altitude tropical lakes in the Bolivian Altiplano. *Environ. Sci. Technol.* 52(17), 9758-9767. https://doi.org/10.1021/acs.est.8b01885

Bravo, A. G., Peura, S., Buck, M., Ahmed, O., Mateos-Rivera, A., Herrero Ortega, S., Schaefer, J. K., Bouchet, S., Tolu, J., Björn, E., Bertilsson, S., 2018. Methanogens and iron-reducing bacteria: the overlooked members of mercury-methylating microbial communities in boreal lakes. *Appl. Environ. Microbiol.* 84(23), e01774-18. https://doi.org/10.1128/AEM.01774-18

Bravo, A. G., Cosio, C., 2020. Biotic formation of methylmercury: a bio–physico–chemical conundrum. *Limnol. Oceanogr*, *65*(5), 1010-1027. https://doi.org/10.1002/lno.11366

Coelho-Souza, S. A., Guimaraes, J. R., Mauro, J. B., Miranda, M. R., Azevedo, S. M., 2006. Mercury methylation and bacterial activity associated to tropical phytoplankton. *Sci. Total Environ. 364*(1-3), 188-199. https://doi.org/10.1016/j.scitotenv.2005.07.010

Eckley, C. S., Hintelmann, H., 2006. Determination of mercury methylation potentials in the water column of lakes across Canada. *Sci. Total Environ. 368*(1), 111-125. https://doi.org/10.1016/j.scitotenv.2005.09.042

Enright, J.T., 1977. Diurnal vertical migration: adaptive significance and timing. Part 1. Selec- tive advantage: a metabolic model 1. *Limnol. Oceanogr.* 22 (5), 856-872. https://doi.org/10.4319/lo.1977.22.5.0856

Gallorini, A., & Loizeau, J. L., 2021. Mercury methylation in oxic aquatic macro-environments: a review. *Journal of Limnology*, *80*(2). https://doi.org/10.4081/jlimnol.2021.2007

Garcia, E., Amyot, M., & Ariya, P. A., 2005. Relationship between DOC photochemistry and mercury redox transformations in temperate lakes and wetlands. *Geochim. Cosmochim. Acta. 69*(8), 1917-1924. https://doi.org/10.1016/j.gca.2004.10.026

Gascón Díez, E., Loizeau, J.-L., Cosio, C., Bouchet, S., Adatte, T., Amouroux, D., Bravo, A.G., 2016. Role of settling particles on mercury methylation in the oxic water column of freshwater systems. *Environ. Sci. Technol*. 50, 11672-11679. https://doi.org/10.1021/acs.est.6b03260

Gignac Brassard, S., Rautio, M., Bertolo, A., 2022. The relative roles of predation and resources on zooplankton vertical distribution across a gradient of fish predation in boreal lakes. Freswhat. Biol. In revision

Gorski, P.R., Armstrong, D.E., Hurley, J.P., Shafer, M.M., 2006. Speciation of aqueous methyl- mercury influences uptake by a freshwater alga (*Selenastrum capricornutum*). *Environ. Toxicol. Chem.* 25 (2), 534-540. https://doi.org/10.1897/04-530R.1

Gorsky, G., M. D. Ohman, M. Picheral, S. Gasparini, L. Stemmann, L. B. Romagnan, A. Cawood, S. Pesant, and others., 2010. Digital zooplankton image analysis using the ZooScan integrated system. *J. Plankton Res*. 32: 285-303. https://doi.org/10.1093/plankt/fbp124

Grégoire, D.S., Poulain, A.J., 2018. Shining light on recent advances in microbial mercury cycling. *Facets* 3, 858-879. https://doi.org/10.1139/facets-2018-0015.

Grieb, T. M., Bowie, G. L., Driscoll, C. T., Gloss, S. P., Schofield, C. L., Porcella, D. B., 1990. Factors affecting mercury accumulation in fish in the upper Michigan peninsula. *Environ. Toxicol. Chem*. *9*(7), 919-930. https://doi.org/10.1002/etc.5620090710

Guevara, S. R., Queimaliños, C. P., del Carmen Diéguez, M., Arribére, M., 2008. Methylmercury production in the water column of an ultraoligotrophic lake of Northern Patagonia, Argentina.ù*Chemosphere*, *72*(4), 578-585. https://doi.org/10.1016/j.chemosphere.2008.03.011

Hatch, J. R., Leventhal, J. S., 1992. Relationship between inferred redox potential of the depositional environment and geochemistry of the Upper Pennsylvanian (Missourian) Stark Shale Member of the Dennis Limestone, Wabaunsee County, Kansas, USA. *Chem. Geol.*, *99*(1-3), 65-82. https://doi.org/10.1016/0009-2541(92)90031-Y

Huguet, L., Castelle, S., Schäfer, J., Blanc, G., Maury-Brachet, R., Reynouard, C., Jorand, F., 2010. Mercury methylation rates of biofilm and plankton microorganisms from a hy- droelectric reservoir in French Guiana. *Sci. Total Environ.* 408, 1338-1348. https://doi.org/10.1016/j.scitotenv.2009.10.058

Jitaru, P., Adams, F., 2004, December, Toxicity, sources and biogeochemical cycle of mercury. In Journal de Physique IV (Proceedings) (Vol. 121, pp. 185-193). EDP sciences. https://doi.org/10.1051/jp4:2004121012

Krabbenhoft, D. P., Hurley, J. P., Olson, M. L., Cleckner, L. B., 1998. Diel variability of mercury phase and species distributions in the Florida Everglades. *Biogeochemistry*, *40*(2), 311-325. https://doi.org/10.1023/A:1005938607225

Lampert, W., 2011. *Daphnia*: development of a model organism in ecology and evolution. In: Kinne, O. (Ed.) Series: Excellence in Ecology. International Ecology Institute.

Lange, T. R., Royals, H. E., Connor, L. L. (1993). Influence of water chemistry on mercury concentration in largemouth bass from Florida lakes. *Trans. Am. Fish. Soc. 122*(1), 74-84. https://doi.org/10.1577/1548-8659(1993)122<0074:IOWCOM>2.3.CO;2

Leclerc, M., Planas, D., Amyot, M., 2015. Relationship between extracellular low-molecular-weight thiols and mercury species in natural lake periphytic biofilms. *Environ. Sci. Technol. 49*(13), 7709-7716. https://doi.org/10.1021/es505952x

Le Faucheur, S., Campbell, P. G., Fortin, C., Slaveykova, V. I., 2014. Interactions between mercury and phytoplankton: speciation, bioavailability, and internal handling. *Environ. Toxicol. Chem.* 33(6), 1211-1224. https://doi.org/10.1002/etc.2424

Le Jeune, A. H., Bourdiol, F., Aldamman, L., Perron, T., Amyot, M., Pinel-Alloul, B., 2012. Factors affecting methylmercury biomagnification by a widespread aquatic invertebrate predator, the phantom midge larvae Chaoborus. *Environ. Pollut. 165*, 100-108. https://doi.org/10.1016/j.envpol.2012.02.003

Mason, R. P., Reinfelder, J. R., Morel, F. M., 1996. Uptake, toxicity, and trophic transfer of mercury in a coastal diatom. *Environ. Sci. Technol.* 30(6), 1835-1845. https://doi.org/10.1021/es950373d

Møller, E.F., 2005. Sloppy feeding in marine copepods: prey-size-dependent production of dis-solved organic carbon. *J. Plankton Res*. 27 (1), 27-35. https://doi.org/10.1093/plankt/fbh147

Newman, M. C., 2009. Fundamentals of ecotoxicology. *CRC press.*

Parks, J.M., Johs, A., Podar, M., Bridou, R., Hurt, R.A., Smith, S.D., Tomanicek, S.J., Qian, Y., Brown, S.D., Brandt, C.C., Palumbo, A.V., Smith, J.C., Wall, J.D., Elias, D.A., Liang, L., 2013. The genetic basis for bacterial mercury methylation. *Science* 339, 1332-1335. https://doi.org/10.1126/science.1230667.

Picheral, M., Colin, S., Irisson, J. O., 2017. EcoTaxa, a tool for the taxonomic classification of images. URL: http://ecotaxa.obs-vlfr.fr

Pinedo-Gonzalez, P., West, A. J., Rivera-Duarte, I., Sanudo-Wilhelmy, S. A., 2014. Diel changes in trace metal concentration and distribution in coastal waters: Catalina Island as a study case. *Environ. Sci. Technol* 48(14), 7730-7737. https://doi.org/10.1021/es5019515

Poulin, B.A., Ryan, J.N., Tate, M.T., Krabbenhoft, D.P., Hines, M.E., Barkay, T., Schaefer, J., Aiken, G.R., 2019. Geochemical factors controlling dissolved elemental mercury and methylmercury formation in Alaskan wetlands of varying trophic status. *Environ. Sci. Technol.* 53, 6203-6213. https://doi.org/10.1021/acs.est.8b06041

Qin, F., Amyot, M., Bertolo, A., 2022. Grazer-mediated regeneration of methylmercury, inorganic mercury, and other metals in freshwater. *Sci. Total Environ.* 829, 154553. https://doi.org/10.1016/j.scitotenv.2022.154553

Quinn, G.P., Keough, M.J., 2002. Chapter 6. Multiple and complex regression. In: Quinn, G.P., Keough, M.J. (Eds.), Experimental Design and Data Analysis for Biologists. *Cambridge University Press*, pp. 111-143.

Ringelberg, J., 2009. Diel vertical migration of zooplankton in lakes and oceans: causal explanations and adaptive significances. *Springer Science & Business Media*

Simonin, H. A., Loukmas, J. J., Skinner, L. C., Roy, K. M., 2008. Lake variability: key factors controlling mercury concentrations in New York State fish. *Environ. Pollut. 154*(1), 107-115. https://doi.org/10.1016/j.envpol.2007.12.032

Tsui, M. T., Wang, W. X., 2004a. Uptake and elimination routes of inorganic mercury and methylmercury in Daphnia magna. *Environ. Sci. Technol. 38*(3), 808-816. https://doi.org/10.1021/es034638x

Tsui, M. T., Wang, W. X., 2004b. Temperature influences on the accumulation and elimination of mercury in a freshwater cladoceran, Daphnia magna. *Aquat. Toxicol.* 70(3), 245-256. https://doi.org/10.1016/j.aquatox.2004.09.006

Ullrich, S. M., Tanton, T. W., Abdrashitova, S. A., 2001. Mercury in the aquatic environment: a review of factors affecting methylation. *Crit. Rev. Environ. Sci. Technol*. 31(3), 241-293. https://doi.org/10.1080/20016491089226

Watras, C. J., Bloom, N. S. 1994. The vertical distribution of mercury species in Wisconsin lakes: accumulation in plankton layers. *Mercury pollution: integration and synthesis*, 137-152.

Wiener, J. G., Martini, R. E., Sheffy, T. B., Glass, G. E., 1990. Factors influencing mercury concentrations in walleyes in northern Wisconsin lakes. *Trans. Am. Fish. Soc. 119*(5), 862-870. https://doi.org/10.1577/1548-8659(1990)119<0862:FIMCIW>2.3.CO;2

Wood, S. N., 2006. Generalized additive models: an introduction with R. *chapman and hall/CRC.*

Wu, Y., Wang, W. X., 2011. Accumulation, subcellular distribution and toxicity of inorganic mercury and methylmercury in marine phytoplankton. *Environ. Pollut. 159*(10), 3097-3105. https://doi.org/10.1016/j.envpol.2011.04.012

Yin, X., Wang, L., Liang, X., Zhang, L., Zhao, J., Gu, B., 2022. Contrary effects of phytoplankton Chlorella vulgaris and its exudates on mercury methylation by iron-and sulfate-reducing bacteria. *J. Hazard. Mater. 433*, 128835. https://doi.org/10.1016/j.jhazmat.2022.128835

Tables

Table 1. Characteristics of the selected lakes in La Mauricie National Park of Canada, Quebec, Canada. Fish: 1 = presence; 0 = absence. K_{dPAR} = light attenuation coefficient for visible light. The lakes are ordered following a gradient of transparency.

Lake	Coordinates	Fish	Secchi depth (m)	Upper thermocline (m)	Lower thermocline (m)	$K_{d\ PAR}$	Maximum depth (m)
Solitaire	46°45'01.7"N 72°49'45.6"W	0	9.5	6	> 9	0.3	35
Chevaux	46°44'59.9"N 72°50'12.6"W	1	7.4	5	7	0.7	18.5
Fou	46°46'54.8"N 72°52'42.0"W	1	1.9	4	6	1.2	30
Noir	46°46'24.3"N 72°49'46.1"W	0	1.5	2	4	1.5	10

Table 2. Explanatory variables used to model the concentration of Hg species in the water column during a 24 h cycle in the four study lakes.

Variable		Description	Data type	Range
Depth		Sampled depth begin with 1 m under surface water, samples were taken at each 1 m until 9 m depth. (m)	ordinal	1–9
Time		Samples were taken at noon (12:00) and midnight (0:00)	categorical	noon / midnight
pH		pH measured at each 1 m until 12 m depth (only 9 m for lake Noir)	continuous	3.75–6.39
Temperature		Temperature was measured at each 1 m until 12 m depth (only 9 m for lake Noir) (^{o}C)	continuous	3.3–20.6
DOC		Concentration of dissolved organic carbon measured at each 1 m until 9 m depth. (mg L^{-1})	continuous	2.6–13.1
Fe		Concentration of Fe in each 1 m water layer until 9 m, the values were log transformed in GAMs models due to the great variation between lakes	continuous	0.1–3.7
SO_4^{2-}		Concentration of sulfate in each 1 m water layer until 9 m (µmol L^{-1})	continuous	10.4–29.5
Chao		Calculated abundance of Chaoborus (individual L-1) in each 1 m water layer until 9 m, used as an indicator indirect for fish predation on zooplankton (individual L^{-1})	continuous	0–0.4
Algae density		Density recorded continuously with fluoroprobe until 12 m in the water column (only 9 m for lake Noir)	continuous	0–20
Zooplankton	Taxon	Calculated abundance of zooplankton (individual L^{-1}) per taxon in each 1 m water layer until 9 m. The taxon was separated roughly into copepods and Cladocera based on detected species (individual L^{-1})	continuous	0.7–22.7
	Size	Calculated abundance of zooplankton (individual L^{-1}) per size in each 1 m water layer until 9 m. The size was separated roughly into 3 class based on the inspection of size frequency in all samples. (individual L^{-1})	continuous	0–21.8

Table 3. GAMs models established for each dependant variables. The interaction term between time and the smooth function for depth (fixed terms), as well the random factor lake was included in all the models since they represented the sampling design. The automatic model selection was thus applied only on the other variables. The smooth function for other explanatory variables has been determined based on a pre-screening (see methods section for more details). For each model, bold indicates the variables for which we expect the strongest effects based on a priori hypothesis.

	Variable	GAMs models
Concentrations	Dissolved Hg	= s(depth x time) + time + pH + temperature + **DOC** + SO_4^{2-} + Fe + Chao + **s(algae)** + **zooplankton**
	Total Hg	= s(depth x time) + time + pH + s(temperature) + **DOC** + SO_4^{2-} + Fe + Chao + **s(algae)** + **zooplankton**
	Dissolved MeHg	= s(depth x time) + time + pH + s(temperature) + **s(DOC)** + s(SO_4^{2-}) + s(Fe) + Chao + **algae** + **zooplankton**
	Total MeHg	= s(depth x time) + time + pH + s(temperature) + **DOC** + s(SO_4^{2-}) + s(Fe) + Chao + **algae** + **zooplankton**
Ratios	Dissolved fraction of MeHg DFM = (dissolved/total) MeHg	= s(depth x time) + time + pH + temperature + **DOC** + SO_4^{2-} + Fe + Chao + **algae** + **zooplankton**
	Proxy of methylation rate PMR = dissolved (MeHg/Hg)	= s(depth x time) + time + pH + s(temperature) + **s(DOC)** + SO_4^{2-} + s(Fe) + Chao + **algae** + **zooplankton**
	Dissolved fraction of total Hg DFH = (dissolved/total) Hg	= s(depth x time) + time + pH + temperature + **DOC** + SO_4^{2-} + Fe + Chao + **algae** + **zooplankton**
	Fraction of total MeHg FTM = total (MeHg/Hg)	= s(depth x time) + time + pH + s(temperature) + **DOC** + s(SO_4^{2-}) + Fe + Chao + **algae** + **zooplankton**

Table 4. Summary of weighted coefficients and confidential intervals (CI) for linear explanatory variables with significant effect on the concentrations of Hg and MeHg based on the 95% set of models (i.e., those with a cumulative weight < = 0.95). Note that here only variables with a CI not including the zero value are shown. (CopM, CopL = abundance of medium- and large-size copepods, respectively; CladoM = abundance of medium-size Cladocera; SumCop = abundance of the sum of copepod). Since it is not possible to estimate weighted coefficients for explanatory variables modeled with a smooth function (indicated by an asterisk), here we only show the ones retained in the 95% set of models together with their relative weight (Wt). For these variables, we show predicted values based on the best-ranking model containing the variable based on the AICc (see Fig. 4 for more information).

Hg data	Variables	Weighted coefficient	Lower CI	Upper CI	Wt
Dissolved Hg	DOC	1.19e-01	5.75e-02	1.81e-01	0.95
	pH	-4.92e-01	-6.16e-01	-3.67e-01	0.95
	Diel variation	1.15e-01	1.56e-03	2.29e-01	0.95
	Phytoplankton*				0.89
	SO_4^{2-}	-3.00e-02	-5.03e-02	-9.63e-03	0.58
	CladoM	-4.47e-02	-8.47e-02	-4.55e-03	0.36
	CopL	-2.77e-01	-5.40e-01	-1.41e-02	0.26
Total Hg	DOC	1.50e-01	1.00e-01	2.00e-01	0.94
	pH	-5.99e-01	-7.79e-01	-4.18e-01	0.94
	Phytoplankton*				0.94
	Temperature*				0.94
	Diel variation	1.37e-01	2.62e-02	2.48e-01	0.94
	CopM	-4.04e-02	-6.25e-02	-1.84e-02	0.87
	SumCop	-2.52e-02	-4.37e-02	-6.68e-03	0.07
Dissolved MeHg	phytoplankton	2.07e-02	1.28e-02	2.86e-02	0.94
	DOC*				0.94
	Fe*				0.94
	SO_4^{2-}*				0.87
	Temperature*				0.01
Total MeHg	phytoplankton	4.85e-02	3.85e-02	5.85e-02	0.95
	SO_4^{2-}*				0.95
	Temperature*				0.73
	DOC	2.15e-02	9.95e-04	4.21e-02	0.35
	Fe*				0.26

Table 5. Summary of weighted coefficients and confidential intervals for explanatory variables with significant effect on the calculated ratios of Hg data based on selected GAM models (cumulative weight < = .95) (CladoS, CladoM = abundance of small and medium size Cladocera per depth, respectively). Non-linear explanatory variables (with *, see Fig. 3 for more information) only show their importance on the response variables.

Hg ratios	Variables	Weighted coefficient	Lower CI	Upper CI	Wt
DFM	Fe	6.49e-02	8.62e-03	1.21e-01	0.63
	phytoplankton	3.03e-02	2.59e-02	3.48e-02	0.95
	Fe*				0.95
PMR	CladoM	-1.52e-02	-2.85e-02	-1.99e-03	0.73
	pH	-6.68e-02	-1.00e-01	-3.34e-02	0.68
	CladoS	1.03e-02	9.57e-04	1.97e-02	0.48
	DOC*				0.08
	Temperature*				< 0.01
DFH	phytoplankton	-2.31e-02	-3.97e-02	-6.59e-03	0.82
FTM	phytoplankton	1.25e-02	9.51e-03	1.55e-02	0.95
	SO_4^{2-}*				0.95
	Temperature*				0.22

Figures

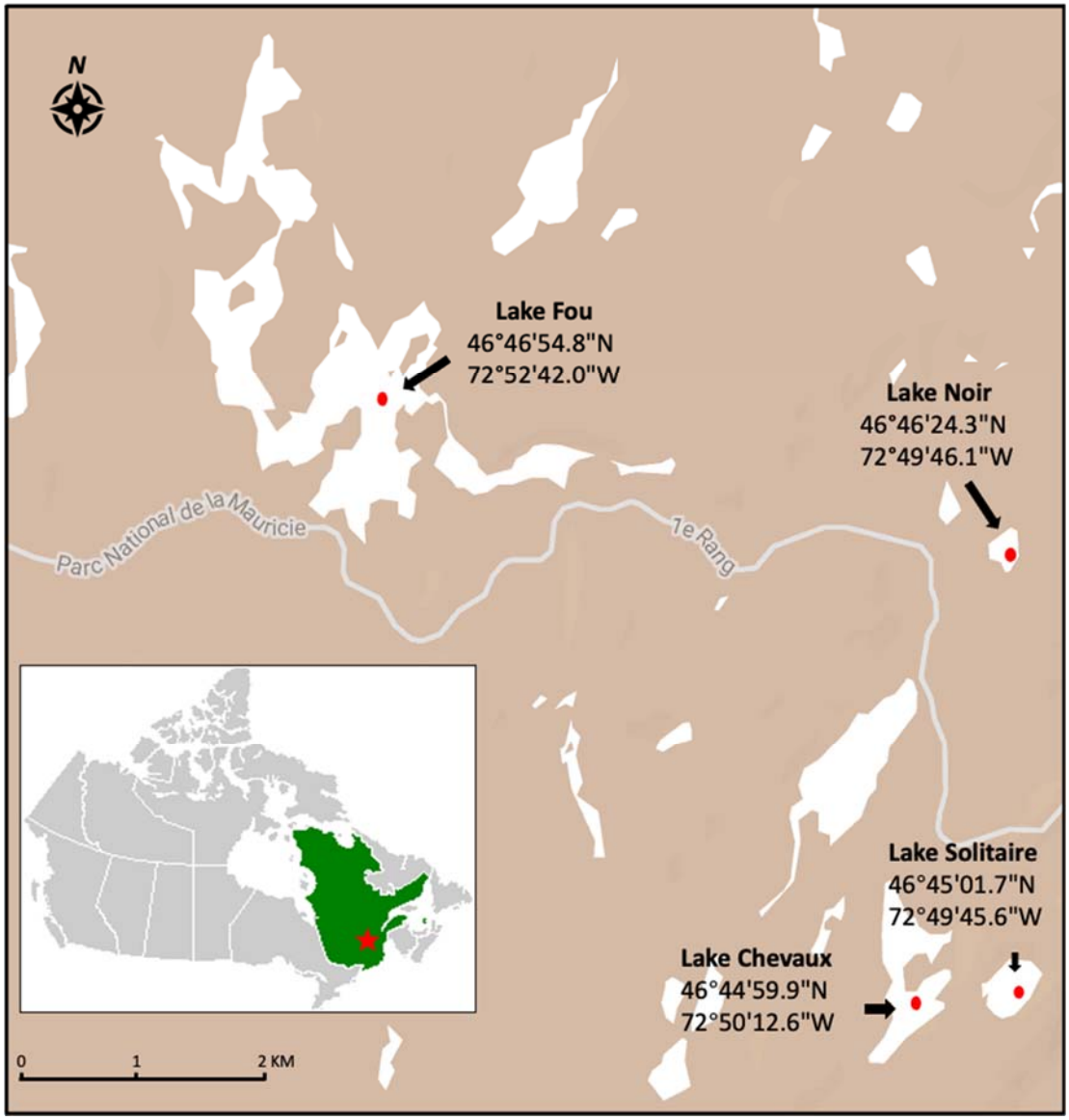

Fig. 1. Sampling site in La Mauricie National Park of Canada. Red star in the map of Canada indicates the location of the Park. Red triangles show the selected lakes with lake Fou (with fish, dark water) at upper right of the map, lake Noir (fishless, dark water) at the upper left side, lake Chevaux (with fish, clear water) at the lower right, and lake Solitaire (fishless, clear water) at the lower left. Red points show the sampling location in each lake (see Table 1 for more detailed information).

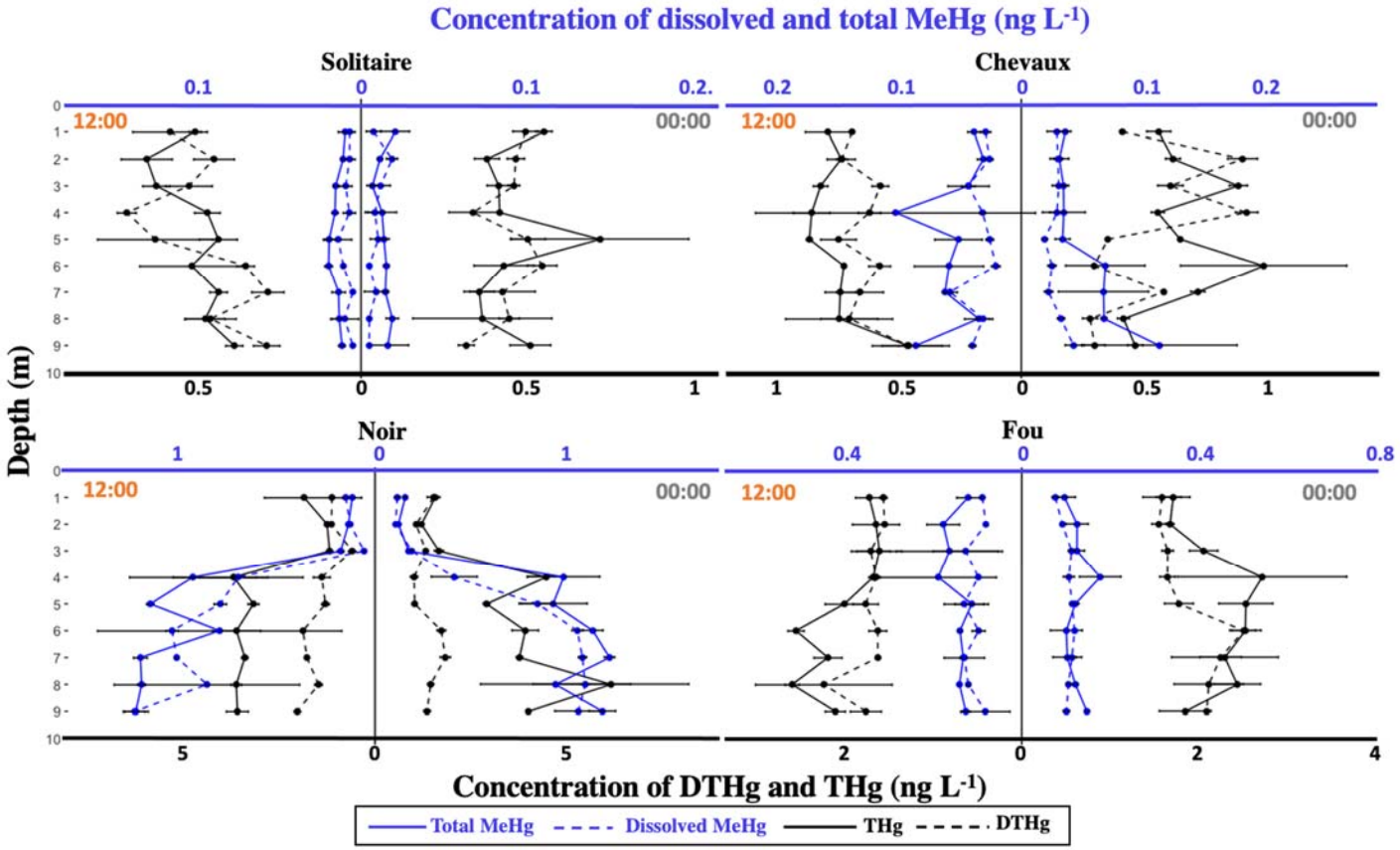

Fig. 2. Vertical profiles of the concentrations of Hg (black) and MeHg (blue) in the study lakes. Solid lines represent total concentrations whereas dashed lines represent the concentrations of dissolved forms. The upper x-scale represents the concentrations of dissolved and total MeHg, whereas the lower scale represents the concentration of dissolved and total Hg. Within each panel, the left side represents sampling from the daytime and the right side represents sampling from the nighttime. Note that the x axes are scaled differently for each lake. Left: fishless lakes; Right: lakes with fish. Upper panels: clearwater lakes; Lower panel: colored lakes.

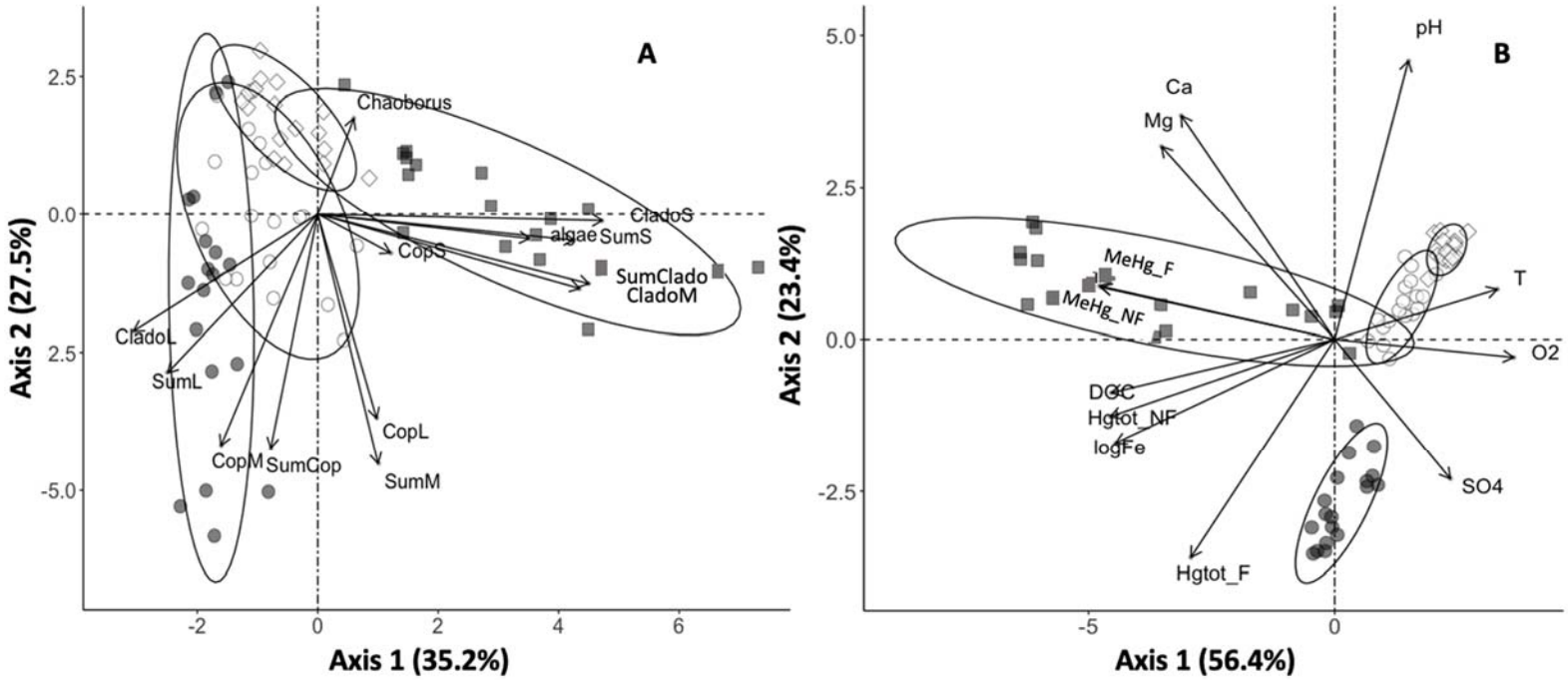

Fig. 3 A) PCA on biotic variables: SumClado, CladoS, CladoM, CladoL = abundance of the sum, small-, medium-, and large-size of Cladocera, respectively; SumCop, CopS, CopM, CopL = abundance of the sum, small-, medium-, and large-size of copepods, respectively; SumS, SumM, SumL = abundance of the total small-, medium, and large-size zooplankton); algae = phytoplankton abundance); B) PCA on physic-chemical variables (Hgtot_F = concentration of dissolved Hg per depth; Hgtot_NF = concentration of total Hg per depth; MeHg_F = concentration of dissolved MeHg per depth; MeHg_NF = concentration of total MeHg per depth; DOC = dissolved organic carbon). Squares: fishless lakes; Circles: lakes with fish. Gray symbols: dark lakes; Open symbols: clear lakes.

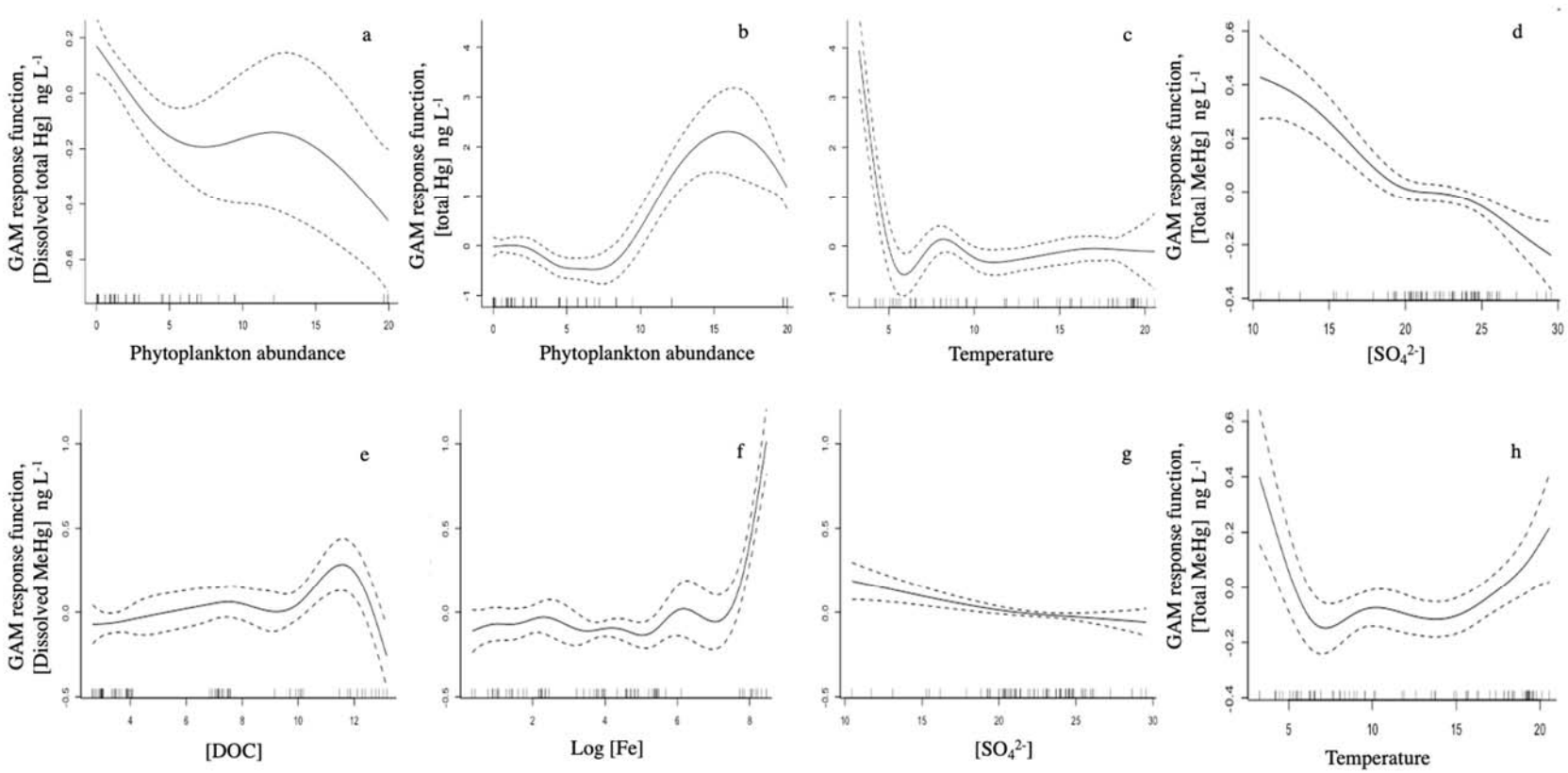

Fig. 4. Predicted values of GAM models for the variables models with a smooth function for the concentrations of Hg and MeHg included in the 95% CI set of models (see Table 4): dissolved total Hg in panel (a); total Hg in panels (b) and (c); dissolved MeHg in (e)-(g), total MeHg in (d) and (h). This graphic summary is based on the selected top model for each of the response variables, which are shown on the y-axis as a centered smoothed function scale to ensure valid pointwise 95% confidence bands. The covariables are shown on x-axis. Solid curves are the cubic smoothing spline fits for each continuous covariate conditioned on all other covariates in the GAM model (see Table 4). Dotted curves are pointwise 95% confidence curves around the fits.

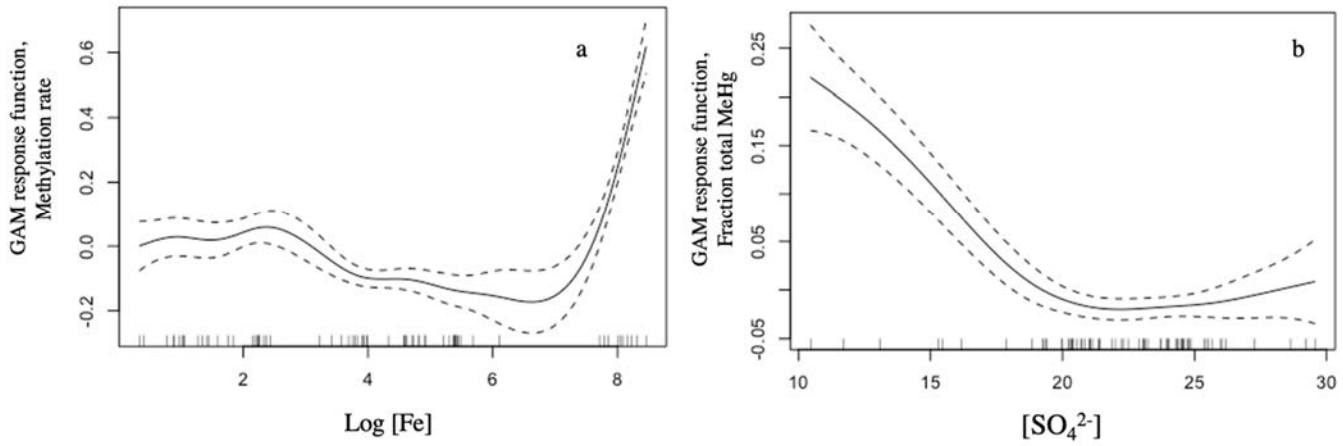

Fig. 5. Predicted values of GAM models for the non-linear covariates for the calculated Hg ratios in Table 5: PMR ratio (proxy of methylation rate) in panel (a); FTM (fraction of the total MeHg) in panel (b). This graphic summary is based on the selected top model for each of the response variables, which are shown on the y-axis as a centered smoothed function scale to ensure valid pointwise 95% confidence bands. The covariables are shown on x-axis. Solid curves are the cubic smoothing spline fits for each continuous covariate conditioned on all other covariates in the GAM model (see Table 5). Dotted curves are pointwise 95% confidence curves around the fits.

Supplentary Tables and Figures

Table S1. Summary of the models retained in the 95% confidence interval (CI) set for dissolved Hg. The coefficients are shown for each of the explanatory variables together with the degrees of freedom (df) AIC_c and ΔAIC_c values associated with the model and both its weight (w_i) and cumulative weight (Cum w_i). The models are ranked based on their AIC_c value. A total of 61 models were included in the 95% CI set of models. For simplicity, only models with a $\Delta AIC_c < 2$ are shown. Depth (with smooth function) and sampling time (categorical) were always presented in the models; thus, they were not present in the table. The best model (i.e., the one with the lowest AIC_c value) had a R^2adj of 0.868.

DOC	CopL	CladoM	pH	SO_4^{2-}	s(algae)	df	AIC_c	ΔAIC_c	w_i	Cum. w_i
0.113		-0.0389	-0.482	-0.028	*	14	15.5	0.00	0.154	0.154
0.102	-0.231		-0.538	-0.026	*	14	16.4	0.88	0.099	0.253
0.093			-0.525	-0.032	*	13	16.9	1.36	0.079	0.332

Table S2. Summary of the models retained in the 95% confidence interval (CI) set for total Hg. The coefficients are shown for each of the explanatory variables together with the degrees of freedom (df) AIC_c and ΔAIC_c values associated with the model and both its weight (w_i) and cumulative weight (Cum w_i). The models are ranked based on their AIC_c value. A total of 2 models were included in the 95% CI set of models. Depth (with smooth function) and sampling time (categorical) were always presented in the models; thus, they were not present in the table. The best model (i.e., the one with the lowest AIC_c value) had a R^2adj of 0.969.

DOC	CopM	SumCop	pH	s(algae)	s(T)	df	AIC_c	ΔAIC_c	w_i	Cum. w_i
0.151	-0.040		-0.603	*	*	15	84.4	0.00	0.867	0.867
0.146		-0.025	-0.539	*	*	15	89.5	5.04	0.070	0.937

Table S3. Summary of the models retained in the 95% confidence interval (CI) set for dissolved MeHg. The coefficients are shown for each of the explanatory variables together with the degrees of freedom (df) AIC_c and ΔAIC_c values associated with the model and both its weight (w_i) and cumulative weight (Cum w_i). The models are ranked based on their AIC_c value. A total of 5 models were included in the 95% CI set of models. Depth (with smooth function) and sampling time (categorical) were always presented in the models; thus, they were not present in the table. The best model (i.e., the one with the lowest AIC_c value) had a R^2adj of 0.971.

algae	CopS	CladoL	CladoM	s(DOC)	s(Log[Fe])	$s(SO_4^{2-})$	s(T)	df	AIC_c	ΔAIC_c	w_i	Cum. w_i
0.020			-0.011	*	*	*		16	-102.3	0.00	0.853	0.853
0.023			-0.020	*	*			14	-96.4	5.83	0.046	0.899
0.022		0.018	-0.021	*	*			15	-94.8	7.49	0.020	0.919
0.027				*	*	*	*	17	-94.1	8.13	0.015	0.934
0.023	0.003		-0.020	*	*			15	-93.4	8.85	0.010	0.944

Table S4. Summary of the models retained in the 95% confidence interval (CI) set for total MeHg. The coefficients are shown for each of the explanatory variables together with the degrees of freedom (df) AIC_c and ΔAIC_c values associated with the model and both its weight (w_i) and cumulative weight (Cum w_i). The models are ranked based on their AIC_c value. A total of 84 models were included in the 95% CI set of models. For simplicity, only models with a $\Delta AIC_c < 2$ are shown. Depth (with smooth function) and sampling time (categorical) were always presented in the models; thus, they were not present in the table. The best model (i.e., the one with the lowest AIC_c value) had a R^2adj of 0.956.

algae	DOC	CopL	CladoM	CladoS	pH	s(Log[Fe])	$s(SO_4^{2-})$	s(T)	df	AIC_c	ΔAIC_c	w_i	Cum. w_i
0.044	0.022						*	*	14	-91.6	0.00	0.071	0.071
0.051					-0.045		*	*	14	-91.4	0.17	0.065	0.136
0.044	0.032			-0.013			*	*	15	-90.7	0.84	0.047	0.183
0.044	0.019	0.073					*	*	15	-90.5	1.03	0.043	0.226
0.049			0.012		-0.050		*	*	15	-90.3	1.32	0.037	0.263
0.050					-0.126	*	*		14	-90.0	1.58	0.032	0.295
0.048	0.013				-0.028		*	*	15	-89.8	1.81	0.029	0.324
0.050		0.057			-0.038		*	*	15	-89.6	1.96	0.027	0.351

Table S5. Summary of the models retained in the 95% confidence interval (CI) set for DFM ratio (dissolved fraction of MeHg). The coefficients are shown for each of the explanatory variables together with the degrees of freedom (df) AIC_c and ΔAIC_c values associated with the model and both its weight (w_i) and cumulative weight (Cum w_i). The models are ranked based on their AIC_c value. A total of 1253 models were included in the 95% CI set of models. For simplicity, only models with a $\Delta AIC_c < 2$ are shown. Depth (with smooth function) and sampling time (categorical) were always presented in the models; thus, they were not present in the table. The best model (i.e., the one with the lowest AIC_c value) had a R^2adj of 0.162.

algae	DOC	CopS	CladoL	CladoM	CladoS	s(Log[Fe])	pH	SO_4^{2-}	T	df	AIC_c	ΔAIC_c	w_i	Cum. w_i
						0.053				9	34.4	0.00	0.013	0.013
-0.015		0.039				0.083				11	34.5	0.05	0.013	0.026
-0.021	0.057	0.036								11	34.5	0.12	0.013	0.039
-0.021					0.026	0.073				11	34.8	0.42	0.011	0.050
-0.022		0.031			0.024	0.082				12	34.9	0.49	0.010	0.060
-0.012						0.069				10	34.9	0.50	0.010	0.070
-0.036	0.049	0.042							-0.034	12	34.9	0.53	0.010	0.080
		0.027				0.058				10	35.1	0.65	0.010	0.090
-0.017	0.049									10	35.3	0.85	0.009	0.099
-0.020	0.031	0.037				0.042				12	35.8	1.40	0.007	0.106
-0.023		0.041	-0.060			0.091				12	35.9	1.43	0.007	0.113
-0.015		0.034				0.077		-0.010		12	36.1	1.70	0.006	0.119
	0.031									9	36.2	1.81	0.005	0.124
-0.019	0.051	0.040					-0.048			12	36.3	1.84	0.005	0.129
-0.016			-0.043			0.073				11	36.3	1.85	0.005	0.134
-0.022	0.073	0.054		-0.029						12	36.3	1.86	0.005	0.139
						0.051		-0.008		10	36.4	1.95	0.005	0.144
-0.022		0.036		-0.033	0.043	0.092				13	36.4	1.97	0.005	0.149

Table S6. Summary of the models retained in the 95% confidence interval (CI) set for PMR (proxy of methylation rate). The coefficients are shown for each of the explanatory variables together with the degrees of freedom (df) AIC_c and ΔAIC_c values associated with the model and both its weight (w_i) and cumulative weight (Cum w_i). The models are ranked based on their AIC_c value. A total of 73 models were included in the 95% CI set of models. For simplicity, only models with a $\Delta AIC_c < 4$ are shown. Depth (with smooth function) and sampling time (categorical) were always presented in the models; thus, they were not present in the table. The best model (i.e., the one with the lowest AIC_c value) had a R^2adj of 0.971.

algae	Chao	CopL	CladoM	CladoS	pH	s(DOC)	s(Log[Fe])	df	AIC_c	ΔAIC_c	w_i	Cum. w_i
0.030			-0.018	0.010	-0.068		*	14	-200.4	0.00	0.249	0.249
0.023			-0.013		-0.067	*	*	15	-197.9	2.58	0.068	0.317
0.030			-0.008		-0.062		*	13	-197.6	2.83	0.060	0.377
0.033			-0.018	0.011			*	13	-197.4	3.06	0.054	0.431
0.033		0.039	-0.023	0.013			*	14	-196.8	3.62	0.041	0.472
0.033	0.115		-0.020	0.012			*	14	-196.7	3.69	0.039	0.511

Table S7. Summary of the models retained in the 95% confidence interval (CI) set for DFH ratio (dissolved fraction of Hg). The coefficients are shown for each of the explanatory variables together with the degrees of freedom (df) AIC_c and ΔAIC_c values associated with the model and both its weight (w_i) and cumulative weight (Cum w_i). The models are ranked based on their AIC_c value. A total of 215 models were included in the 95% CI set of models. For simplicity, only models with a $\Delta AIC_c < 2$ are shown. Depth (with smooth function) and sampling time (categorical) were always presented in the models; thus, they were not present in the table. The best model (i.e., the one with the lowest AIC_c value) had a R^2adj of 0.399.

algae	DOC	CopL	CopM	CladoL	CladoS	s(Log[Fe])	pH	SO_4^{2-}	df	AIC_c	ΔAIC_c	w_i	Cum. w_i
-0.026		-0.320	0.018						11	11.3	0	0.015	0.015
-0.021						-0.053	-0.083		11	11.4	0.08	0.014	0.029
-0.020		-0.199				-0.046	-0.099		12	11.5	0.22	0.013	0.042
-0.021		-0.386	0.015	0.051					12	11.9	0.56	0.011	0.053
-0.020		-0.250	0.019			-0.025			12	11.9	0.58	0.011	0.064
-0.024		-0.303		0.062					11	11.9	0.6	0.011	0.075
-0.019	-0.016	-0.272	0.019						12	12.1	0.73	0.01	0.085
-0.026						-0.030			10	12.3	0.94	0.009	0.094
-0.030		-0.202							10	12.6	1.24	0.008	0.102
-0.024	-0.020								10	12.7	1.33	0.008	0.110
-0.016		-0.316	0.017	0.048		-0.024			13	12.8	1.45	0.007	0.117
-0.022			0.012			-0.037			11	12.8	1.48	0.007	0.124
-0.025		-0.42	0.018	0.071	0.020				13	13	1.64	0.007	0.131
-0.024		-0.340	0.016					0.008	12	13.2	1.84	0.006	0.137
-0.020	-0.023	-0.230					-0.072		12	13.2	1.92	0.006	0.143
-0.033									9	13.3	1.93	0.006	0.149

Table S8. Summary of the models retained in the 95% confidence interval (CI) set for FTM ratio (fractio of total MeHg). The coefficients are shown for each of the explanatory variables together with the degrees of freedom (df) AIC_c and ΔAIC_c values associated with the model and both its weight (w_i) and cumulative weight (Cum w_i). The models are ranked based on their AIC_c value. A total of 84 models were included in the 95% CI set of models. For simplicity, only models with a $\Delta AIC_c < 2$ are shown. Depth (with smooth function) and sampling time (categorical) were always presented in the models; thus, they were not present in the table. The best model (i.e., the one with the lowest AIC_c value) had a R^2adj of 0.885.

algae	Chao	CopL	CopM	CopS	SumClado	CladoL	Cla-doM	CladoS	SumCop	Log[Fe]	$s(SO_4^{2-})$	s(T)	df	AIC_c	ΔAIC_c	w_i	Cum. w_i
0.013									0.002		*		12	-249.3	0.000	0.028	0.028
0.012							0.008	-0.005			*		13	-249.3	0.030	0.028	0.056
0.013											*		11	-248.7	0.660	0.020	0.076
0.015										0.011	*	*	14	-248.6	0.710	0.020	0.096
0.012							0.004				*		12	-248.5	0.830	0.018	0.114
0.015							0.004			0.011	*	*	15	-248.4	0.890	0.018	0.132
0.014				0.005						0.012	*	*	15	-248.4	0.970	0.017	0.149
0.013	0.066								0.002		*		13	-248.2	1.130	0.016	0.165
0.012		0.026									*		12	-248.2	1.130	0.016	0.181
0.013			0.002								*		12	-247.9	1.470	0.013	0.194
0.012						0.007	0.004				*		13	-247.6	1.700	0.012	0.206
0.012										0.004	*		12	-247.6	1.740	0.012	0.218
0.012	0.054						0.008	-0.006			*		14	-247.4	1.880	0.011	0.229
0.012			0.002				0.004				*		13	-247.4	1.930	0.011	0.240
0.015					0.002					0.012	*	*	15	-247.3	1.980	0.010	0.250
0.012									0.002	0.003	*		13	-247.3	2.000	0.010	0.260

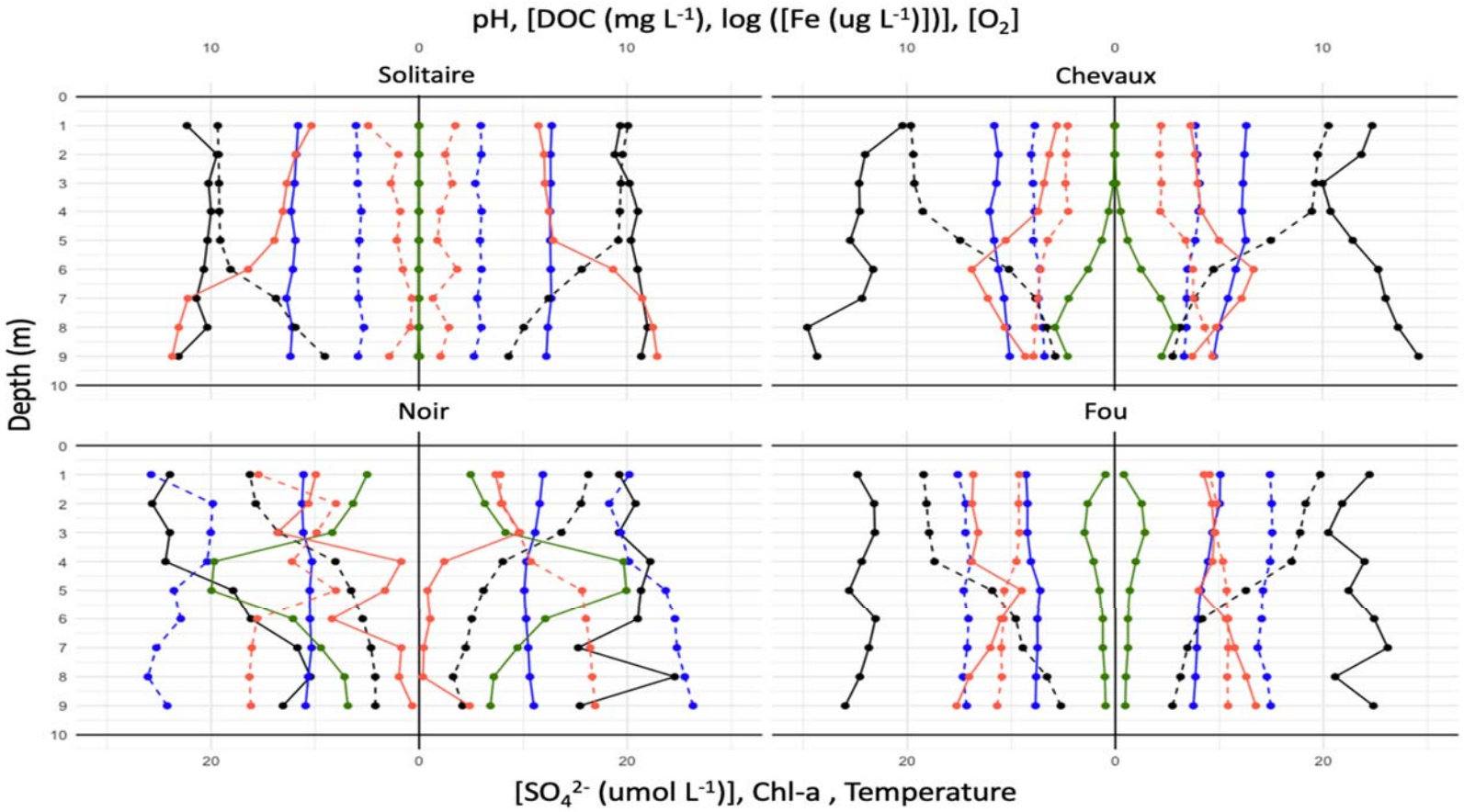

Fig. S1. Vertical profiles for biotic and abiotic variables in the sampled lakes. The left and the right side of each panel represent, respectively, daytime and nighttime sampling. The lower x scale represents the abundance of phytoplankton (green line), the concentration of sulfate (black line) and temperature (dashed black line). The upper x scale represents for pH (blue line), DOC concentration (dashed blue line), log concentration of Fe (dashed red line), and concentration of O2 (red line). Note that for Chl-a we took the profiles only at midday (the mirror night profile is shown only for reference).

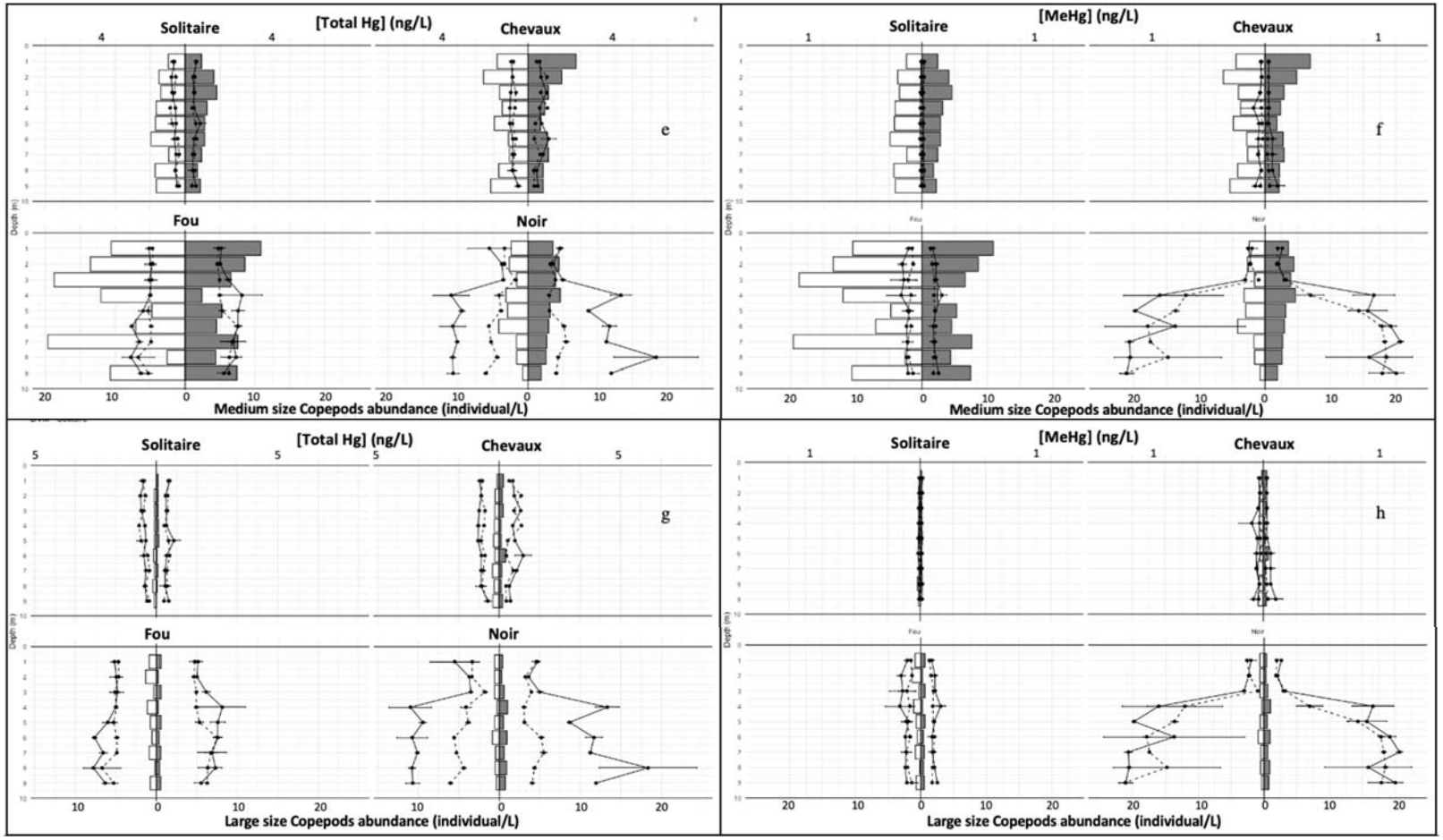

Fig. S2. Mirror plot of copepods abundance versus the concentrations of total Hg and MeHg in each of the four lakes: Sum abundance of copepods in panel (a) and (b); small size copepods in panels (c) and (d); medium size copepods in panels (e) and (f); big size copepods in panels (g) and (h). Concentrations of dissolved (dashed line) and total (solid line) Hg are in panel (a), (c), (e), and (g); concentrations of dissolved (dashed line) and total (solid line) MeHg are in panel (b), (d), (f), and (h). In each panel, lakes are presented by the gradient of water clarity: lake Solitaire (top left); lake Chevaux (top right); lake Fou (lower left), and lake Noir (lower left).

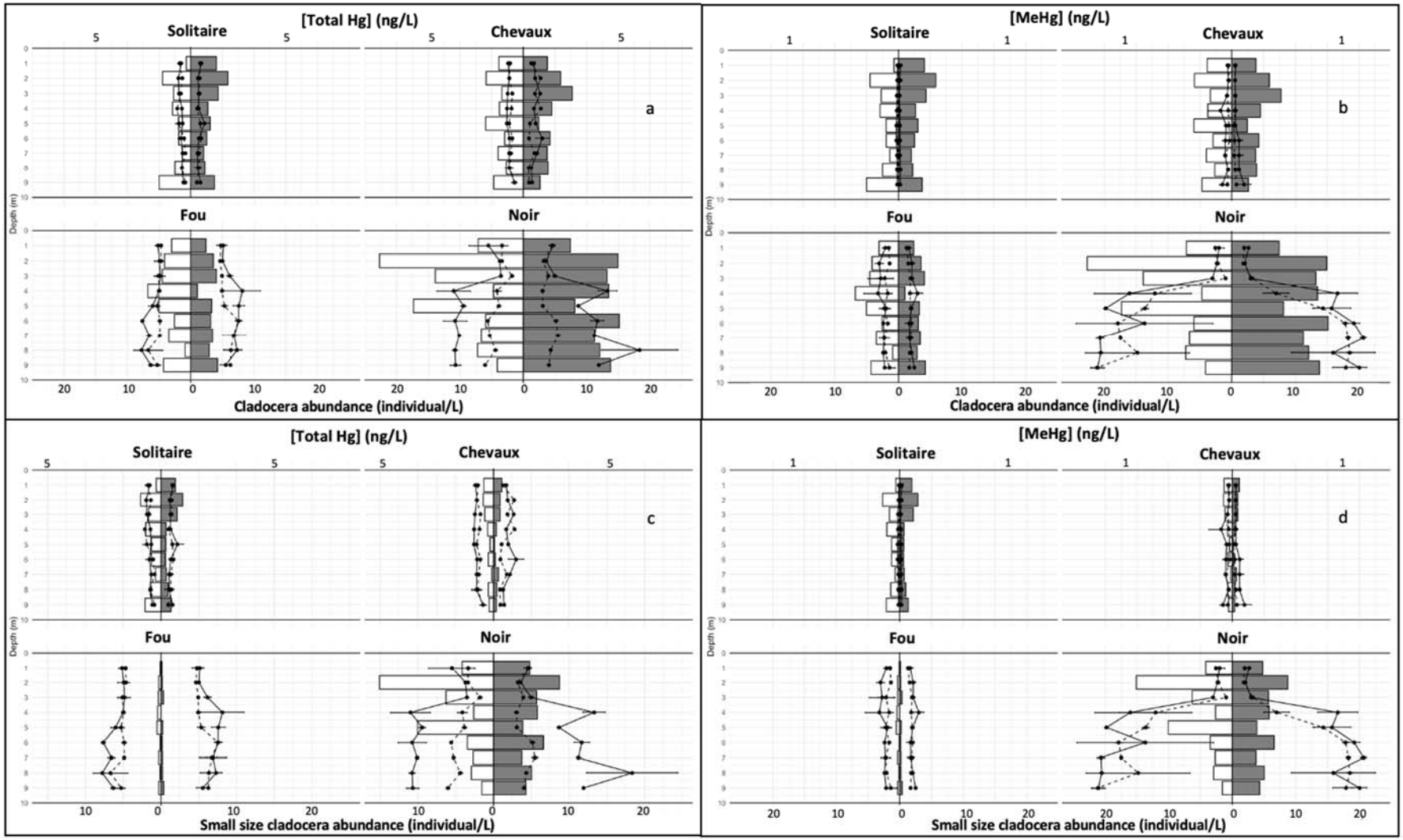
[Total Hg] (ng/L)
Solitaire
Chevaux
Fou
Noir
a
Depth (m)
Cladocera abundance (individual/L)
[MeHg] (ng/L)
b
[Total Hg] (ng/L)
c
Small size cladocera abundance (individual/L)
[MeHg] (ng/L)
d
Small size cladocera abundance (individual/L)

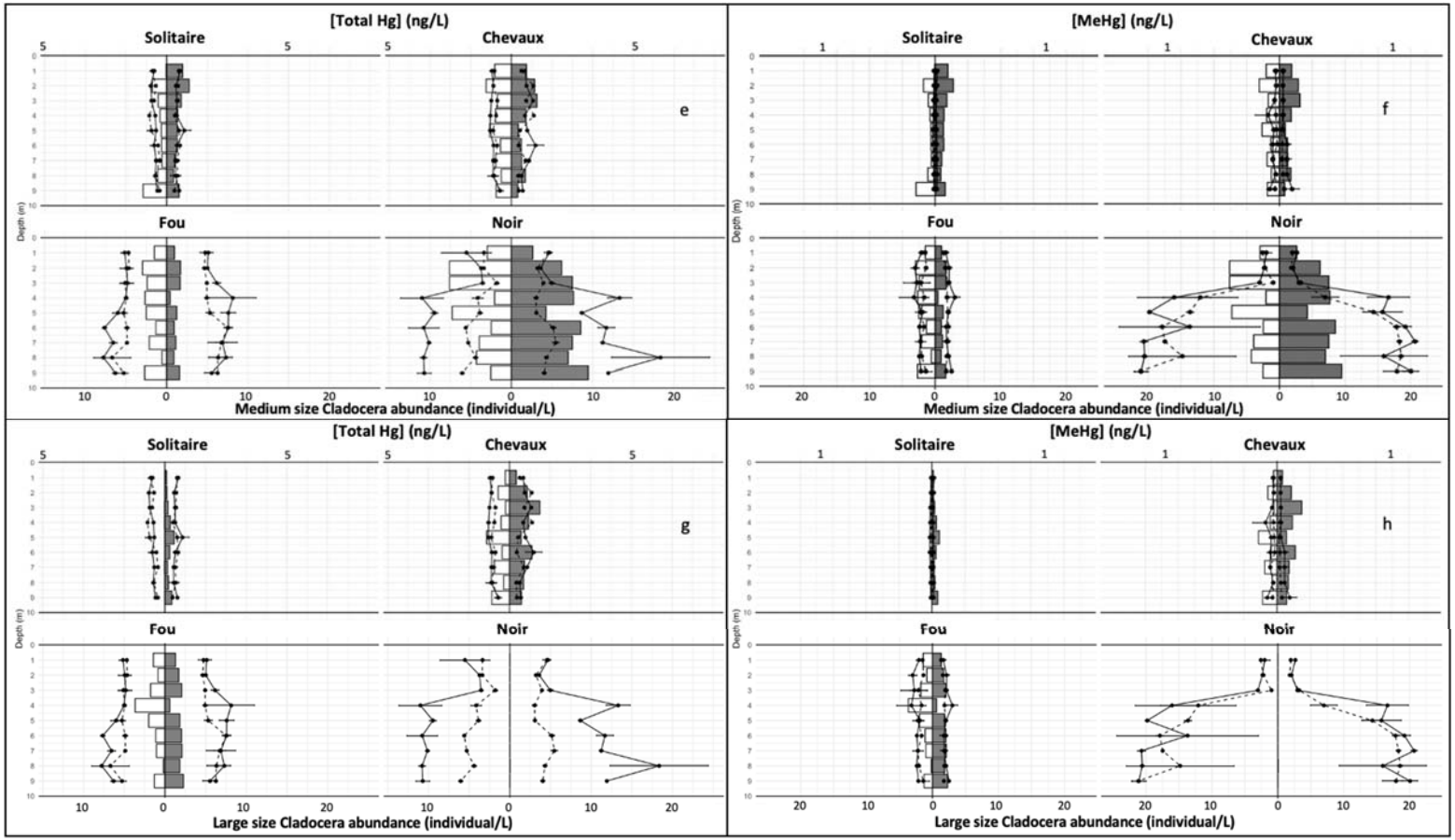

Fig. S3. Mirror plot of cladocerans abundance versus the concentrations of total Hg and MeHg in each of the four lakes: Sum abundance of cladocerans in panel (a) and (b); small size cladocerans in panels (c) and (d); medium size cladocerans in panels (e) and (f); big size cladocerans in panels (g) and (h). concentrations of dissolved (dashed line) and total (solid line) Hg are in panel (a), (c), (e), and (g); concentrations of dissolved (dashed line) and total (solid line) MeHg are in panel (b), (d), (f), and (h). In each panel, lakes are presented by the gradient of water clarity: lake Solitaire (top left); lake Chevaux (top right); lake Fou (lower left), and lake Noir (lower left).

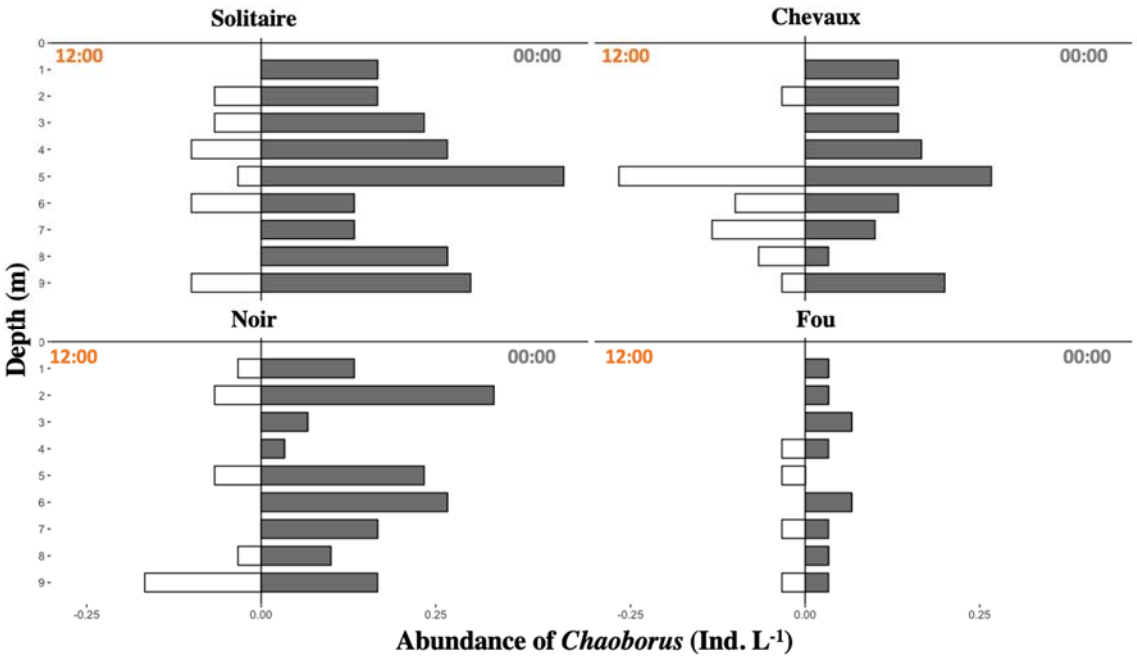

Fig. S4. Mirror plot of *Chaoborus* abundance in sampled lakes. Left panels: fishless lakes; Right panels: lakes with fish. Upper panels: clearwater lakes; Lower panels: colored lakes.

CONCLUSION

Bien que le zooplancton soit considéré comme une composante importante dans le transfert trophique du Hg dans les réseaux trophiques aquatiques, on en sait encore très peu au sujet de son rôle potentiel dans le cycle du Hg dans les lacs par d'autres voies. Dans le cadre de cette thèse doctorale, nous avons étudié les effets sur le cycle du Hg de multiples facteurs concernant les activités du zooplancton dans les lacs boréaux, tels que le broutage, la distribution verticale et les fluctuations de température. Nous avons utilisé des approches expérimentales dans des conditions contrôlées pour mieux comprendre les mécanismes à l'origine de certains facteurs spécifiques (p. ex., le broutage du zooplancton, la fluctuation de température) sur le cycle du Hg en eau douce et l'observation sur le terrain pour étudier les effets de l'abondance du zooplancton sur l'hétérogénéité verticale du Hg à plus grande échelle.

Tandis que les trois chapitres dans cette thèse sont développés autour de différentes problématiques, ils se sont connectés en étudiant les effets des comportements du zooplancton sur le cycle de Hg dans les écosystèmes de l'eau douce, qui sont peu étudiés dans le temps passé. Tel que démontré dans le premier chapitre, le broutage du zooplancton libère du Hg inorganique (IHg) et du MeHg dans l'eau douce durant la période de sloppy feeding, mais les concentrations de IHg/MeHg total diminuent après 30 min dans le microcosme. Cependant, ces effets semblent être espèce-spécifiques, dépendant à la fois de la taxonomie du zooplancton et de la spéciation du Hg dans l'eau. Plus précisément, le broutage par les copépodes libère plus d'éléments traces dans la phase particulaire, alors que le broutage par les cladocères a montré plus d'impact sur la phase dissoute des éléments traces. Ces résultats sont partiellement confirmés par notre étude sur terrain en étudiant la relation entre l'abondance du zooplancton, qui est lié au comportement de la migration verticale journalière, et l'hétérogénéité du profil de Hg dans la colonne d'eau. En effet, une corrélation significative (négative) a été observée entre l'abondance du zooplancton dans une profondeur donnée et la concentration de Hg total (THg) et de Hg total dissout (DTHg), qui est peut-être causé par un broutage plus efficace par le zooplancton. Le temps d'échantillonnage sur terrain (midi et minuit) correspond à

la période d'échantillonnage prolongé dans les expériences de chapitre I (Ringelberg, 2009). Néanmoins, les impacts de l'abondance du zooplancton étaient spécifiques, en fonction de la taxonomie du zooplancton, de la taille du zooplancton et de la spéciation du Hg dans l'eau des lacs. Plus précisément, les gros copépodes et les cladocères de taille moyenne diminuent significativement la concentration de Hg dissous dans l'eau, alors que la présence de copépodes moyens diminue significativement la concentration de Hg total. Ces résultats sur les comportements du zooplancton (migration et broutage) *vs* les concentrations de Hg/MeHg dans l'eau ont le potentiel d'affecter le mode d'accumulation de ces contaminants dans le réseau trophique, comme il a montré dans le chapitre II de cette thèse. Nous avons observé que l'accumulation de IHg était diminuée de manière significative dans des conditions de fluctuation de la température via les voies trophique et aqueuse par rapport au traitement à température constante dans des conditions contrôlées. Cependant, l'accumulation de MeHg n'était réduite que dans la voie trophique mais augmentée par la voie aqueuse. Cette étude jette ainsi un nouvel éclairage sur l'accumulation de polluants métalliques traces dans des conditions de température plus représentatives des milieux naturels. Comme souligné déjà par plusieurs chercheurs, les résultats observés à température constante ne permettent pas de reproduire le phénomène observé dans les conditions naturelles où la température fluctue rapidement (Hagstrum and Hagstrum. 1970; Niehaus et al. 2012; Vasseur et al. 2014), et les conclusions tirées sur les effets de la température sur l'accumulation de Hg dans les réseaux trophiques obtenues à température expérimentale constante peuvent être trompeuses. Cependant, les effets de la fluctuation de température sur les comportements, comme l'efficacité de filtration par les *Daphnia*, reste à confirmer dans les futures études.

Comme le rôle du broutage du zooplancton est souvent ignoré dans le cycle des polluants métalliques traces dans les écosystèmes d'eau douce, les résultats de cette thèse contribuent à combler le manque de connaissances sur le cycle du Hg en reconsidérant le rôle du zooplancton qui est non seulement important dans le transfert trophique, mais aussi dans le cycle biogéochimique du Hg dans les écosystèmes d'eau douce. En broutant dans la colonne d'eau, le zooplancton a le potentiel de modifier les micro-environnements dans la couche d'eau oxique. Des études récentes ont montré que les producteurs primaires

pourraient être de sites importants sur la production de MeHg (Coelho-Souza et al., 2006; Gascón Díez et al., 2016; Yin et al., 2022). Les effets du broutage du zooplancton sur cette production et son transfert ultérieur dans les réseaux trophiques n'est pas encore connu. En outre, il a été prouvé que la « neige de lac » peut également être un site important pour la production de MeHg en raison des conditions d'hypoxie-anoxie au centre des agrégats de matière organique particulaire (Alldredge and Cohen, 1987; Glud et al., 2015; Ortiz et al., 2015). Le broutage du zooplancton a le potentiel de modifier la structure de ces agrégats et donc la production de MeHg, entraînant des changements à la biogéochimie du Hg dans les écosystèmes aquatiques. Le Hg inorganique libéré pendant le broutage pourrait contribuer à la production de MeHg an s'ajoutant à celle due au périphyton dans les lacs peu profonds, un autre site important sur la production de MeHg dans la colonne d'eau (Leclerc et al., 2015; Branfireun et al., 2020). Tous les éléments mentionnés ci-dessus nécessitent une attention supplémentaire pour pouvoir comprendre pleinement le cycle du Hg dans les écosystèmes d'eau douce et son transfert dans le réseau trophique, en particulier dans les lacs peu profonds.

En effectuant la migration verticale, la bioaccumulation de métaux traces dans le zooplancton peut être modifiée et amplifiée par la fluctuation des températures. On ne connaît toujours pas ce qui cause cette accumulation accrue de polluants organiques à l'état de trace (p. ex., MeHg) dans le zooplancton migrateur. Plus de travail devrait être effectué à de grandes échelles d'échantillonnage sur le terrain et au niveau subcellulaire pour mieux comprendre les mécanismes derrière cette amplification. En outre, certains poissons ont également adopté un comportement migratoire, soit vertical ou horizontal, entre le jour et la nuit. Ces changements dans l'environnement, en particulier le changement des conditions de température, doivent être étudiés davantage, afin de mieux comprendre le transfert trophique de multiples polluants dans la chaîne alimentaire. De plus, un nouveau cadre d'étude et une nouvelle norme expérimentale devraient être établis, car nous savons maintenant qu'il est incorrect d'étudier l'accumulation de polluants sous des températures constantes non réalistes dans des conditions contrôlées en laboratoire.

Bien que nous sommes bien conscients que la contribution de cette thèse ne reste que partielle, elle apporte un nouvel éclairage sur différents aspects pouvant relier le zooplancton au cycle du mercure, en montrant que ces organismes méritent une attention particulière si nous voulons avoir un portrait plus complet de la place de ce contaminant dans les écosystèmes aquatiques. Nous espérons que cette contribution saura stimuler des nouveaux axes de recherche pouvant nous renseigner aussi bien sur les patrons en nature que sur les mécanismes sous-jacents ceux-ci.

RÉFÉRENCES BIBLIOGRAPHIQUES

Achá, D., Hintelmann, H., Yee, J., 2011. Importance of sulfate reducing bacteria in mercury methylation and demethylation in periphyton from Bolivian Amazon region. *Chemosphere* 82, 911-916. https://doi.org/10.1016/j.chemosphere.2010.10.050.

Alldredge, A. L., Cohen, Y., 1987. Can microscale chemical patches persist in the sea? Microelectrode study of marine snow, fecal pellets. *Science*, *235*(4789), 689-691. https://doi.org/10.1126/science.235.4789.689

Bollens, S., Roliwagen-Bollens, G., Quenette, J.A., Bochdansky, A.B. 2011. Cascading migrations and implications for vertical fluex in pelagic ecosystems. *J Plankton Res* 33:349-55. https://doi.org/10.1093/plankt/fbq152

Bouchet, S., Goñi-Urriza, M., Monperrus, M., Guyoneaud, R., Fernandez, P., Heredia, C., Tessier, E., Gassie, C., Point, D., Guédron, S., Achá, D., Amouroux, D., 2018. Lin-ing mi- crobial activities and low-molecular-weight thiols to Hg methylation in biofilms and periphyton from high-altitude tropical lakes in the Bolivian Altiplano. *Environ. Sci. Technol 52(17), 9758-9767.* https://doi.org/10.1021/acs.est.8b01885.

Branfireun, B. A., Cosio, C., Poulain, A. J., Riise, G., Bravo, A. G., 2020. Mercury cycling in freshwater systems-An updated conceptual model. *Sci. Total Environ.* 745, 140906. https://doi.org/10.1016/j.scitotenv.2020.140906

Cleckner, L.B., Gilmour, C.C., Hurley, J.P., Krabbenhoft, D.P., 1999. Mercury methylation in periphyton of the Florida Everglades. *Limnol. Oceanogr.* 44, 1815-1825. https://doi.org/10.4319/lo.1999.44.7.1815

Coelho-Souza, S. A., Guimaraes, J. R., Mauro, J. B., Miranda, M. R., Azevedo, S. M., 2006. Mercury methylation and bacterial activity associated to tropical phytoplankton. *Sci. Total Environ. 364*(1-3), 188-199. https://doi.org/10.1016/j.scitotenv.2005.07.010

Compeau, G. C., Bartha, R., 1985. Sulfate-reducing bacteria: principal methylators of mercury in anoxic estuarine sediment. *Appl. Environ. Microbiol. 50*(2), 498-502. https://doi.org/10.1128/aem.50.2.498-502.1985

Dalin, C., Outhwaite, C. L., 2019. Impacts of global food systems on biodiversity and water: the vision of two reports and future aims. *One Earth*, *1*(3), 298-302. https://doi.org/10.1016/j.oneear.2019.10.016

Eckley, C. S., Hintelmann, H., 2006. Determination of mercury methylation potentials in the water column of lakes across Canada. *Sci. Total Environ. 368*(1), 111-125. https://doi.org/10.1016/j.scitotenv.2005.09.042

FAO. 2020. The State of World Fisheries and Aquaculture 2020. Sustainability in action. Rome. https://doi.org/10.4060/ca9229en

Fleming, E. J., Mack, E. E., Green, P. G., Nelson, D. C., 2006. Mercury methylation from unexpected sources: molybdate-inhibited freshwater sediments and an iron-reducing bacterium. *Appl. Environ. Microbiol. 72*(1), 457-464. https://doi.org/10.1128/AEM.72.1.457-464.2006

Gascón Díez, E., Loizeau, J.-L., Cosio, C., Bouchet, S., Adatte, T., Amouroux, D., Bravo, A.G., 2016. Role of settling particles on mercury methylation in the oxic water column of freshwater systems. *Environ. Sci. Technol*. 50, 11672-11679. https://doi.org/10.1021/acs.est.6b03260

Glud, R. N., Grossart, H. P., Larsen, M., Tang, K. W., Arendt, K. E., Rysgaard, S., ... & Gissel Nielsen, T., 2015. Copepod carcasses as microbial hot spots for pelagic denitrification. *Limnol. Oceanogr.* 60(6), 2026-2036. https://doi.org/10.1002/lno.10149

Golden, C.D., Koehn, J.Z., Shepon, A. et al., 2021. Aquatic foods to nourish nations. *Nature* 598, 315–320 https://doi.org/10.1038/s41586-021-03917-1

Gorski, P.R., Armstrong, D.E., Hurley, J.P., Shafer, M.M., 2006. Speciation of aqueous methyl- mercury influences uptake by a freshwater alga (*Selenastrum capricornutum*). *Environ. Toxicol. Chem.* 25 (2), 534-540. https://doi.org/10.1897/04-530R.1

Grégoire, D.S., Lavoie, N.C., Poulain, A.J., 2018. Heliobacteria reveal fermentation as a key pathway for mercury reduction in anoxic environments. *Environ. Sci. Technol*. 52 (7), 4145-4153. https://doi.org/10.1021/acs.est.8b00320.

Grossart, H. P., Simon, M., 1993. Limnetic macroscopic organic aggregates (lake snow): occurrence, characteristics, and microbial dynamics in Lake Constance. *Limnol. Oceanogr. 38*(3), 532-546. https://doi.org/10.4319/lo.1993.38.3.0532

Guimarães, J.R.D., Mauro, J.B.N., Meili, M., Sundbom, M., Haglund, A.L., Coelho-Souza, S.A., Hylander, L.D., 2006. Simultaneous radioassays of bacterial production and mercury methylation in the periphyton of a tropical and a temperate wetland. *J. Environ. Manag*. 81, 95-100. https://doi.org/10.1016/j.jenvman.2005.09.023.

Hagstrum, D. W., Hagstrum, W. R., 1970. A simple device for producing fluctuating temperatures, with an evaluation of the ecological significance of fluctuating temperatures. *Ann. Entomol. Soc. Am*. *63*(5), 1385-1389. https://doi.org/10.1093/aesa/63.5.1385

Hamelin, S., Amyot, M., Barkay, T., Wang, Y., Planas, D., 2011. Methanogens: principal methylators of mercury in lake periphyton. *Environ. Sci. Technol*. 45(18), 7693-7700. https://doi.org/10.1021/es2010072

Hudson, R.J.M., Gherini, S.A., Watras, C.J., Porcella, D.B., 1994. Modeling the Biogeochem- ical Cycle of Mercury in Lakes: The Mercury Cycling Model (MCM) and Its Application to the MTL study Lakes, In Mercury Pollution: Integration and Synthesis (pp. 473-522). *Lewis Publishers* https://doi.org/1-566 70-066-3/94

Huguet, L., Castelle, S., Schäfer, J., Blanc, G., Maury-Brachet, R., Reynouard, C., Jorand, F., 2010. Mercury methylation rates of biofilm and plankton microorganisms from a hy- droelectric reservoir in French Guiana. *Sci. Total Environ.* 408, 1338-1348. https://doi.org/10.1016/j.scitotenv.2009.10.058

Jitaru, P., Adams, F., 2004. Toxicity, sources and biogeochemical cycle of mercury. In *Journal de Physique IV (Proceedings)* (Vol. 121, pp. 185-193). *EDP sciences.* https://doi.org/10.1051/jp4:2004121012

Kainz, M. J., Fisk, A. T., 2009. Chapiter 5. Integrating Lipids and Contaminants in Aquatic Ecology and Ecotoxicology. In: Kainz, M. J., M. T. Brett, & M. T. Arts., (eds). Lipids in aquatic ecosystems (pp. 94-113). New York: *Springer-Verlag.*

Kerin, E. J., Gilmour, C. C., Roden, E., Suzuki, M. T., Coates, J. D., Mason, R. P., 2006. Mercury methylation by dissimilatory iron-reducing bacteria. *Appl. Environ. Microbiol*. *72*(12), 7919-7921. https://doi.org/10.1128/AEM.01602-06

Leclerc, M., Planas, D., Amyot, M., 2015. Relationship between extracellular low-molecular-weight thiols and mercury species in natural lake periphytic biofilms. *Environ. Sci. Technol*. 49(13), 7709-7716. https://doi.org/10.1021/es505952x

Lehnherr, I., 2014. Methylmercury biogeochemistry: a review with special reference to Arctic aquatic ecosystems. *Environmental Reviews. 22*(3), 229-243. https://doi.org/10.1139/er-2013-0059

Le Jeune, A-H., Bourdiol, F., Aldamman, L., Perron, T., Amyot, M., Pinel-Alloul, B., 2012. Factors affecting Methylmercury biomagnification by a widespread aquatic invertebrate predator, the phantom midge larvae Chaoborus. *Environ. Pollut.* 165: 100–08. https://doi.org/10.1016/j.envpol.2012.02.003

Li, Y., Gai, G., Makler-Pick, V., Waite, A.M., Bruce, L.C., Hipsey, M.R. 2014. Examination of the role of the microbial loop in regulating lake nutrient stoichiometry and phytoplankton dynamics. *Biogeosciences* 11:2939-2960. https://doi.org/10.5194/bg-11-2939-2014

Lovley, D. R., Phillips, E. J., 1987. Competitive mechanisms for inhibition of sulfate reduction and methane production in the zone of ferric iron reduction in sediments. *Appl. Environ. Microbiol. 53*(11), 2636-2641. https://doi.org/10.1128/aem.53.11.2636-2641.1987

Mason, R.P., Reinfelder, J.R., Morel, F.M.M., 1996. Uptake, Toxicity, and Trophic Transfer of Mercury in a Coastal Diatom. *Environ. Sci. Technol.* 30(6), 1835-1845. https://doi.org/10.1021/es950373d

Mason, R. P., Choi, A. L., Fitzgerald, W. F., Hammerschmidt, C. R., Lamborg, C. H., Soerensen, A. L., Sunderland, E. M., 2012. Mercury biogeochemical cycling in the ocean and policy implications. *Environ. Res. 119*, 101-117. https://doi.org/10.1016/j.envres.2012.03.013

Niehaus, A. C., Angilletta Jr, M. J., Sears, M. W., Franklin, C. E., Wilson, R. S., 2012. Predicting the physiological performance of ectotherms in fluctuating thermal environments. *J. Exp. Biol*. *215*(4), 694-701. https://doi.org/10.1242/jeb.058032

Ortiz, V. L., Mason, R. P., Ward, J. E., 2015. An examination of the factors influencing mercury and methylmercury particulate distributions, methylation and demethylation rates in laboratory-generated marine snow. *Mar. Chem. 177*, 753-762. https://doi.org/10.1016/j.marchem.2015.07.006

Poulain, A. J., Amyot, M., Findlay, D., Telor, S., Barkay, T., Hintelmann, H., 2004. Biological and photochemical production of dissolved gaseous mercury in a boreal lake. *Limnol. Oceanogr. 49*(6), 2265-2275. https://doi.org/10.4319/lo.2004.49.6.2265

Qin, F., Amyot, M., Bertolo, A., 2022. Grazer-mediated regeneration of methylmercury, inorganic mercury, and other metals in freshwater. *Sci. Total Environ. 829*, 154553. https://doi.org/10.1016/j.scitotenv.2022.154553

Ringelberg. 2009. Diel Vertical Migration of Zooplankton in Lakes and Ocean. *Springer Science & Business Media*.

Steffan, R. J., Korthals, E. T., Winfrey, M. R., 1988. Effects of acidification on mercury methylation, demethylation, and volatilization in sediments from an acid-susceptible lake. *Appl. Environ. Microbiol*. *54*(8), 2003-2009. https://doi.org/10.1128/aem.54.8.2003-2009.1988

Tsui, M. T., Wang, W. X., 2004. Temperature influences on the accumulation and elimination of mercury in a freshwater cladoceran, Daphnia magna. *Aquat. Toxicol.*, *70*(3), 245-256. https://doi.org/10.1016/j.aquatox.2004.09.006

Ullrich, S. M., Tanton, T. W., Abdrashitova, S. A., 2001. Mercury in the aquatic environment: a review of factors affecting methylation. *Crit. Rev. Environ. Sci. Technol.* 31(3): 241-293. https://doi.org/10.1080/20016491089226

Vasseur, D. A., DeLong, J. P., Gilbert, B., Greig, H. S., Harley, C. D., McCann, K. S., Savage, V., Tunney, T. D., O'Connor, M. I. (2014). Increased temperature variation poses a greater risk to species than climate warming. *Proc. R. Soc. B*. *281*(1779), 20132612. https://doi.org/10.1098/rspb.2013.2612

Watras, C. J., Bloom, N. S., 1994. The vertical distribution of mercury species in Wisconsin lakes: accumulation in plankton layers. In *Mercury pollution: integration and synthesis*, 137-152.

Watkins, B., Simkiss, K., 1988a. The effect of oscillating temperatures on the metal ion metabolism of Mytilus edulis. *J. Mar. Biol. Assoc. U. K. 68*(1), 93-100. https://doi.org/10.1017/S0025315400050128

Watkins, B., Simkiss, K., 1988b. Effects of temperature oscillations on the distribution of ^{65}Zn on cytoplasmic proteins. *Comp. Biochem. Physiol., Part C: Toxicol. Pharmacol. 89*(1), 53-55. DOI: https://doi.org/10.1016/0742-8413(88)90144-2

Winder, M., Spaak, P., Moou, W.M., 2004. Trade-offs in Dphania Habitat Selection. *Ecology* 85 :2027-36. https://doi.org/10.1890/03-3108

Yin, X., Wang, L., Liang, X., Zhang, L., Zhao, J., Gu, B., 2022. Contrary effects of phytoplankton Chlorella vulgaris and its exudates on mercury methylation by iron-and sulfate-reducing bacteria. *J. Hazard. Mater. 433*, 128835. https://doi.org/10.1016/j.jhazmat.2022.128835